Faculty of Engineering – Department of Civil Engineering

Nottingham Transportation Engineering Centre (NTEC)

SELF-HEALING OF CYCLIC LOADING DAMAGE IN ASPHALT MIXTURES

By

SIHAM IDAN SALIH

B.Sc (Survey Eng.) and M.Sc (Highway & Trans.Eng.)

Thesis submitted to the University of Nottingham for the degree of Doctor of Philosophy in Civil Engineering

بسم الله الرحمن الرحيم

In the Name of Allah, the Most Gracious, the Most Merciful

ABSTRACT

One of the essential phenomena that impacts on the properties of asphalt mix is the self-healing. This phenomenon has been explored for about four decades. However, many researchers are trying to investigate artificial methods to accelerate it. The present study was primarily aimed to investigate the optimum moment in the life of asphalt, where self-healing is maximized. Three different self-healing techniques have been investigated, namely infra-red heating, induction heating, and encapsulated healing agents. Accomplishing this aim would enable self-healing to be incorporated into a maintenance plan of the pavement.

This study commenced with a literature review concerning the asphalt self- healing phenomenon, in order to identify the current gaps that must be researched. There are no previous studies about the optimum moment to implement artificial self-healing. For this reason, further research in this thesis was arranged to assess the self -healing capability of hot asphalt mixtures in further detail. Three different asphalt mixtures were used such as; Porous asphalt (PA), Dense asphalt (DA), and Stone mastic asphalt (SMA). Three methods were utilized to generate self-healing: Infra-red heating, Induction heating and Capsules containing rejuvenators. In addition, many tests were carried out : (i) 3-point bending fatigue test to quantify self-healing, (ii) X-Ray Computed Tomography (CT Scans) to assess air void distribution before and after heal-

ing, and (iii) Additional testing related to self-healing for example; Thermal expansion, Stiffness module's (ITSM), and Fourier Transformed Infrared Spectroscopy (FTIR). These test methods covered the three following aspects.

The first aspect of research used infrared heating to simulate solar radiation. It explored the effect of air voids content and their interconnectivity on the capacity of asphalt mixtures to heal fatigue cracks when a thermal infrared treatment is applied. Results showed that contiguous air voids are required to optimise healing. In samples with a lower void content, the thermal expansion of bitumen and its flow through cracks can exceed the pore network's capacity. Therefore, the internal pressure can increase enough to produce material damage instead of healing. Also, the fatigue life of dense asphalt mixes is still significantly longer than that of porous asphalt mixtures. On the contrary, asphalt mixtures with percolated air void content got higher fatigue life extensions than denser asphalt mixtures, to the point of tripling their lifetime.

The second aspect researched used another self-healing method namely induction heating to evaluate self-healing ability. Electrically conductive particles in the form of steel wool fibres were added into porous asphalt (PA). In previous publications, it was found that this technique can significantly extend the fatigue life of the material but the optimum moment to apply the treatment had still unknown not been investigated in -depth by other researchers.

In the present investigation, fatigue tests were carried out at different loading levels and the optimum time in the life of the material to apply the induction treatment was found to be at 35% of the failure life based on statistics and Computed Tomography

scans. The results also show that Induction heating reduces the diameter of the air voids. As a consequence, this has lead to enhancement of the life of the pavement.

The third aspect considered of a study of the self-healing of asphalt mixture enhanced by capsules. The self-healing properties of cracks were then examined under repeated loading in dense, porous, and Stone Mastic Asphalt (SMA) asphalt mixtures, which are the most commonly used asphalt types worldwide. The study determined the optimum time that is represented 35% of number of cycles $N_{0.5}$ (probability of breaking) when the capsules should break to maximise the self-healing. It also gave an insight into the type of cracks that already heal and the breaking mode of the capsules due to repeated loading.

Based on the results obtained for three aspects above, a good understanding of the self- healing of asphalt was achieved. This thesis concludes by discussing these important aspects of constructing of pavements with high durability provided by self-healing abilities. Self-healing asphalt is not only a dream; it works. In addition, porous and stone mastic asphalt healed more efficiently than dense asphalt.

Publications

Salih, S, B Gómez-Meijide, M Aboufoul, and A Garcia. 2018. **"Effect of porosity on infrared healing of fatigue damage in asphalt"**, Construction and Building Materials, 167: 716-25.

A. Garcia-Hernández, S. Salih , B. Gomez-Meijide, "**Optimum moment to heal cracks in asphalt roads by means electromagnetic induction**", Construction & Building Materials, Volume 238, 30 March 2020, 117627.

A. Garcia-Hernández, S. Salih, I. Ruiz-Rianchoa, J. Norambuena-Contrerasa,c, R. Hudson-Griffithsd, B. Gomez-Meijidea, "**Self-healing of reflective cracks in asphalt mixtures by the action of encapsulated agents"**, Construction & Building Materials, Volume 252, 28 August 2020, 118929.

Gomez-Meijide, B., Salih, S., Ajam, H. & Garcia, A. 2018. "**Effect of binder thermal expansion on healing performance of asphalt mixtures"**. ISAP, Conference paper.



EDICATION

To the Messenger Mohammad (Peace and blessing be upon him) for his endless guidance toward the right path. . . .

To the pure souls of my mother and father who had dreamt to witness these moments. . . .

To my all family's brothers, sisters, son of sisters and brother worm herded thanks prayer, encouragements and kindness

To spirit immortal of my brother (the Martyr "Mohamad")

. . . . From the depth of the past wounds, hopes are born . . . .

. . . . We have made a promise and loyalty that crush the impossible. . . .

. . . . through the buried, we send immortal a spirit from death that will not be defeated. . . .

. . . . for the one who gain a paradise in his spirit. . . .

. . . .and inherited the splendour to a sister for the sake of his love, ……

. . . . she struggled with difficulties. . . .

. . . and the eyes of his relatives are wishing for his murderer to destruction. . . .

. . . .and with defiance and an honest word they achieved their goal. . . .

. . . . by his blood and spirit that chanted the humanity. . . .

Siham

DECLARATION

This is to declare that the contents of this thesis are my own work and were performed at the Nottingham Transportation Engineering Centre, Civil Engineering Department, the University of Nottingham. This thesis has not been submitted to any other institution for another degree or another of university.

Siham Idan Salih

University of Nottingham,

Email: evxss7@nottingham.ac.uk

sihamsalih15@gmail.com

Suhamedan_almaliky@yahoo.com

DECLARATION

We declare that the contents and the work described in this thesis were performed at University of Nottingham, Faculty of Engineering from October 2015 to September 2019 under our supervision.

Alvaro Garcia Hernandez
Assistant Professor
Faculty of Engineering
alvaro.garcia@nottingham.ac.uk

Nick Thom
Assistant Professor
Faculty of Engineering
Email: nicholas.thom@nottingham.ac.uk

ACKNOWLEDGMENTS

First and the foremost, I would like to thank “ALLAH”, the Almighty, who created me and gave me an opportunity to live. Without His guidance and blessing, this study would never have been completed.

Sincere appreciation is due to the Al- Shuhdda foundation /Ministry of Higher Education and Scientific Research in Iraq and Al Mustansiriyah University for providing a Scholarship to conduct this PhD study. I would like to thank the Iraqi Cultural Attaché and Mr. Liath Shakur for continuing support.

It is my great pleasure to express my warmest thanks to the people that supported me during my study. I would like to express my sincere gratitude to my supervisors, Dr. Alvaro Garcia, Dr.Nick Thom and Dr. Breixo Gomez-Meijide for providing me the opportunity to do this research with valuable guidance, interest and encouragement over the years. I want to say for Dr. Alvaro and Dr.Nick I proud to work with you.

In addition, I appreciate the valuable advices, kindness and encouragement from Prof. Dr. Gordon Airey, my internal assessor, through my first- and second-year report.

I would like to extend my appreciation to all staff members of University of Nottingham / Pavement research for providing facilities and support to this project. My gratitude also goes to the technical laboratory staff: Mr. Richard Blackmore, Mr. Martyn

Barrett, Mr. Lawrence Pont, Mr. Jonathan Watson, Mr. Matthew Thomas, Mr. Antony Beska, Miss. Laura Weatherby and Miss. Margrata Pawlak. Nottingham Transportation Engineering Centre (NTEC) for all their valuable assistance regarding laboratory experimental works.

Warm hearted thanks go to my brother, Asaad and Asal, and sisters Salima , Anam, Ahlam Bushra Azhar Aseel Anas, and their husbands, Haider, Ayad and Ali, Also, their son's Kahdeer, Rawan Ali, Mohamad Hassan, Ameer. Hussain, Mohamad Asaad Layan Asaad, and Ali Asaad, I appreciate their prayer, encouragements and kindness, and I ask God to bless them all.

LIST OF CONTENT

ABSTRACT ---------- **I**

ACKNOWLEDGMENTS ---------- **VIII**

TABLE OF CONTENTS ---------- ERROR! BOOKMARK NOT DEFINED.

TABLE OF FIGURES ---------- **XIII**

LIST OF TABLES ---------- **XVII**

CHAPTER 1: INTRODUCTION

1.1 Background ---------- **1**

1.2 Research motivation and problem statement ---------- **3**

1.3 Aim and Objectives ---------- **4**

1.4 Thesis overview ---------- **7**

CHAPTER 2: LITERATURE REVIEW

2.1 Summary of the chapter ---------- **9**

2.2 Hot mix asphalt ---------- **9**

2.2.1 Dense asphalt mixture ---------- **11**

2.2.2 Stone mastic asphalt mixture ---------- **12**

2.2.3 Open graded asphalt mixture ---------- **13**

2.3 Asphalt fatigue cracking phenomenon. ---------- **14**

2.4 Self –Healing Materials ---------- **20**

2.5 Introduction to asphalt self-healing ---------- **22**

2.6 Capillary flow ---------- **24**

2.7 Factors influencing Self –Healing of Bituminous Materials ---------- **28**

2.7.1 Internal Factors influencing the self-healing ---------- **28**

2.7.2 External Factors ---------- **30**

2.8 Self-Healing Techniques for Asphalt Pavements ---------- **34**

2.8.1 Induction heating of asphalt concrete ---------- **35**

2.8.2 Healing of crack by infrared heating ---------- **38**

2.8.3 Liquid-based self-healing material systems ---------- **38**

2.9 Summary of literature review ----------42

CHAPTER 3: MATERIALS AND METHODS

3.1 General ----------43

3.2 Raw materials ----------44

3.2.1 Virgin limestone aggregates ----------44

3.2.2 Bitumen ----------45

3.2.3 Self- healing additives ----------45

3.2.3.1 Conductive Particles (Steel wool fibres) ----------45

3.2.3 .2 Encapsulated healing agents ----------45

3.3 Asphalt mixture's composition ----------47

3.4 Manufacturing and geometry of test specimens ----------49

3.5 Method to quantify asphalt self-healing ----------50

3.6 Methods to induce self-healing ----------55

3.6.1 Self- healing by infra-red heating ----------55

3.6.2 Self-healing by induction heating ----------56

3.6.3 Encapsulated rejuvenators ----------58

3.7 X ray Computed Tomography (CT) Scans ----------60

3.7.1 Connectivity of pore network test ----------62

3.7.2 Use of CT scans to determine the percentage of cracks healed -------63

3.8 Bulk density and air void content ----------64

3.9 Thermal expansion test ----------65

3.10 Indirect tensile stiffness modulus (ITSM) ----------66

3.11 Fourier Transform Infrared Spectroscopy (FTIR) ----------67

3.12 Summary ----------69

CHAPTER 4: EFFECT OF ASPHALT

4.1 Introduction ----------70

4.2 Experimental summary ----------71

4.3 Results and Discussion ----------73

4.3.1 Service life of asphalt samples ----------73

4.3.2 Asphalt test sample temperatures during the heating treatment ----75

4.3.3 Service life extension by infrared heating ----------77

4.3.4 Effect of temperature on asphalt self-healing ----------83

4.3.5 Evolution of internal air voids distribution after heating ----------85

4.3.6 Thermal expansion of asphalt during the heating treatment ---------88

4.3.7 Influence of pore network connectivity on asphalt self-healing ------89

4.4 Summary of Chapter ----------91

CHAPTER 5: OPTIMUM MOMENT TO HEAL CRACKS IN ASPHALT ROADS BY MEANS ELECTROMAGNETIC

5.1 Introduction ---------- 92
5.2 Experimental program ---------- 93
5.3 Results and discussion ---------- 94
5.3.1 Fatigue durability of asphalt samples ---------- 94
5.3.2 Temperatures of asphalt test samples during the heating treatment 97
5.3.3 Effect of induction heating on the healing index. ---------- 99
5.3.4 Effect of natural healing on extension to service life. ---------- 102
5.3.5 Hypothesis for the healing mechanism of damage caused by cyclic loading ---------- 105
5.4 Summary of Chapter 5 ---------- 112
CHAPTER 6: INFLUENCE OF MIXTURE TYPE ON SELF-HEALING OF ASPHALT ENHANCED WITH CAPSULES
6.1 Introduction ---------- 113
6.2 Experimental summary ---------- 114
6.3 Results and Discussion ---------- 116
6.3.1 Density and air void properties of asphalt mixture with capsules. 116
6.3.2 Repeated loading durability of asphalt mixture with capsules. ---- 117
6.3.3 Oil released from the capsules during the repeated loading tests. - 119
6.3.4 Self-healing of crack in PA, DA, and SMA by the action of encapsulated oil ---------- 124
6.4 Summary of Chapter 6 ---------- 128
CHAPTER 7: CONCLUSIONS AND RECOMMENDATIONS
7.1 Review of Aims and Objectives ---------- 129
7.2 Conclusions of Chapter 4: "Finding of Using infrared healing to assess the porosity in fatigue damage" ---------- 131
7.3 Conclusions of Chapter 5: "Finding the optimum moment to heal asphalt roads by means electromagnetic induction" ---------- 133
7.4 Conclusions of Chapter 6: "Using capsules to induce self-healing of cracks in asphalt mixture" ---------- 135
7.5 Suggestions and recommendations for future work ---------- 137
REFERENCES ---------- 139
APPENDIX A: ---------- 5-A
APPENDIX B: ---------- 5-B
APPENDIX C: ---------- 5-E

LIST OF FIGURES

Figure 2.1: Asphalt road layers, [15] 10

Figure 2.2: Scheme of hot mix asphalt classification: (a) dense–graded mix. (b) stone mastic asphalt (c) open–graded asphalt, [19]. 11

Figure 2.3: Typical gradation curve of dense graded asphalt, [20]. 12

Figure 2.4: Typical gradation curve of stone mastic asphalt, [19]. 13

Figure 2.5: Typical gradation curve of open graded asphalt, [24]. 14

Figure 2.6: Effects of fatigue on pavement structures, after[51]. 15

Figure 2.7: Fatigue crack (author, Siham Salih). 17

Figure 2.8: Set-ups to induce fatigue loading in asphalt, [15]. 19

Figure 2.9: Self- healing of cracks by (a) melting of the the fibres, (b) breaking the brittle fibre under load, which releases healing agents,[64]. 21

Figure 2.10: Self-healing of a crack in asphalt, [66] 22

Figure 2.11: (a) No rest. (b) Vehicles passing over the pavement, after [67]. 23

Figure 2.12: Effect of rest interval, after [8]. 24

Figure 2.13: Capillary flow experiment,[139] 25

Figure 2.14: The healing mechanism diagram in bitumen,[87]. 27

Figure 2.15: The micro-damage boundary during crack growth in indirect tensile fatigue test,after [117]. 32

Figure 2.16: Components of a basic induction heating setup, [125]. 35

Figure 2.17: Concept of oil release to heal the crack though asphalt mix, after 40

Figure 2.18: A capsule broken during inderect tensile test , after [142]. 41

Figure 3.1: Steel wool fibre 46

Figure 3.2: Capsules used in the study. 47

Figure 3.3: (a) Configuration setup of Loading , (b) Scheme representation of the modified 3-point bending test used. (c) Universal machine used. 51

Figure 3.4: Criterion of failure analysis by using Image J software. 1. The sample tested after several cycles (but before failure). 2. The specimen tested until failure. 52

Figure 3.5: An example of an asphalt beam with 21% air voids content, a) the beam after three point bending fatigue test, and b) the beam processed in image J..... 53

Figure 3.6: Scheme of how the number of cycles with 50% probability of breaking can be obtained based on Weibull probability distribution. 53

Figure 3.7: Scheme of how the number of cycles and service life extension can be evaluated. 54

Figure 3.8: Infrared Heating setup..... 55

Figure 3.9: Scheme of infrared lamps setup for farm..... 56

Figure 3.10: Self-healing under induction heating..... 57

Figure 3.11: Schematic diagram of the manufacturing process of capsules by ionotropic gelation of alginate Capsule presentation, based on [140]. 60

Figure 3.12: XRadia Versa XRM-500 scanner machine in Sutton Bonington 61

Figure 3.13: The X-ray scanning (plan view) illustration after [161]..... 62

Figure 3.14: Binary 2D images of pore networks with a range of air void content and their correlation to the Euler number (χ)..... 63

Figure 3.15: Setup for thermal expansion for mixture. 65

Figure 3.16: Indirect tensile stiffness test setup..... 67

Figure 3.17: Fourier Transform Infrared device. 68

Figure 3.18: FTIR curves for asphalt mixture samples with and without oil..... 68

Figure 4.1: Experimental methodology used in Chapter 4. 72

Figure 4.2: Probability of breaking and number of cycles for a probability of 0.5. 73

Figure 4.3: Probability of breaking obtained for the studied materials with different air voids contents. 74

Figure 4.4: Evolution of temperature with the heating time for different distances between sample and lamps. 75

Figure 4.5: Steady-state temperatures reached by samples with different air voids. 76

Figure 4.6: Healing index obtained for samples with different air voids content. ... 77

Figure 4.7: Schematic simplification of obtained curves subjected to thermal heating at different numbers of cycles..... 78

Figure 4.8: Optimum number of cycles and healing index. 79

Figure 4.9: Optimum number of cycles obtained for samples with a range of air void contents. 80

Figure 4.10: Phenomena happening inside dense (top) and porous asphalt (bottom) during heating..... 83

Figure 4.11: Healing index obtained for samples with 5% air voids content that have been subjected to thermal heating at different numbers of cycles and temperatures and different distances (110cm, 70cm, and 30cm). 84

Figure 4.12: Air voids distribution for samples with 5% (a) and 21% (b) after production (new) and at the optimum number of cycles before (optimum) and after applying thermal heating (healing). 87

Figure 4.13: Thermal expansion of asphalt samples with different air voids contents and at different temperatures. 88

Figure 4.14: Euler number obtained for test samples with different air voids content. 90

Figure 5.1: Summary of the methodology used in Chapter 5. 93

Figure 5.2: Probability of breaking the test samples at the load levels studied..... 95

Figure 5.3: Wöhler curve for $N_{0.5}$ probability. 96

Figure 5.4: Infrared image of asphalt sample containing 1.1 % steel wool under induction heating. 97

Figure 5.5: Evolution of the asphalt's surface temperature over heating time. 98

Figure 5.6: Healing index versus the number of cycles (Nh) for porous asphalt with 1.1% of steel wool. 99

Figure 5.7: Healing index versus the Weibull probability for breaking the test samples. 100

Figure 5.8: Optimum number of cycles to apply healing treatment (Nh) and extra number of cycles survived after induction heating (Nt)..... 102

Figure 5.9 : Number of cycles versus healing index and probability for breaking versus number of cycles subjected to 2 kN repeated loading. 103

Figure 5.10: Healing index of beams under both- natural and induction healing ... 104

Figure 5.11: Air voids of a 0.5cm width test section (a) before testing, (b) after cyclic loading, (c) after induction heating..... 105

Figure 5.12: Change of air void content with the percentage of $N_{0.5}$. when the load is 0.5 kN..... 106

Figure 5.13: Change of air void content with the percentage of $N_{0.5}$. when the load is 0.7 kN..... 107

Figure 5.14: Change of air void size with the percentage of $N_{0.5}$. when the load is 0.5 kN..... 109

Figure 5.15: Change of air void size with the percentage of $N_{0.5}$. when the load is 0.7 kN..... 111

Figure 6.1: Summary of test programme in Chapter 6. 115

Figure 6.2: Distribution functions of the number of cycles resisted by SMA without capsules (WO) at different loading levels..... 117

Figure 6.3: Wöhler curves for dense asphalt (D), Stone Mastic Asphalt (SMA), and Porous Asphalt (PA), with (W/C) and without (WO/C) capsules. 118

Figure 6.4: Area under the FTIR curve for bitumen modified with various percentages of sunflower oil. 120

Figure 6.5: Oil released from the capsules embedded in SMA. 121

Figure 6.6: Oil released from the capsules embedded in SMA beams versus the probability of breaking the beams. 122

Figure 6.7: Oil released from the capsules embedded in PA, SMA, and DA subjected to 2 kN repeated loading 123

Figure 6.8: Healing index vs number of loading cycles for SMA without capsules. 124

Figure 6.9: Healing index vs probability of cracking for SMA without capsules. . 125

Figure 6.10: Healing index of all the types of asphalt studied at 2kN. 126

Figure 6.11: Average probability for breaking the asphalt test samples at the highest heading index. 127

Figure B.1: a Fibre steel, -(a)- distributes steel fibres in sample, (b)- dimeter of steel fibre, in CT scan image 5-B

Figure B.2: Manufacturing of Hot Mix Asphalt 5-B

Figure B.3: Asphalt mixture slabs produced beams and cylinders. 5-C

Figure B.4: a)Example for samples (a)white marking spray paint, (b) Samples before and after testing. 5-C

Figure B.5: Asphalt mixture beams for CTscan test for Chapter 5. ..... 5-D

Figure B.6: Average values of the stiffness modulus of PA specimens with (W/SF), and without (WO/SF), relationship between stiffness modulus of the PA specimens measured in longitudinal (Y) and cross (X) directions. 5-D

Figure C.1: Distribution functions of the number of cycles resisted by PA without capsules (WO) at different loading levels. (b), and Porous Asphalt (PA), with (W/C) capsules. 5-E

Figure C.2: Distribution functions of the number of cycles resisted by DA without capsules (WO) at different loading levels. (b), and Porous Asphalt (DA), with (W/C) capsules 5-E

Figure C.3: Distribution functions of the number of cycles resisted by SMA without capsules (WO) at different loading levels. (b), and Ston Mastic Asphalt (SMA), with (W/C) capsules. 5-F

Figure C.4: Healing index vs number of loading cycles for, (a) SMA without capsules,(b) SMA with capsules 5-F

Figure C.5: Healing index vs number of loading cycles for(a) PA without capsules, (b)PA with capsules. 5-G

Figure C.6: Healing index vs number of loading cycles for(a) DA without capsules, (b)DA with capsules. 5-G

Figure C.7: Healing index vs probability of cracking for, (a) SMA without capsules, (b)SMA with capsule. 5-H

Figure C.8: Healing index vs probability of cracking for, (a) PA without capsules, (b)PA with capsule. 5-H

Figure C.9: Healing index vs probability of cracking for, (a) DA without capsules, (b)DA with capsule. 5-I

LIST OF TABLES

Table 2.1: Summary of factors influencing the self-healing of asphalt. 34

Table 3.1: Summary of materials and experiments. 43

Table 3.2: Aggregate size distributions used. 44

Table 3.3: Additives to promote theself-healing used intheThesisand mass percentage intheasphalts (thecomposition of the asphalts can be found in Section(3.3).. 45

Table 3.4: Composition of the asphalts used in the Thesis. 48

Table 3.5: ITSM test configuration depending on [153]..... 66

Table 4.1: Comparison between thenumbers of cyclesresisted by test samples without thermal treatment($N_{0.5}$)and total numberof cycles resisted by test samples after applying a thermal treatment. 80

Table 5.1: Number of Cycles ($N_{0.5}$) with different loads applied. 96

Table 5.2: $N_{0.5}$ cycles for different Load..... 101

Table 5.3: Stiffness Modulus (SM) before and after induction heating 108

Table A.1: Asphalt maintenance techniques [60]. 5-A

LIST OFABBREVIATIONS AND NOTATIONS

HMA	Hot Mix asphalt
SMA	Stone Mastic Asphalt
DA	Dense Asphalt
PA	Porous Asphalt
N_f	Sum number of load repetitions
N_i	Number of load repetitions for crack initiation
N_p	Number of load repetitions for Macro crack
FTIR	Fourier Transform Infrared spectrometry
DSR	Dynamic Shear Rheometer
Ifs	Internal Factors of self-healing
MMHC	Methyl plus methylene hydrogen to carbon
NMR	Nuclear Magnetic Resonance
VFB	Voids filled with bitumen
VA	The volume of air voids
VMA	Voids in Mineral Aggregate
SBR	Styrene-Butadiene Rubber
GIL	Gilsonite
IDT	Indirect Tensile Test
ASTM	American Society of Testing and Materials
CaCl2	Calcium chloride
C6H7O6Na	Sodium alginate
CT-Scans	Computed tomography scans

BSI	British Standard Institution
HI	Healing Index
LVDT	Linear Variable Differential Transformer
AVC	Air Void Content
N_{opt}	Optimum number of cycles
T	temperature
d	distance from the centre of the coil
N_h	Optimum number of cycles to apply healing treatment
BD	Bulk Density
W/C	with capsules
WO/C	without capsules
kN	Kilo Newton
kHz	Kilo hertze
kW	Kilo watt
G*	dynamic shear modulus
ρ_m	maximum density
ρ_b	bulk density

Chapter 1: Introduction

1.1 Background

Asphalt is a self-healing material; when a crack opens in it, bitumen can flow into and repair the crack. This may lead to reduced maintenance, extend service life and decrease gas emissions [1]. According to reference [2], promoting the self-healing of asphalt is the best way to improve the economic and environment sustainability of roads.

The service life of an asphalt road is often approximately 20 years [3]. It deteriorates because of the action of the environment (ageing, water ingress) and heavy traffic loading. According to [4], to preserve the properties of asphalt until the end of the service life of the roads, it should be maintained and repaired regularly. An example of a maintenance technique for roads is crack sealing, which is used to repair cracks, preventing further deterioration. Appendix A lists a fuller set of treatment.

A limitation is that the normal use of the pavement is interrupted for the duration of the repair. For this reason, the development of road maintenance techniques that do not reduce the functionality of roads is required.

One of the most common failure mechanisms in asphalt pavements is fatigue damage, which is defined as damage and deterioration of the structural capacity of a road, generated by a series of repetitive loads. This damage can be affected by different factors such as loading type, [5], loading frequency, [[6] , [7]], working temperature, [[8] ,[9]] and bitumen content in the mixture, [10].

According to reference [11], air void content is the main factor affecting the fatigue durability of roads. These authors show that the air void content should be no more than 3% to produce pavements with excellent strength, service fatigue life, durability, and resistance to ravelling, rutting and moisture damage; however , according to reference [3], lower air void content could lead to bleeding of asphalt mixture.

According to reference [4] asphalt is as a self-healing material. Self-healing means that when cracks appear in the road, they can automatically disappear. This happens if the viscosity of bitumen is low enough and the cracks have enough time to close [2]. Since the viscosity of bitumen is temperature dependant, temperature is one of the factors that most affects self-healing.

This thesis focuses on self-healing of asphalt. Since, asphalt is self-healing material, it means that when the crack appears it automatically starts to disappear. In this thesis, different methods will be used to examine this phenomenon; firstly, by using infrared heating to mimic solar energy; secondly induction heating to accelerate self-healing; and thirdly, encapsulated healing agents to restore aged bitumen.

These methods have been carried out in three hot mix asphalt types, namely dense asphalt, porous asphalt and stone mastic asphalt, because these are commonly used to construct roads throughout the world.

1.2 Research motivation and problem statement

Asphalt mixtures are the main material used in the construction of roads across the world; they consist of a mixture of aggregates and bitumen, [10]. The aggregates give structural strength to the material, enabling it to resist the different traffic loads exerted on the roads. Bitumen is a liquid with temperature-dependant viscosity that keeps the aggregates together.

The durability of asphalt roads is between 15-20 years [12]. However, this durability can be enhanced due to the material's self-healing nature, caused by the bitumen's ability to flow and drain between the aggregates. If the viscosity is too high, for example, at low temperatures, bitumen does not flow in the cracks. Therefore, lower viscosity will accelerate the self-healing of cracks. Because of the high viscosity of bitumen, the self-healing process can be very slow and cracks or potholes may develop faster than they heal [2].

On the other hand, on sunny days the black colour of asphalt enables the material to absorb a lot of solar energy. Consequently, the temperature of the asphalt increases, and the viscosity of bitumen reduces. Thus, if a crack appears, it can be repaired automatically as low viscosity bitumen will flow into the crack and seal it. Furthermore, in very warm weather asphalt can begin to age and bitumen becomes stiffer, hence reducing its ability to heal well.

To accelerate the self-healing, researchers have carried out investigations to develop techniques that can artificially reduce the viscosity of bitumen. These include infrared heating, induction heating, and capsules containing rejuvenators, all of which will be evaluated in this Thesis.

Infrared heating is a technology that is widely used to repair roads [11]. It increases the surface temperature of asphalt by using infrared lights as a heating source. The heat is simply conducted to the bottom layers of the road.

Induction heating consists of mixing steel or other metals with excellent electrical or magnetic properties into the asphalt mixture. These conductive metal particles can be heated up using an electromagnetic field, which reduces the viscosity of bitumen and promotes its flow into the cracks. The dimensions of metal particles are typically less than 1 mm in length and diameter [11].

The third method utilizes encapsulated oil, which is a good bitumen solvent. The capsules are mixed into the asphalt mixture and typically have a diameter between one and three millimetres. When a crack occurs, the capsule breaks and will release the oil, which diffuses into the bitumen. Subsequently, the bitumen viscosity may reduce, drain and fill the crack [12].

1.3 Aim and Objectives

Considering the statements above the overarching theme, is that this work concerns the subject of the self-healing phenomenon and how can be integrated through the use of different asphalt mixtures. The project aim is now stated regarding this:

- To investigate the optimum moment in the life of an asphalt, where a self-healing technique can be applied, and the self-healing is maximised. Three different self-healing techniques will be investigated, namely infrared heating, induction heating, and encapsulated healing agents.

- To investigate differences in the self-healing performance of asphalt using infrared, induction heating, and encapsulated rejuvenators to accelerate the self-healing.
- To investigate differences in the self-healing performance in different types of asphalt.
- To give an insight into the asphalt properties that most affect the self-healing.

In order to given specific objectives of this study, but are not limited to the following:

- **Effect of porosity on infrared healing of fatigue damage in asphalt**

The main objective is to understand the effect of air void content on the healing capacity of asphalt mixtures. Since this is a fundamental study it was decided that natural, i.e. infra-red, heating was appropriate. The factors analysed in this study are (i) the extension of fatigue life, (ii) the optimum number of cycles at which to apply the thermal treatment, (iii) the evolution of internal pore structure during both cracking and healing processes, (iv) and finally, material thermal expansion.

- **Optimum moment to heal cracks in asphalt roads by means of electromagnetic induction**

The aim of this objective is to provide an indication of the best moment to heal an asphalt road in order to repair cracks, something which has not been tested before.
In order to accelerate the self-healing, electrically conductive will be added to the

asphalt, the advantage of electrically conductive asphalt is that it can be heated using induction energy [2], which may lead to reduce the crack in roads[7], which will be subjected to mechanical damage and, once it is cracked, heated by applying an alternating electromagnetic field. In addition, in order to understand the optimum time to apply the induction heating treatment and its effect on the material's properties, fatigue tests have been carried out at different loading levels.

- **Influence of aggregate gradation on self-healing of asphalt enhanced with capsules**

This objective aims to evaluate the effectiveness of using encapsulated oil in order to improve the self-healing properties of asphalt mixture with a range of gradations, namely dense asphalt, porous asphalt, and stone mastic asphalt. It includes measurement of the rate at which the oil is released from the capsules during fatigue cracking, and the improvement of the self-healing. Furthermore, changes in the air void structure due to cyclic loading and self-healing have been analysed and it has been found that the gradation of asphalt is a critical parameter that influences the release of oil from the capsules and therefor the self-healing properties of asphalt.

From the conclusions in the first objective, where in the first objective, it has been found that porous asphalt shows a higher healing ability compared to denser mixtures when infrared heating was used. Therefore, porous asphalt was used in the second objective to evaluate the influence of induction heating to accelerate self-healing. However, in the third objective three different mixtures were used namely, dense, porous and stone mastic asphalt, all these materials were used to evaluate the influence of capsules into the asphalt self-healing.

1.4 Thesis overview

This thesis is arranged into seven chapters; the organization of the thesis is as follows:

Chapter 1. Introduction: This chapter includes the background of the research project, its motivation and the aims and objectives.

Chapter 2. Literature Review: This chapter explains the fundamental principles and techniques relevant to this Thesis. These include types of hot mix asphalt, asphalt fatigue cracking, the self-healing phenomenon, and the methods to improve the self-healing artificially. In addition, in order to discover the research needs in the field of asphalt self-healing, a critical evaluation of previous studies related to the self-healing phenomenon has been made.

Chapter 3. Materials and Methods: This chapter summarizes the methodology followed to accomplish the objectives of this research project. It also explains the characterization of the different materials used. In addition, the materials that were used to promote the self-healing, such as steel fibres and encapsulated oil.

Chapter 4. Effect of porosity on infrared healing: This chapter presents the experimental results of self-healing promoted by infrared heating. Furthermore, this chapter shows the effect of thermal expansion on self-healing.

Chapter 5. Optimum moment to heal cracks by means of electromagnetic induction: This chapter presents the effect of using induction-heating to repair cracks in porous asphalt. Porous asphalt has been used rather than other types of asphalt, because in the previous chapter it was found that this is the material has excellent self-healing

properties. The chapter provides an indication of the best moment to heat an asphalt road in order to repair crack.

Chapter 6. Influence of aggregate gradation on self-healing of asphalt enhanced with capsules: This chapter presents the effect of adding capsules on the self-healing of asphalt mixtures with a range of aggregate gradations, namely dense asphalt, porous asphalt, and stone mastic asphalt, which are the most commonly used asphalt types worldwide. Furthermore, the effect of cyclic loading on the air void structure of these mixtures has been analysed.

Chapter 7. Conclusions and Recommendations: This chapter gives a reflective comment on the various aspects of the project. The aims and objectives are restated, summarising how each was achieved, to what level of success and what could be done in the future to improve results. These leads to a list of recommendations for future work.

Chapter 2: Literature review

2.1 Summary of the chapter

The goal of this chapter is to examine the published literature concerning the asphalt self- healing phenomenon, in order to identify the current gaps that must be researched. The chapter includes definition of the most commonly used types of asphalt, its damage mechanisms, the self-healing properties, and techniques to improve the self-healing. Finally, a critical evaluation is made in order to find the limitations that need to be overcome on this topic.

2.2 Hot mix asphalt

An asphalt mixture is composed of aggregates and bitumen. In order to manufacture hot mix asphalt, aggregates must be first heated above 100 ^{o}C to evaporate the moisture, and the mixture of bitumen and aggregates can be made at temperatures ranging from 140 ^{o}C to 180 ^{o}C. Hot mix asphalt is used in the construction of roads due to qualities such as; durability, high resilience and waterproofing and it is used to protect the foundations of a road from the direct action of traffic due to its superior stiffness [13]. A pavement which includes hot mix asphalt, is composed of layers made of different materials, see Figure 2.1. The higher quality materials are closer to the surface [14] and are designed to achieve the required skid resistance [15].

The failures that occur in roads depend mainly on the load that is carried and the behaviour mechanisms by which stress is transferred between the particles of aggregate [16].

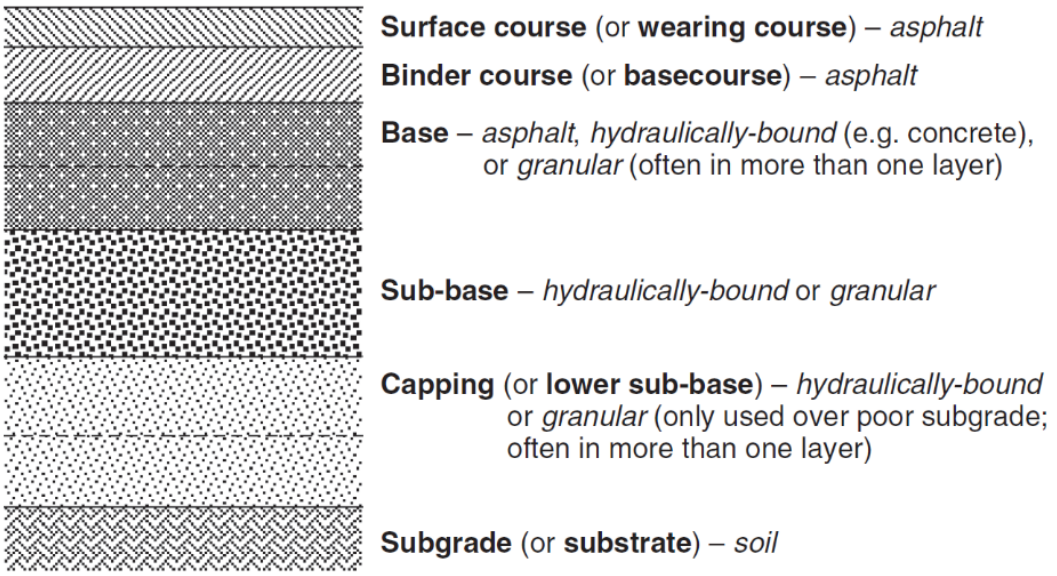


Figure 2.1: Asphalt road layers, [15]

The properties of the components of hot mix asphalt such as bitumen, aggregate and additives affect the performance of this mixture, in addition to the proportion of these components in the mixture. The additives may be polymers, latex or fibres [17].

There are three main types of hot mix asphalt, depending on the purpose and gradation, namely, dense-graded, stone mastic asphalt and open-graded asphalt, see Figure 2.2.

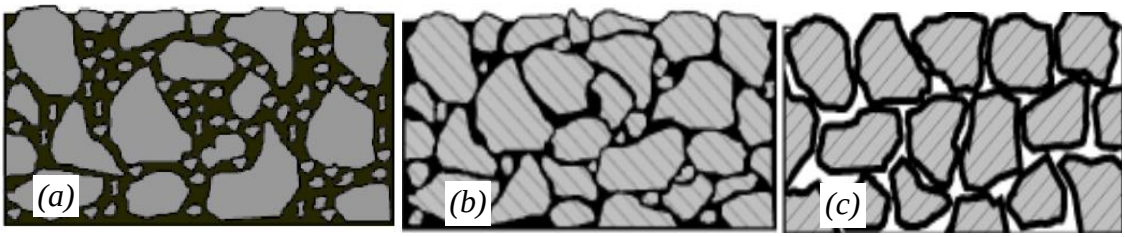


Figure 2.2 : Scheme of hot mix asphalt classification: (a) dense–graded mix. (b) stone mastic asphalt (c) open–graded asphalt, [19].

2.2.1 **Dense asphalt mixture**

Dense asphalt mixture is the material most commonly used worldwide to build road surfaces. This mixture is well-graded, which means that the aggregate gradation is designed to reach the highest aggregate density. It provides excellent resistance to water penetration from the surface [20]. Dense mixtures contain fine and coarse aggregates and, typical maximum nominal particle sizes of aggregates are 4.75 mm, 9.5 mm, 12.5 mm, 19.0 mm and 25.0mm. Furthermore, typical aggregate and binder contents in dense graded mixtures are approximately 95% and 5%, respectively, of the total weight of the mixture. See Figure 2.3 for an example [21].

An advantage of dense asphalt mixture is that its low air void content, typically between 3% and 8% [23], inhibits the entry of water into the pavement, which may be one of the main factors affecting the durability of the road, causing dislodging of aggregates and bitumen loss [23]. In order to ensure mixture workability, the denser the mix, the higher its resulting strength will be, and the strength is a significant property of the mixture. The strength is achieved by using a broad range of particle sizes; usually the maximum size is 40 mm or less, however, it should be no more than 30% of the layer thickness [15].

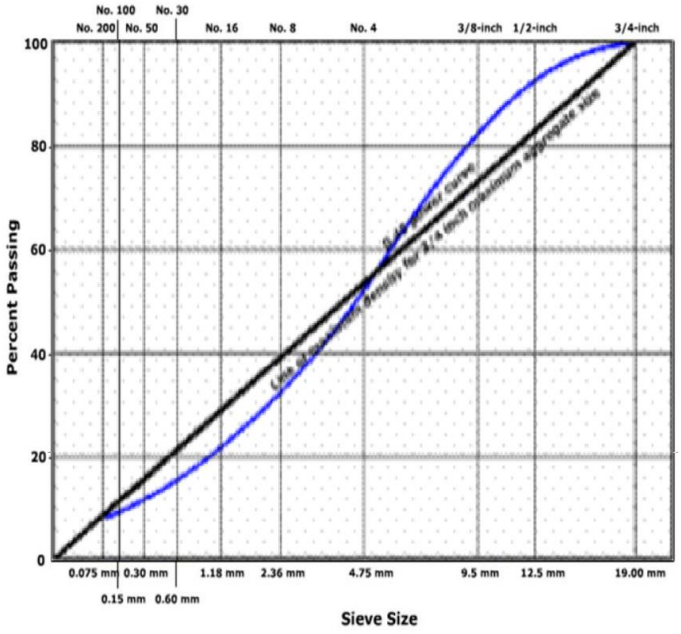


Figure 2.3: Typical gradation curve of dense graded asphalt, [20].

2.2.2 **Stone mastic asphalt mixture**

Stone mastic asphalt is a gap-graded mixture [25], in which intermediate sizes of aggregates are missing, in order to create a strong skeleton of stone and to allow space for the fine aggregate and bitumen [26].This mixture became widely used in USA, Asia, South Africa and Australia to construction the roads in high traffic loading [27],[28],[33].This mixture is used because it is more stable [29], sturdier, and shows improved fatigue behaviour, tensile strength [30], reflection crack and rutting resistance when compared to dense asphalt mixture [31], as well as higher resistance to thermal and cracking [32]. The strength of stone mastic asphalt is given by the coarse aggregate-to coarse aggregate interaction. The gradation of SMA is gap graded, where the mastic is fill of voids rather than air [33]. The rich bitumen content provides high durability, however, create a strong skeleton of stone gives a deformation resistant surface [34]. See Figure 2.4 for an example of the aggregate gradation.

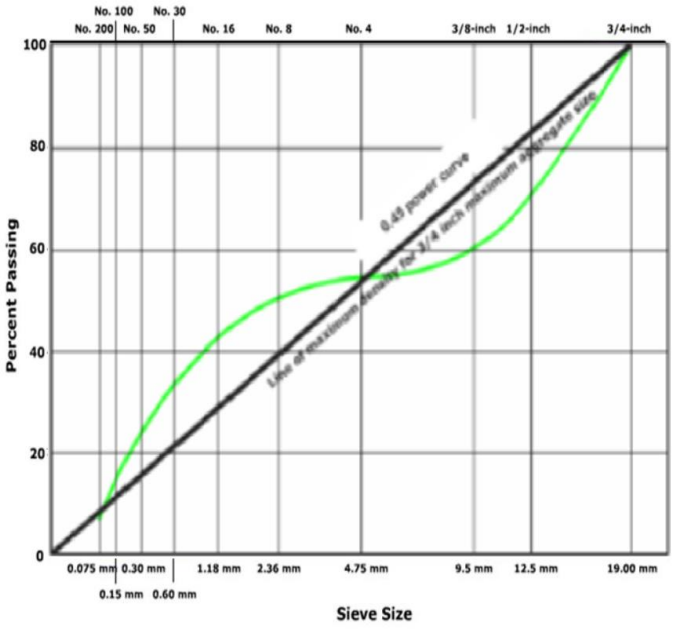


Figure 2.4: Typical gradation curve of stone mastic asphalt, [19].

2.2.3 **Open graded asphalt mixture**

Open-graded asphalt is a mix that is designed to be permeable to water[35]. It is designed with a high air voids content in excess of 20% [36] by mixing crushed rock and a percentage of fine particles [37]. This material has very good friction at high speeds, reduces spray and may also reduce noise of traffic [39]. The FHWA (Federal Highway Administration) [38] reported that 1.25 of the 5.8 million vehicle crashes per year in the United States are weather-related. One of the ways used to solve this issue is selecting paving materials to decrease the potential for hydroplaning while providing a long-term performance, and open- graded asphalts allow this problems include the fact that the pores in this asphalt tend to clog [40] and that it has lower durability than dense asphalt or stone mastic asphalt .Finally, porous asphalt is more expensive per cubic meter than dense asphalt mixture, but the unit weight of the mixture when

in-place is lower, which partially offsets the higher per-ton cost [41]. Figure 2.5 shows a gradation curve for open graded asphalt.

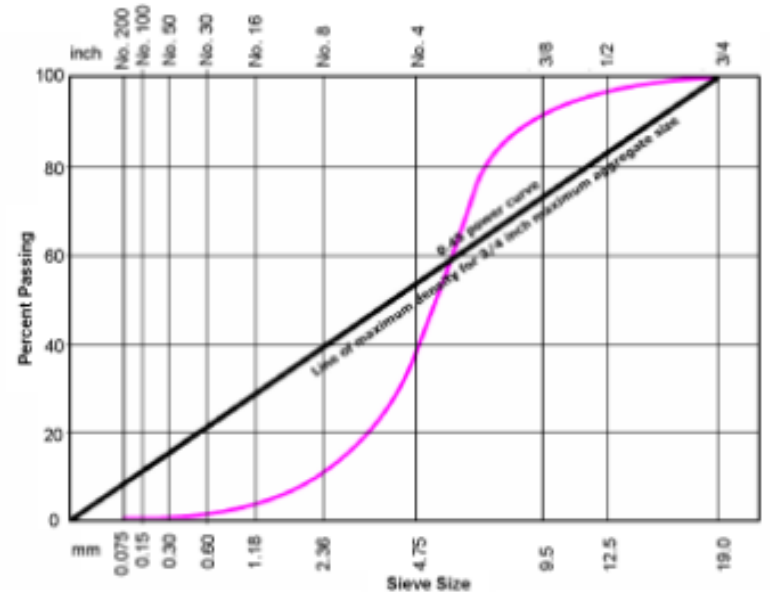


Figure 2.5: Typical gradation curve of open graded asphalt, [24].

2.3 Asphalt fatigue cracking phenomenon.

This review will now move to the fatigue characteristics of asphalt. Fatigue cracking is one of the most common failure mechanisms in asphalt roads. In flexible pavement, fatigue is produced by repeated heavy axles loads, causing the layer of asphalt to flex, as shown in Figure 2.6. Cracking is produced of the repeating by horizontal tensile stresses and strains which are induced by the repeated cyclic loading and unloading action [42]. Fatigue failure happens when the number of cumulative loading cycles exceeds the fatigue capacity. Fatigue cracking is often first visible as a fine a longitudinal crack in the wheel path [43].

From the asphalt pavements agencies , fatigue cracking is illustrated as an accumulation of damage and deterioration of structural capacity produced by a series of repeated loads [15] defining damage as decrease in stiffness of the pavement structure under repeating loading.

Fatigue cracking is one of the major distress modes of asphalt pavements. Basically, the study of asphalt materials fatigue has been made analyzing their fatigue laws. These fatigue laws are obtained by mathematical relationships between the imposed strain and the number of cycles needed to fatigue the mixture. Usually, laboratory tests were used to find fatigue laws.

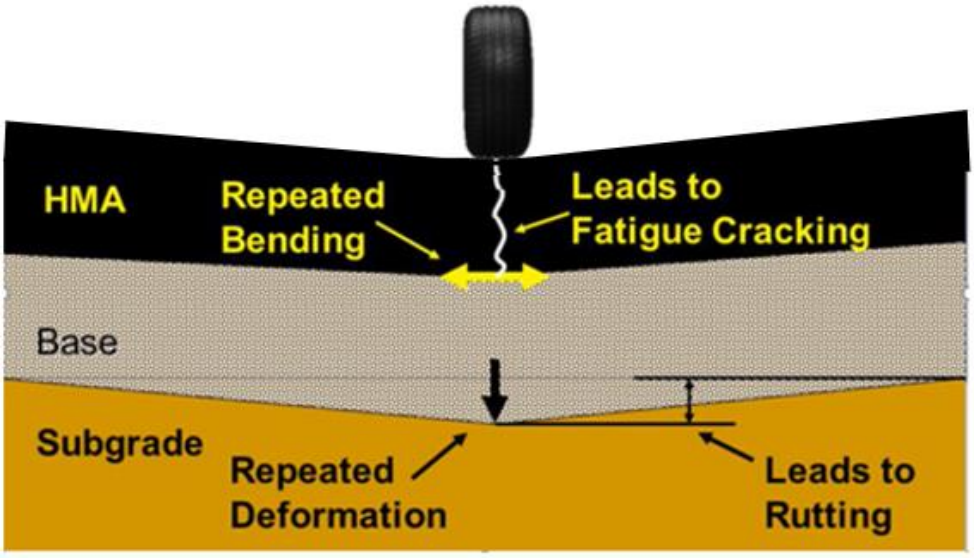


Figure 2.6: Effects of fatigue on pavement structures, after[51].

Van Dijk [46] stated that that fatigue-cracking development is a three-stage process; The first stage is the crack initiation stage that produces hairline cracks. This is only a

small portion of the fatigue life. In the second stage, hairline cracks widen and a network of cracks form which propagate because of tensile strain. The number of load repetitions required to reach this stage is 4 times larger than that required to reach the first stage. Finally Stage three is where real cracks are formed. The number of load repetitions required to reach this final stage is more than 20 times larger than that required to reach the first stage. Apart from traffic loading and temperature variation, fatigue life of a pavement can be affected by mode of loading, loading pattern and mixture variables. [48].

The asphalt mixtures have complex behaviour, their response depends on temperature[44], degree of humidity, speed of load application, and stress level, inter alia. Thus, researchers sought to reproduce highway conditions in the laboratory, as far as this is possible. However, due to the substantial difficulty of this task, conditions which are impossible or difficult to reproduce are simplified[45] .

The mode of loading could be either stress controlled, or strain controlled [48]. In the controlled stress mode of loading, the stress is held constant and the strain gradually increases as the specimen is damaged until failure. In the controlled strain mode of loading, the strain is held constant and the stress gradually decreases as the specimen is damaged. It is important in the design process to consider fatigue characteristics over a range of traffic and environmental conditions to ensure adequate pavement service life. n [49],[50].



Figure 2.7: Fatigue crack (author, Siham Salih).

When a tensile strain exists, a crack can happen anywhere [54], an example of fatigue crack in Nottingham city see Figure 2.7. Three areas are distinguished such as Firstly, under a load in the lower part of pavement layers. Secondly, in the tire tread of the contact surface area and Finally, on the surface on the edges of the load part.

The phenomenon of fatigue in asphalt mixtures is evaluated by using methods such as the bending beam fatigue test and the indirect tensile test. In beam tests, a simple beam is used with a third point or centre point loading. In an indirect tensile test, the repeated load is applied, as shown in Figure 2.8.

Figure 2.8 illustrates the direction of the applied loading which causes fatigue failure in each type of test. There are many advantages and disadvantages to each test. The methods assess fundamental properties of fatigue test in varying apparatus types. Variables are:

- The configuration of loading,
- Stress distribution,
- Loading wave form, and.
- Loading frequency,

Zeiada [18]. and Pell [52] stated that field stresses are three-dimensional, and tri-axial loading best replicates these stresses.

Furthermore, due to the specimen's trapezoid shape in the two point-loading, therefore, is considered advantageous because it does not induce a stress concentration at the point of loading. Meanwhile, Hung,[53] recommended using the four-point loading and the three-point loading because the middle third part of the specimen has a constant bending moment.

For this reason, the specimen will fail at any weak spot that there may be in the material due to non-uniformity. Since, asphalt is considered a non-homogeneous material, the results of this type of testing tend to be more consistent [53].Previous researchers have specified that failure in a fatigue test occurs when the sample is broken into two pieces and has collapsed at the end of the test due to tensile strains [55].

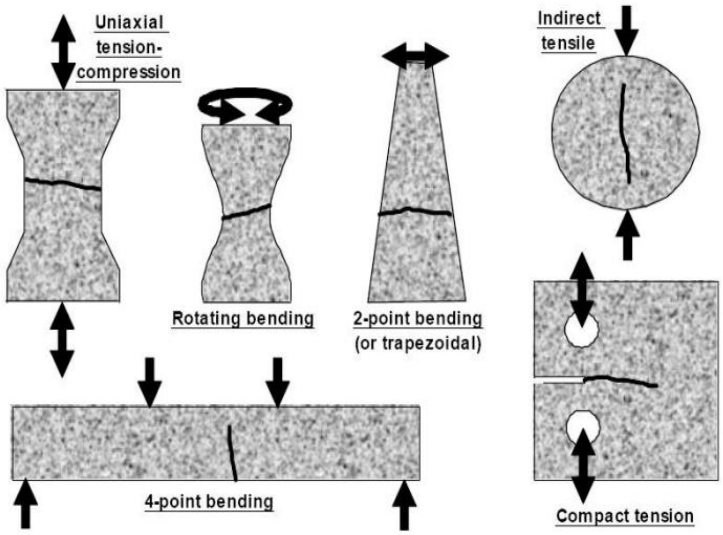


Figure 2.8: Set-ups to induce fatigue loading in asphalt, [15].

- **Fatigue failure mechanism**

According to Thom, [15] there are two mechanisms that lead to deformation of the asphalt's aggregate skeleton under strain (i) compression at particle contacts and (ii) inter-particle slip, combined with particle rotation and separation. This process leads to gradual weakening of the structure and causes fracture.

According to Little [57], fatigue is a two-stage process, (i) micro-crack growth and healing and (ii) macro-crack growth and healing. The growth of micro-cracks leads to a series of macro-cracks [58]. The mechanism of fracture also depends on rest periods between the loads and temperature, the critical situation being when there is a decrease in temperature, because the binder stiffens, and with reduced rest periods, because the self-healing is reduced.

The inter-particle movement is restricted when the binder is stiffer, which will lead to an increase of stress in the bitumen, which may increase the cracking probability [15]. With high temperatures, the stress is decreased in the binder, and the phenomenon of healing can occur, where the viscosity of bitumen decreases and it flows into the fractures [[59],[60]].

In addition, rest periods (periods without loading) and higher temperatures promote healing of the fracture areas due to the decrease of bitumen's viscosity. So far, there is no model of pavement degradation that incorporates the self-healing, partly because the phenomenon is not well understood.

2.4 Self –Healing Materials

Self-healing has been recognized for many years by pavement engineers, and researchers have detected the great healing potential of asphalt. Researchers have suggested various novel methods to make and develop the capability of self-healing in asphalt mixture, and therefore, to increase the service life of asphalt roads [60]. Asphalt is generally a required material in roads engineering. However, after many years of service, asphalt pavements become damaged under cyclic vehicle loading.

With time, asphalt binder becomes brittle due to ageing and environmental effects, and as a result, the micro-cracks start and then grows to a larger size which increases the damaging process and finally leads to distresses types such as ravelling, potholes and cracking. Bazin [62], stated that the temperature was related with the healing phenomenon in asphalt mix after loadings. Since then, the healing phenomenon in bitumen has drawn the attention of several researchers.

- **Concept of asphalt self-healing**

Self-healing is known as the capability of a material to automatically heal (repair) the cracking happening through its service life [[59],[63]]. The first attempt to design an artificial self-healing composite was done in 1994 by Dry [64], see Figure 2.9. Two approaches were tested. In the first approach, see Figure 2.9 (a), a fibre filled with methyl methacrylate was placed inside a hard, polymeric matrix. When a crack appeared in the matrix, heat was applied, which melted the wax and released the methyl methacrylate into the crack. Heat also helped the methyl methacrylate to polymerize and close the crack.

In the second approach, see Figure 2.9 (b), a brittle fibre, filled with glue, with the shell made of glass was used. When a crack appeared the fibre broke, released the glue, which filled the crack.

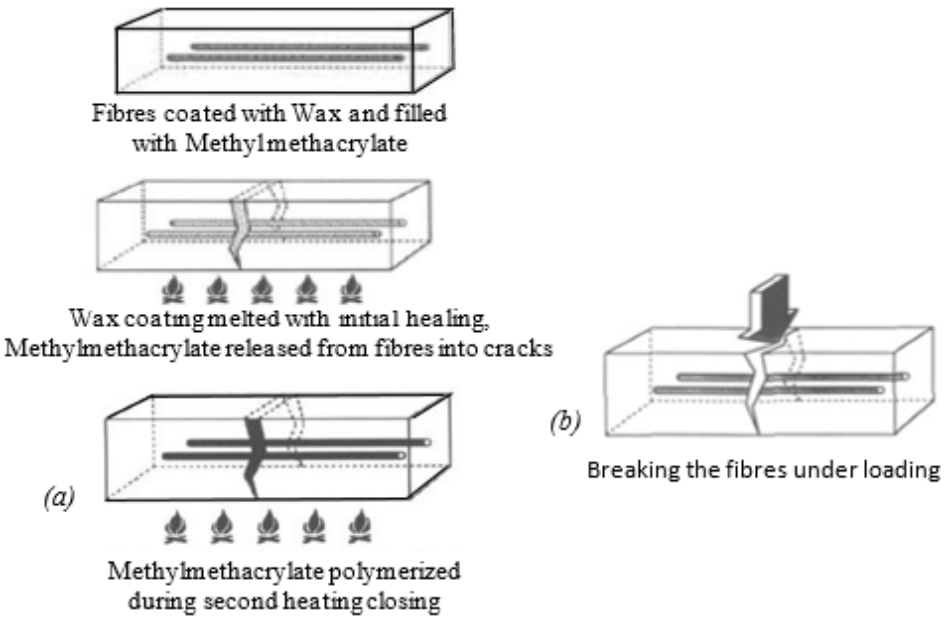


Figure 2.9: Self- healing of cracks by (a) melting of the the fibres, (b) breaking the brittle fibre under load, which releases healing agents,[64].

2.5 Introduction to asphalt self-healing

Asphalt mixture is a self-healing material, since it can repair its cracks autonomously and recover its stiffness and strength when it is subjected to rest periods [65]. The self-healing ability of asphalt mixtures has been noted both in laboratory tests and in the field since the 1960s [[63],[64]]. See Figure 2.10 for an example of self-healing of cracks in asphalt.

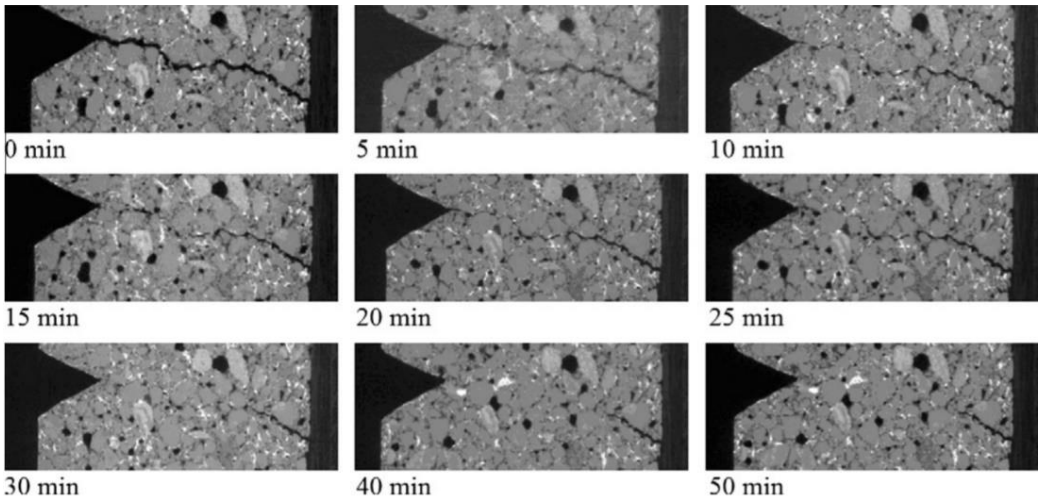


Figure 2.10: Self-healing of a crack in asphalt, [66].

Usually, the analysis of fatigue in asphalt is carried out by means of fatigue laws which are represented mathematically by the relationship between stress or strain and the number of load cycles [65] The fatigue laws are obtained from experimental studies in the laboratory, usually with a dynamic test with loading cycles which are repeated continuously without any rest period of zero loads as seen in Figure 2.11 (a).

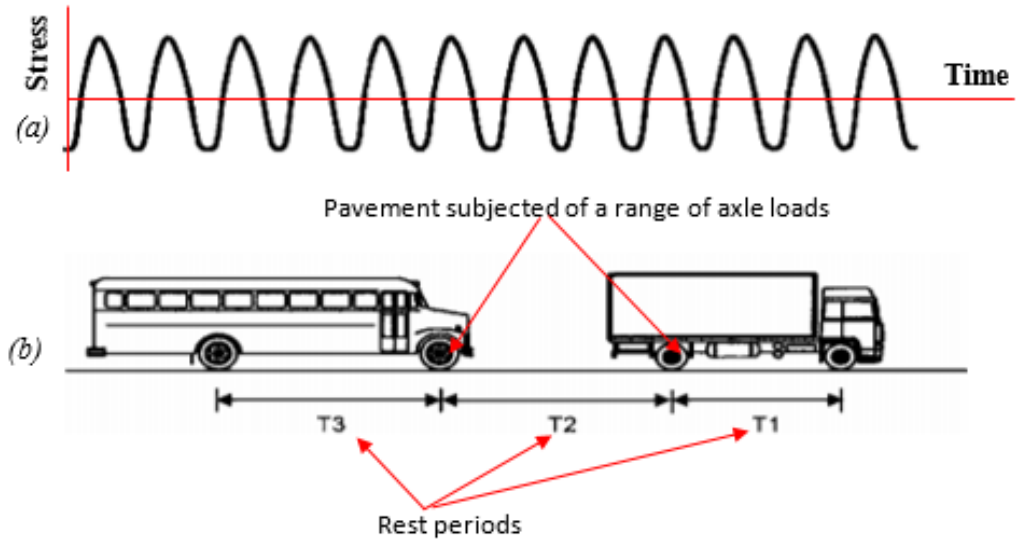


Figure 2.11: (a) No rest. (b) Vehicles passing over the pavement, after [67].

In contrast, Figure 2.11 (b) shows the pavement which is exposed to loads with rest periods and related to the time that passes between two sequential axles of the same of vehicles or the time between vehicles [67].

Figure 2.12 shows that the modulus value during a fatigue test is reduced according to the curve ABD, if a rest period is inserted into the test, author showed that a restoration of modulus occurs (AM=C-B), implying that mixture healing has taken place during the rest period [[67],[68]].

After a rest period, Castro [67] explained that the modulus would follow the curve (CE), which implies that an additional number of cycles $\Delta N = F-B$ has been added to the material's life After F, the shape of the curve is almost parallel to that obtained without rest periods as shown in Figure 2.12.

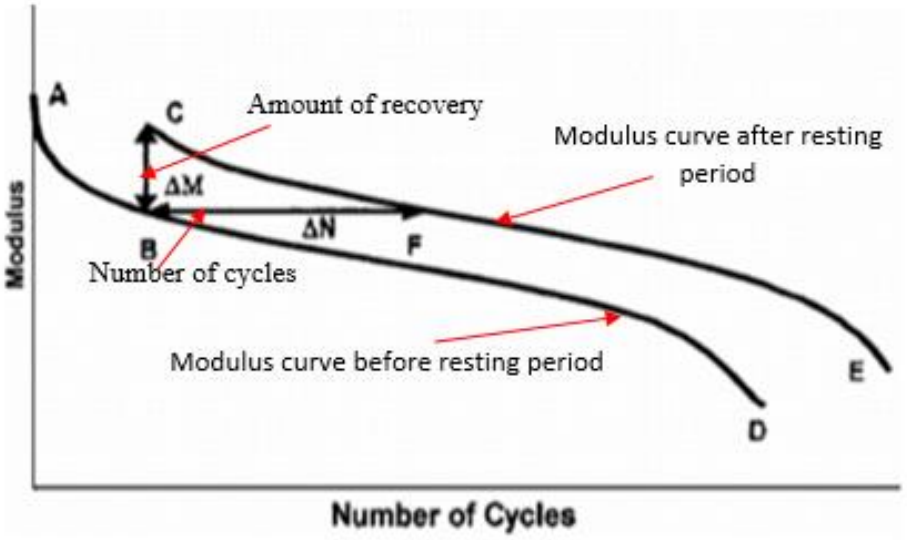


Figure 2.12: Effect of rest interval, after [8].

According to Bazin [62] asphalt concrete beams at a temperature of 25 ºC would recover 90% of their original resistance when left to rest under pressure, after testing to failure under uniaxial tensile loads.

2.6 Capillary flow

Capillary flow of bitumen can be considered a key factor influencing asphalt self-healing [69] see Figure 2.13. The reason is because bitumen may behave like a Newtonian fluid at temperatures ranging from 30ºC to 70ºC when the temperature is high enough [70]; viscosity starts to reduce at the higher temperatures, leading to the closing of cracks in the asphalt, through a sort of capillary flow [71].

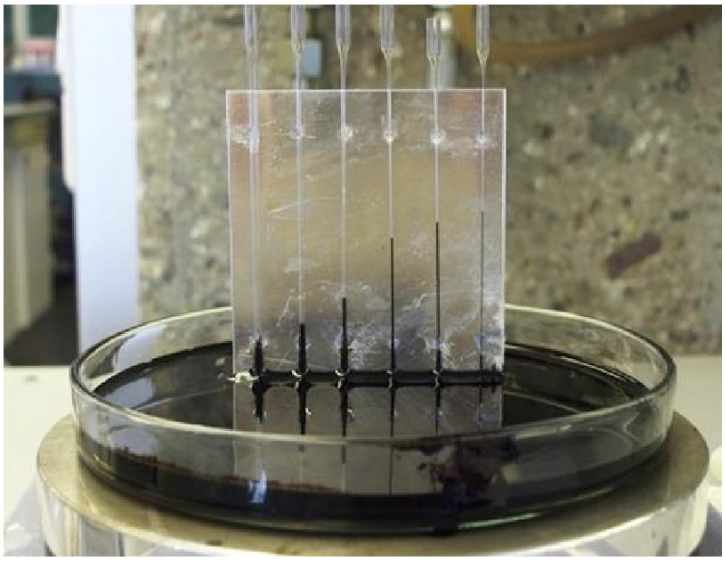


Figure 2.13: Capillary flow experiment,[139]

This contributes to the flow of bitumen through the cracks by the effect of surface tension and gravity [72]. Since gravity is a very important parameter influencing the self-healing of asphalt, the capillary flow of bitumen improves and the healing is faster when the cracks are deeper within the pavement [72].

Furthermore, the viscosity of bitumen decreases with the increase of temperature, which may lead to an increased rate of capillary flow [73]. According to [74] the softening point of bitumen can be used as an ideal healing temperature for base asphalt binders.

- **Explanation of self –healing of asphalt mixes**

Healing is the phenomenon that occurs within an asphalt mix to recover its stiffness and strength by closing internal cracks. The mechanism of healing for asphalt mixtures has been reported by many researchers [[75]- [77]]. In general, it is believed that there

is a relation between healing and the sol-gel properties of bitumen [77]. Bitumen is considered as a binder (colloidal) system, including high molecular weight asphaltenes micelles scattered or resolved in the lower molecular weight oily melting bitumen [[78],[75]]. In the sol-gel bitumen system, the conversion occurs reversibly from sol to gel or gel to sol due to the changing of temperatures or stresses [80].

At high temperatures, the structure of bitumen transforms from sol to gel, and the healing may take place Bonemazz [81]. If there is enough time, the cracks can be filled, and the self-healing completed. However, at low temperature, recovery would only be partial, because rest periods do not allow the healing of the structural damage growth caused by the loading cycle [82]. Also Garcia [83], stated that the viscosity of bitumen plays a vital role in the ability of self-healing to stop the progress of cracks and restore the asphalt properties. Increasing temperature leads to high workability and recovery of properties [84]. Furthermore, Garcia, [71] stated that self-healing could be artificially induced by increasing the temperature of the road. Consequently, the self-healing of asphalt can be induced by temperature increases [72].

Furthermore, Garcia [83] found that rest periods during cyclic loading improved the self-healing, since this led to increased bitumen flow. For example, Norambuena [85] had resting periods in the middle of the tests. Their results showed that there was an extension in fatigue life by more than 100%. These conditions are unlikely to apply to a real pavement because there will not be enough time for such rest periods.

The fatigue and healing process for cracks are summarised in Figure 2.14, which shows that the mechanism of failure and healing is a three steps process. The first step of crack self-healing in asphalt is flow, which is the development of the contact points

between two cracked surfaces. Flow rate is impacted by the mechanical properties of the material, for example remaining confining stress, brittleness of bitumen and its visco-elastic properties, and in addition surface free energy of bitumen[86].

According to [87], the second step is wetting of bitumen molecules between both faces of a crack and the homogenization of the healing material. Also,[87] stated that the third step is the diffusion of bitumen from the asphalt matrix into the cracks.

Furthermore, Qiu [88] showed that the crack width is an important factor that could impact on the ability of healing in asphalt because bitumen has to flow further within the asphalt. Wider cracks imply less healing [66].

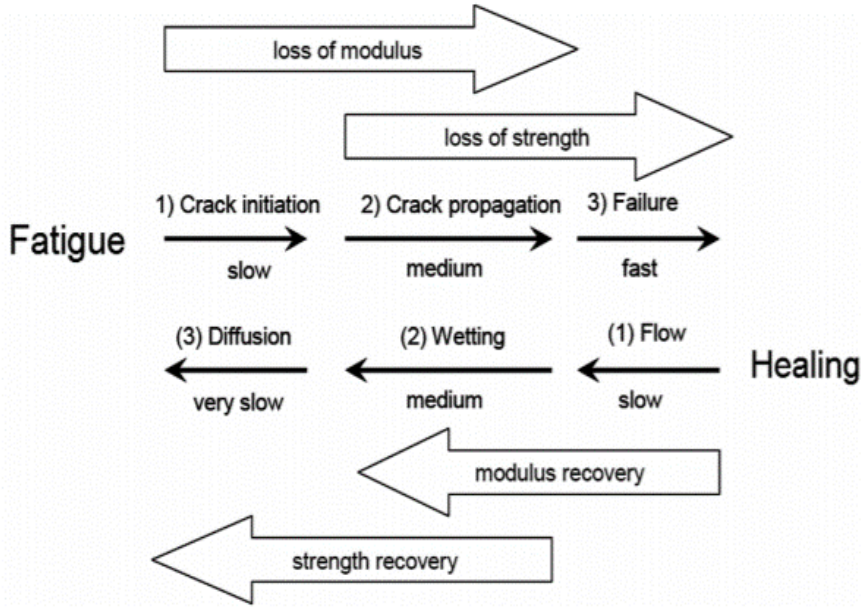


Figure 2.14 : The healing mechanism diagram in bitumen,[87].

In addition, Porto [89] found that the softening point temperature of bitumen and therefore, the optimal self-healing temperature increased with ageing. However, the healing level of binder increased slightly when the temperatures exceeded the softening point [90]. Consequently, the minimum healing time for asphalt depends on the temperature and binder type, where the healing time decreases with the increase of heating temperature and higher penetration grade of bitumen [75].

2.7 Factors influencing Self –Healing of Bituminous Materials

2.7.1 **Internal Factors influencing the self-healing**

The main internal factors influencing the self-healing are physical properties such as softening point of bitumen or penetration, and the composition of the materials.

- Physical properties

Several researchers such as [[91],[92]] have mentioned that the bitumen has higher healing ability when it has a lower softening point and higher penetration grade.

- Chemical composition

In general, many researchers such as [93] have demonstrated that the chemical composition of bitumen and aggregates is considered a strong factor that has an impact on the potential of healing for bitumen. According to [94], different bitumen vary widely in aromatic, amphoteric, and wax content, and the researchers found that better healing occurs with high aromatic and low amphoteric contents .

Kim ,[94], used the methyl plus methylene hydrogen to carbon (MMHC) ratio to assess the self-healing of bitumen. The methyl and methylene hydrogen to carbon (MMHC) ratio is the ratio of the number of methyl and methylene hydrogen atoms to methyl and methylene carbon atoms in independent aliphatic molecules or aliphatic series attached to cycloalkanes or aromatic centres. This ratio can be determined through Fourier Transform-Infrared spectroscopy (FT-IR) and Nuclear Magnetic Resonance (NMR) measurements. It was shown that a higher MMHC ratio corresponds to a lower healing capability.

- Volumetric properties

Asphalt mixtures, [92] have higher self-healing potential with an increase of voids filled with bitumen (VFB). Francken [95] stated that healing increased with a decrease of voids in the mineral aggregate skeleton and a reduction of the volume of air voids.

On the other hand, Lee [96], found that additional factors that affect the healing properties of asphalt mixtures are the aggregate interlock, and film thickness, rather than modifications by polymers. In addition, Lee [96], noticed that SMA mixes have higher self-healing ability when compared with other types of asphalt mix.

- Modifiers

Bahia,[97] tested eight samples, two bitumen's without a modifier, two bitumen modified adding plastomers, two bitumen with added elastomers, and two modified by oxidation. This author found that the modified binders all had a better healing potential than the raw binder.

Therefore, polymer modifications can improve the healing performance. Lee, [96] compared the healing of asphalt mixtures with different modifications, namely: Styrene Butadiene Styrene (SBS), Styrene-Butadiene Rubber (SBR) and Gilsonite (GIL). Lee, [96], found that adding SBS into the asphalt mix gave the best performance for fatigue, rutting and healing. However, Kim, [98] investigated the impact of adding SBS to the asphalt mixture on crack healing, and found there was only a small positive effect on normalized healing rate of mixture. Van [100] noted that there is a distinguishing difference between the healing ability in laboratory.

- Ageing

According to Little aged and field aged mortar samples. Van de bergh stated that a laboratory aged mortar shows a higher ability of healing compared to the raw mortar in stress controlling fatigue healing [99]. However, a field aged mortar, that has a same rheological and chemical properties as the laboratory aged mortar, shows a lower in healing ability compared to the virgin mortar. In addition, Liu [101], stated that ageing simulated in the laboratory showed a little decrease in the healing ability.[102] stated that bitumen ageing has a negative impact on the healing ability of asphalt and caused low healing performance of asphalt concrete, however, Oil of cooking can be improved healing performance and aged binder

2.7.2 **External Factors**

- Resting periods

Many researchers have confirmed the positive effect of rest periods on healing [[63], [66], [72], [103],[104]] , showing that the healing potential increased during the rest

period. In addition, rest periods aid the recovery of stiffness and strength of the material, also prolonging the fatigue life of the asphalt mixture.

Qiu stated that rest period can increase healing ability are ranging from second at least in the intermittent loading related healing to up 100 days in fracture related healing in asphalt concrete[88]. .

- Heating and Temperature

Temperature is considered an important factor that impacts the self-healing of asphalt mixture. It is apparent that when temperatures increase [93] , self-healing is increased also and it occurs more rapidly [103]. Bhasin, [105] evaluated the effect of thermal treatment on the fatigue life of asphalt concrete. Garcia, [66], explained that the self-healing rates change with the temperature and that this could be explained by means of the Arrhenius equation.

- Damage level

The damage level and the history of loading impact the healing in asphalt mixtures [[111],[112]]. The healing is better when the damage is smaller [112]. However, the healing of macro-cracks does not happen [113].

- Loading methodology

The loading methodology is one of the main factors that impact healing in asphalt mixtures [[114], [115], [116]]. Figure 2.15 illustrates the boundary between micro-

and macro- damage during crack growth [117]. Zhang [118] stated that macro-cracks are not formed so long as a specific load threshold is not exceeded. The micro-crack is automatically healed by the aid of temperature or rest periods.

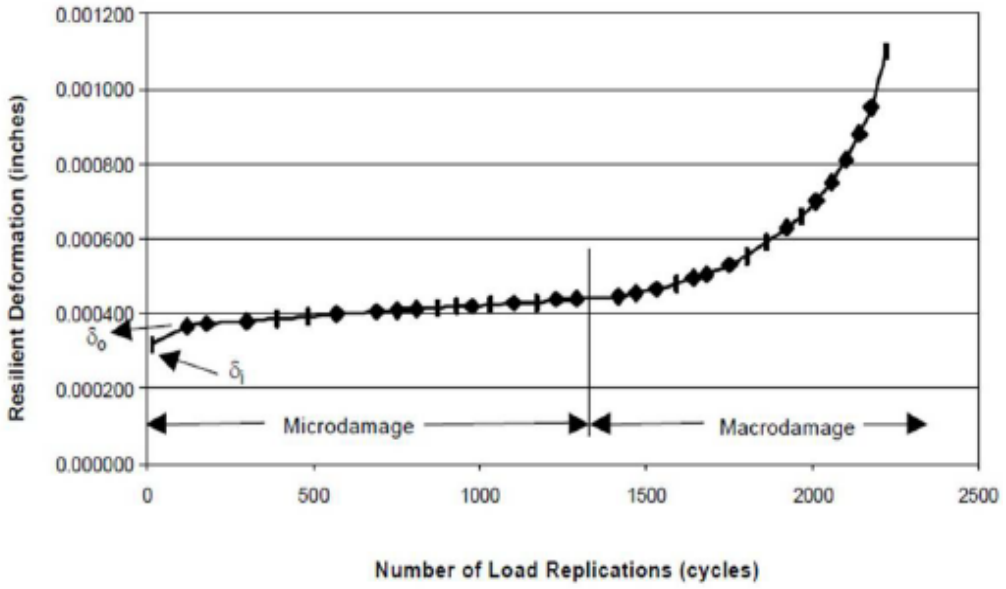


Figure 2.15: The micro-damage boundary during crack growth in indirect tensile fatigue test,after [117].

In addition, Zhang, [119], explained macro- cracks do not heal even through there are rest periods or temperature increases. Furthermore, Lytton et al. [107] have developed a constitutional model for predicting the progress of damage in asphalt mixture, which could address controlled stresses and strains, and randomly applied loading and rest periods.

- Load level

The impact of load level on self-healing has been widely noted in fatigue-related healing tests with intermittent loading [100], it appears that there is a negative impact on

the proportional fatigue life extension caused by healing when at a high tensile stress/ strain level [101]. Qiu [120], developed a two-phase healing test to examine the self-ealing behaviour of pure bitumen. Two phases were distinguished: firstly, is the initial healing phase that happens due to time-dependent healing and secondly gap closure.

- Compressive stress

Bazin [62] noted that applying a compressive stress to the fatigued or fractured sample could lead to accelerated healing. Because this compressive stress can increase the contact between the broken surfaces during the period of healing [[106],[121]].

- Moisture

Qiu [88] pointed out that moisture does not affect the healing. On the other hand, Qiu found that the water has a negative impact on the healing of an adhesive bond.

Thus, there are several factors affecting the healing rate of asphalt mixtures be, and they are summarized in Table 2.1.

Table 2.1: Summary of factors influencing the self-healing of asphalt.

Factor influencing the healing	Effect on healing
Bitumen properties	Increases with lower softening point and higher penetration [74]
Volumetric properties of asphalt	Increases with higher air voids content [72]
Bitumen ageing	Decreases with bitumen ageing [116]
Temperature	Increases with increase of temperature [100]
Level of damage in asphalt	Decreases with increased level of damage [67]
Resting periods	Increases with rest periods [62]

2.8 Self-Healing Techniques for Asphalt Pavements

The ability of self-healing in asphalt was recognized about five decades ago [[52], [62], [91]], and is the capability of repairing crack damage caused by ageing and external factors, for example, a changing climate. The natural self-healing in asphalt pavements may need many days to happen. However, there is an obstacle represented by the continuity of traffic flow. Therefore, researchers have tried to find techniques that increase the rate of asphalt self-healing and prevent further degradation and crack propagation, [[122],[123]]. The sections below summarise the existing methods of artificial healing.

2.8.1 Induction heating of asphalt concrete

Induction heating is a technique which is used to heat asphalt mixture locally in order to recover the mechanical properties of the material [124]. The technique works by adding conductive materials such as steel fibre within the asphalt mixture in order to increase the temperature of the material by means of an electromagnetic field [125].

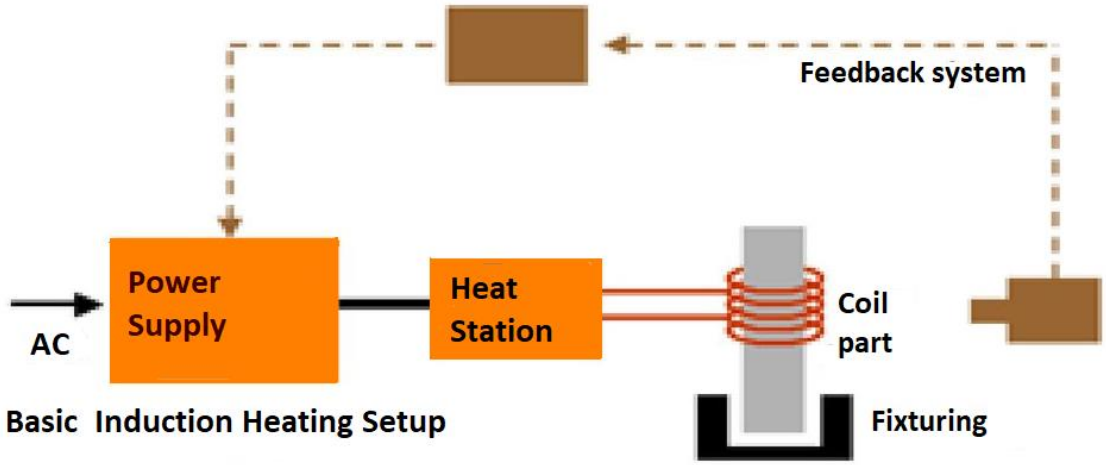


Figure 2.16: Components of a basic induction heating setup, [125].

In 1831, electromagnetic induction was discovered by Michael Faraday, an American physicist, although, Joseph Henry also discovered it independently, according to Texas University [126]. An alternating magnetic field will induce currents in an electrical conductor. The generating of electrical currents in a conductor by means of an alternating magnetic field is called Faraday electromagnetic induction. Also, Figure 2.16 illustrates the basic components of induction heating machine.

The flow of induced current, combined with the electrical resistivity of the conductor creates heat by the Joule effect, the process called induction heating. Electricity in

induction heating, therefore, uses a high frequency in order to heat electrically conductive materials, and the technique has many benefits compared to convection, radiation, open flame or other heating methods:

- Induction heating can convert up to 90% of its energy into heat.
- Induction heating is achieved without touching the asphalt during heating; therefore, the material is not damaged perhaps during heating.
- Depending on Joule's law for heating, the material is heated from within. Therefore, there will be warping and deformation.
- Heating develops immediately and works quickly. In addition, induction heating can be started instantly; therefore, there is no warm-up or cool-down cycle.
- There is no waste heat, no noise, and no harmful emissions.

In asphalt, induction heating heats only the mastic without damaging the aggregate. Therefore, this is considered an exclusive benefit for asphalt mixture. Induction heating has wide applications in modern industrial processes such as bond hardening of soft metals or other conductive materials.

In asphalt roads, the induction heating technique has been applied to increase their temperature, therefore, to close cracks. The first step in an application of induction heating to different asphalt mixtures is to prepare them as electrically conductive, such that they can be heated with induction energy. Many researchers have been successful in preparing conductive asphalt mixtures,[126]. The following paragraphs will give a brief review on conductive asphalt concrete.

- Conductive asphalt concrete

It has already been said that asphalt needs to be electrically conductive in order to induce energy using an electromagnetic field. To achieve electrically conductive asphalt, graphite or fibres which are considered conductive component, have been added to the mixes[126]. The first attempt to make electrically conductive asphalt dates back to the 1960s, and it was for control of the accumulation of snow and ice130]. This conductive asphalt mixture was made by the addition of graphite.

Wu et al. carried out research into the electrically conductive asphalt mixture at the Wuhan University of Technology [131], by adding electrically conductive carbon fibres, carbon black or graphite to asphalt for melting the ice or for self- monitoring. Wu et al [131] explained that the conductivity of an asphalt mixture is proportional to the volume of graphite or electrically conductive fibres added. On the other hand, adding electrically conductive additives above a certain percentage does not decrease the resistivity and influences the mechanical strength and the workability of the mixture.

Wu et al. [131] showed that adding conductive fibres into the mixture is more effective than adding graphite or carbon black to increase the electrical conductivity. Furthermore, Garcia et al.[132] made conductive asphalt mastic by adding steel fibre to the mixture and used induction heating to heat the sample [2] in order to improve its self-healing properties.

Garcia et al. [2] proved that the conductivity is proportional to the volume of electrically conductive particles in the mixture and there is an optimum volume content of electrically conductive particles for each mixture above which the electrical conductivity cannot be improved any more.

- Healing of cracks though induction heating

Garcia et al. [132] tested the healing by means of three-point bending to produce cracks crossing the specimen. Afterwards, they heated the samples for various periods of time ranging from seconds to hours and temperatures, such as 15°C, 30°C, 40°C, 50°C, 70°C, 90°C, and 100°C. After that, the samples were broken again by means three-point bending to measure how much the sample resisted the failure. The healing level of these asphalt mastics was calculated as the ratio of the ultimate force of the beams before and after heating.

2.8.2 Healing of crack by infrared heating

A similar method used for artificial healing is infrared heating, which mimics solar radiation. It heats the asphalt by conduction. When the incident light hits the asphalt's surface, part of the energy is absorbed, and part is reflected. The absorbed energy is conducted to the bottom layers of the pavement at a rate that is given by the thermal conductivity of the material. Since induction heating heats the asphalt from within, it is a much faster method. As an example, Ajam [72], stated that infrared heating required at least 200 min to complete the healing process, while in induction heating this time could be reduced to under 2 min [126].

2.8.3 Liquid-based self-healing material systems

Many agencies have resorted to using asphalt rejuvenators to repair ageing and brittle asphalt pavements. Rejuvenators are oily substances with good penetration in the asphalt. They are normally spread on the surface of roads, and diffuse into the material, restoring its initial properties [133].

The rejuvenators' purpose is to recover the initial properties of the old bitumen by adding, for example, a small amount of oil or raw bitumen. The rejuvenator is described as a softer grade raw bitumen or recycling agent specifically designed to reduce the viscosity. However, Sirin [134] explained the rejuvenators purpose as to penetrate a little into the asphalt concrete and soften (rejuvenate) the bituminous binder.

Their limitation is that they may reduce the skidding resistance of the road [135]. To avoid this problem, researchers have added microcapsules containing healing agents to the asphalt [136]. The objective is that when crack damage happens, the microcapsules break and the healing agent diffuses into the crack, reducing the viscosity of asphalt, which can drain into and fill the crack.

- Mechanism of asphalt self-healing by the action of capsules

During production, capsules are mixed with the asphalt materials, and the capsules have to resist all the loads caused by traffic, temperature [2] and those that occur during mixing. A capsule first suffers a shape change due to compressive loads that occur by an elastic response, without any damage. If this load is sustained, the capsules will undergo permanent deformation and rupture, allowing the rejuvenator to diffuse out of the capsules.

Garcia [142] in Figure 2.17 explained the working mechanism of capsules. Initially, asphalt pavement containing capsules sustains the traffic load, as shown in point 1 in Figure 2.17. After many years the stiffness of the asphalt increases, and the distribution of the force changes the capsules' surface. Therefore, due to all the traffic loading and asphalt ageing, the capsule will break, as shown in point 2 in Figure 2.17. If loading continues at the same level, the capsule suffers permanent deformation, while with

continued increasing of loading, the pressure inside the capsule increases leading to the rejuvenator coming out, Figure 2.17, point 3.

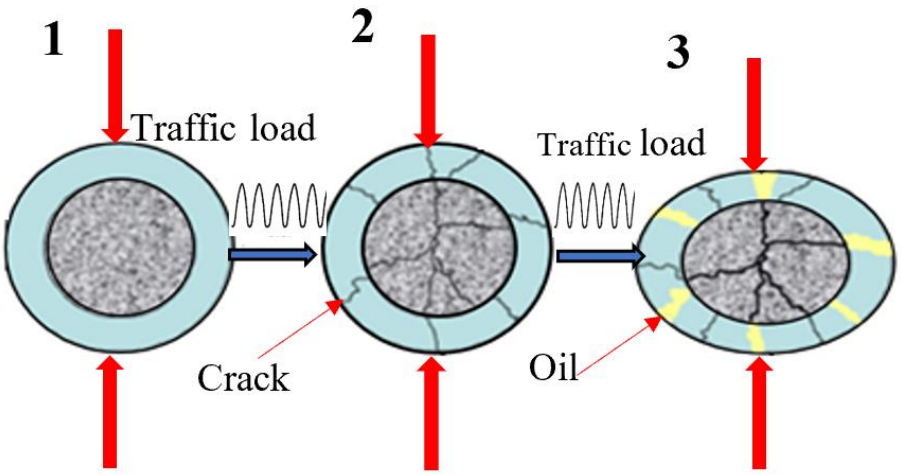


Figure 2.17: Concept of oil release to heal the crack though asphalt mix, after [142].

It has been found that the capsules release about 4% of their content during mixing and compaction [135].Additionally, Garcia.et al, [136] found out that all the capsules in an asphalt crack surface broke during indirect tensile fatigue tests. In addition, capsules may have a negative impact on the asphalt stiffness.

The authors clarified that this happens because, it is possible that the capsules were weaker than they should have been to resist the asphalt testing, this weakness can be overcome by the creation of stronger capsules [137]. In addition, capsules could lead to increased permanent deformation in asphalt [138]. Figure 2.18 shows a capsule broken during direct tensile test. In addition, Al Mansouri [140] found that up to 80% by volume of healing agents was released by the capsules during cyclic loading.

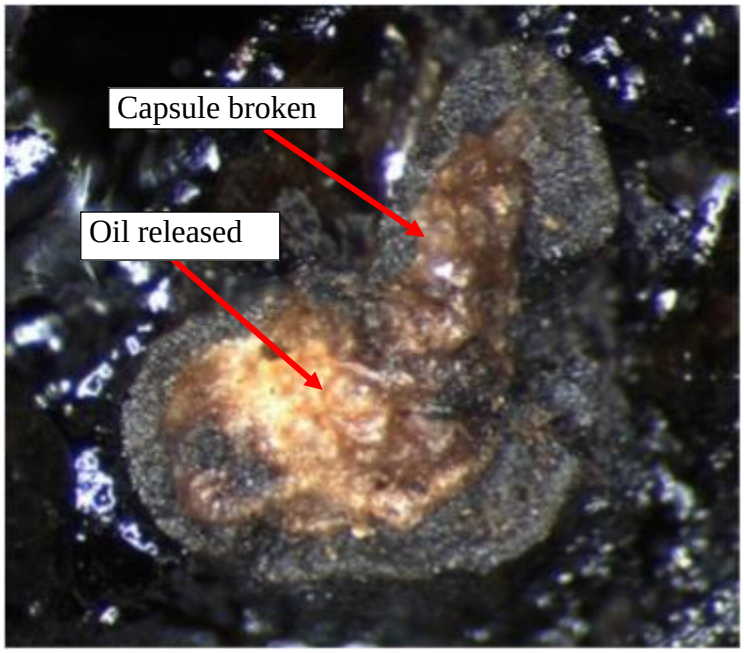


Figure 2.18: A capsule broken during inderect tensile test , after [142].

Al Mansouri[140],] showed that capsules promote the healing of asphalt up to 30^{o}C; at temperature above those, there is no difference between asphalt with and without capsules. In addition, the healing level of the asphalt is proportional to the number of capsules, being 0.5% by total weight in the asphalt in three experiments. Furthermore, the amount of oil released from the capsules increases with the increasing percentage of oil in the material. Erkut, [143] recommended that the diameter of capsules was 2.5 mm and their sunflower oil content 75% by volume. From all these results, it is yet unclear when do the capsules break, or if there is an optimised strength and size for the capsules.

The behaviour of capsule in asphalt self-healing was successful, enabling it to rejuve-nate the aged binder. However. these capsules cannot be able to reuse after they are cracked in which considered one of disadvantages in using. This issue can be studied and recommended with future work.

2.9 Summary of literature review

Based on the literature review, the following conclusions were obtained:

- Asphalt mixtures can recover their strength and stiffness when allowed to rest and if the viscosity of bitumen is low enough.

- According to the literature review, the temperature and viscosity of bitumen are considered as the dominant factors that affects the self-healing behaviour of asphalt.

- The self-healing of asphalt can be promoted by artificial techniques such as induction heating and encapsulated rejuvenators.

- Induction heating consists of adding metallic particles to the asphalt and heating them using an electromagnetic field. As a result, bitumen melts and can fill the cracks. This accelerate the self-healing from hours or days to minutes.

- Encapsulated rejuvenators are drops of oil protected during mixing, compaction and the road's lifetime by hard shells. They are designed to break when cracks appear; because of the release of the oil, the bitumen melts, drains and fills the cracks.

- Finally, there are no previous studies about optimum moment to implement the artificial self-healing. For this reason, the work will focus on this study.

Chapter 3: Materials and Methods

3.1 General

The main objective of this thesis is to assess the self-healing of cracks in different hot asphalt mixtures. The chapter has been divided in two parts. The first part describes the different materials that were used in the present study. The second part summarizes the methodology followed to accomplish the objective of this research project. In Table 3.1, the reader can find a summary of the materials and experiments used.

Table 3.1: Summary of materials and experiments.

Descriptions	**Chapter 4: Healing by infrared heating**	**Chapter 5: healing by induction heating**	**Chapter 6: healing by encapsulated rejuvenators**
Materials	Porous asphalt	Porous asphalt	Porous asphalt
	Dense asphalt		Dense asphalt Stone mastic asphalt
Self-healing induced by:	Infrared heating	Induction heating	Capsules containing rejuvenators
Mechanical test to quantify the self-healing	3-point bending		
X-Ray Computed Tomography (CT Scans)	Air void distribution before and after healing		
Additional testing	Thermal expansion	Stiffness modulus (ITSM)	Fourier Transformed Infrared Spectroscopy (FTIR)

3.2 Raw materials

3.2.1 **Virgin limestone aggregates**

In this investigation, crushed limestone aggregate was used. The density was 2.67 g/cm^3. Before using them, the aggregates were dried at 160^{o}C for 12 h to remove all the moisture. In this study, the nominal sizes of gradation were the following: 20mm, 14mm, 10mm, 6mm, and dust (i.e. < 4mm). The gradation of each nominal size is presented in Table 3.2.

Table 3.2: Aggregate size distributions used.

Sieve size (mm)	20mm		14mm		10mm		6mm		Dust	
	Retain %	Pass. %	Retain %	Pass. %	Retain %	Pass. %	Retain %	Pass. %	Retain. %	Pass. %
31.5										
20.0	14.86	85.14								
16.0	57.22	27.94								
14.0	21.92	6.02	5.54	94.46						
10.0	5.16	0.86	67.66	26.8	7.38	92.62				
8.0	0.09	0.77	21.86	4.94	30.56	62.06				
6.3	0.03	0.74	3.13	1.81	38.5	23.56	4.32	95.68		
4.0	0.01	0.73	0.56	1.25	20.35	3.21	70.66	25.02	1.02	98.98
2.8	0	0.73	0.1	1.15	1.97	1.23	19.82	5.2	4.98	94
2.0	0	0.73	0.05	1.1	0.3	0.93	2.46	2.74	11.39	82.61
1.0	0	0.73	0.06	1.04	0.05	0.87	0.51	2.23	23.13	59.48
0.5	0	0.73	0.04	1	0.02	0.85	0.12	2.11	16.75	42.73
0.25	0	0.73	0.05	0.95	0	0.85	0.06	2.05	10.76	31.97
0.125	0.01	0.72	0.05	0.9	0.02	0.83	0.04	2.01	7.78	24.19
0.063	0.07	0.65	0.1	0.8	0.02	0.81	0.1	1.91	5.4	18.79
Pan	0.63	0.02	0.79	0.01	0.83	-0.02	1.9	0.01	18.79	0
Sum	100		99.99		100		99.99		100	

3.2.2 **Bitumen**

In this study, bitumen with 40/60 pen, with density 1.028g/cm3 was used. This bitumen was provided by Shell. This is the most commonly used type of bitumen in the UK.

3.2.3 **Self- healing additives**

Below the reader can read a description of the additives used in each of the chapters in the Thesis (see also Table 3.3).

Table 3.3: Additives to promote the self-healing used in the Thesis and mass percentage in the asphalts (the composition of the asphalts can be found in Section 3.3).

Additives	Porous Asphalt %	Dense Asphalt %	Stone Mastic Asphalt %	Chapter in the Thesis
Steel fibre	1.1 %*	-	-	Chapter 5
Capsule	0.5%*	0.5%*	0.5%*	Chapter 6

* In mass percentage

3.2.3.1 **Conductive Particles (Steel wool fibres)**

Steel wool fibres were added to the asphalt as a means to accelerate the self-healing process by increasing the temperature of the asphalt (see Chapter 5). This product is as a very fine fibre as shown in Figure 3.1, the range of diameters used was from 16µm to 72µm (the average was 40µm) and the length was from 0.15 mm to 5mm (average length, 1.4mm) (see Figure B.1 in Appendix B) with a density of 7.220 g/cm^3, see

Figure 3.1 The steel wool fibre content was 1.1 % by mass of mix as shown in Table 3.3.

3.2.3.2 **Encapsulated healing agents**

Capsules have been used in this thesis as a method to accelerate the self-healing of cracks in asphalt (see Chapter 6). They are spherical particles of between 1-2 mm diameter that consist of a liquid core protected by a porous membrane able to resist mixing and compaction. The composition of the capsules used in the Thesis is sunflower oil as the healing agent, 75% by mass, and calcium-alginate as the membrane 25 % by mass [143] see Figure 3.2.

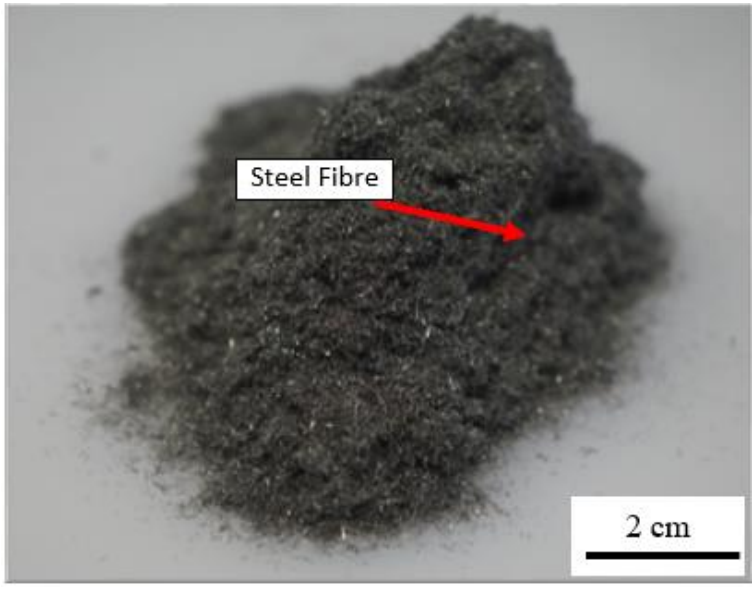


Figure 3.1: Steel wool fibre

The capsules have been previously described by several researchers and it is not the objective of this Thesis to explain how to make them or how their diameter or strength influences the functionality of an asphalt mixture. The manufacturing method can be

found in [143]; their mechanical and thermal properties in [143]; and the properties of asphalt containing capsules in [143]. In addition, examples of capsules made by other researchers can be found in references [134]-[140],[142]- [146]].

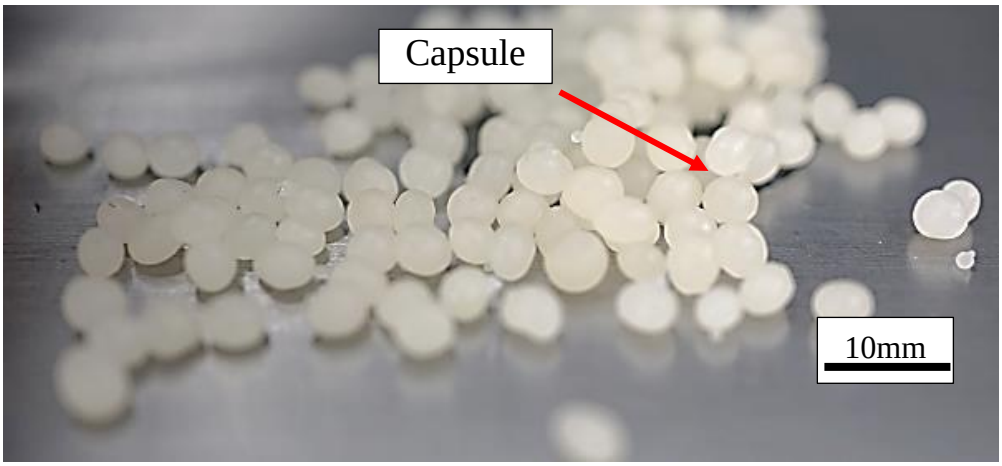


Figure 3.2: Capsules used in the study.

3.3 Asphalt mixture's composition

The types of asphalt used in the Thesis are summarised in Table 3.4. In Chapter 4, Dense Asphalt (DA) (also called 5% because of its air void content) and mixtures with 10%, 13%, 21%, and 26% air void contents were used according to reference[164].In Chapter 5, Porous Asphalt (PA) with fibre addition was used. The steel wool had an average length of 1.4 mm and a diameter 40 µm. Its content was 1.1 % according in reference [152] by mass of mix as shown in Table 3.3. Using of porous asphalt in Chapter 5, therefore, it recommended of chapter 4. In Chapter 6, Dense Asphalt (DA), Stone Mastic Asphalt (SMA), and Porous Asphalt (PA) were used, with and without capsule addition. These mixtures were selected because of their variety of air voids (to know the influence of air voids on the self-healing, in Chapter 4) and representative of

the most commonly used surface courses in Europe. The percentages of self-healing additives in each mixture are presented in Table 3.4.

Table 3.4: Composition of the asphalts used in the Thesis.

Name of the mixture:	DA / 5%	10%	13%	21%	26%	PA	SMA
Size (mm)	Passing (%)						
31.5	100	100	100	100	100	100	100
20	99.1	99.1	99.1	99.1	99.1	99.3	100
16	91.3	91.2	91.2	95.5	91	96.3	100
14	83.3	82.9	82.9	88.1	78.2	94.2	99.7
10	62	58.8	58.8	53.4	27.6	73.1	93.9
8	54.1	48.7	48.7	36.3	17.9	57.7	77.8
6.3	47.8	40.7	40.7	23.1	13.5	44.3	58.4
4	34.3	29.5	29.5	17.8	11.4	23.6	33.3
2.8	28.7	25	25	16.6	10.6	17.9	26.2
2	23.7	20.8	20.8	14	9	14.7	21.7
1	17	15	15	10.2	6.7	10.3	15.5
0.5	12.9	11.3	11.3	7.9	5.2	7.4	11.6
0.25	10.2	9.1	9.1	6.3	4.3	5.7	9.2
0.125	8.1	7.2	7.2	5.1	3.5	4.6	7.4
0.063	6.5	5.7	5.7	4.1	2.9	3.6	6
Bitumen	4.70%	4.50%	4.20%	3.30%	2.70%	4.50%	5.90%
Fibres*						1.10%	
Capsules*	0.50%					0.50%	0.50%
** There are mixtures with and without fibres and capsules. Those without self-healing additives had the same aggregate gradation*							
Air voids	5%	10%	13%	21%	26%	20%	5.5%

All the mixtures were manufactured with crushed limestone aggregates; the nominal maximum size for DA and PA was 20mm, and 14mm for SMA. The air void contents

measured are shown in Table 3.4. In addition, asphalts with and without self-healing additives were manufactured. These mixtures were used in Chapter 6, and were designed according to references [147], [148] and [149],[164] with different amounts of bitumen 5%, 4.5% and 5.9%, for DA, PA and SMA, respectively .

To promote the self-healing, 1.1% of fibres was added to PA, according to reference [152], which is the optimum amount of fibres that maximises the healing and does not affect the mechanical properties, and 0.5% of capsules was added to DA, PA, and SMA, according to advice reference [143],[154]. The asphalt mixes design, the materials additives, air voids content and bitumen content will be used in all the chapters are summarized in Table 3.4.

3.4 Manufacturing and geometry of test specimens

Mixing and compaction of test specimens was developed according to the standard BS EN [151]. Asphalt was manufactured by mixing the pre-heated materials at 160ºC (12 hours for the aggregates and 2h for bitumen). The materials were then compacted using a roller compactor to make slabs until the mixtures reached their target air voids content. In the Thesis, slabs (to cut beams), beams, and cylindrical test specimens were manufactured. Asphalt slab and cylindrical test specimens were manufactured following standard procedures [155]. The slabs dimensions were 307 × 307 x 50 mm^3.The beams were 150 × 60 x 50 mm^3, and the cylinders, 100 x 40 mm^2, (see Figure B.2(stages of preparing the samples), and Figure B.3, Appendix B). 8 beams were cut from each slab. In addition, in order to manufacture test specimens for measuring the

stiffness, cylindrical test specimens were also core from the slabs. Their diameter was 100 mm.

3.5 Method to quantify asphalt self-healing

Self-healing was evaluated according to [75]. The samples were tested to fatigue under modified three-point bending fatigue configuration at 20±2ºC, see Figure 3.3 (b), which ensured the formation of vertical cracks at the midpoint.

Between the bottom bearings and underneath the samples, an elastic membrane was placed to prevent the production of permanent deformations during the test. The test had a frequency of 4 Hz between a maximum value of 2.5kN and a minimum of 0.15 kN, which ensured consistent contact between actuator and sample with dynamic waves of 0.1s duration and a resting period of 0.15 s (see Figure 3.3).

In order to determine the effect of the loading level on the self-healing, in general, four different loads were applied for all the self-healing additives analysed, 1.25 kN, 1.50 kN, 1.75 kN, and 2 kN, for PA and SMA, and 2kN, 2.5kN, 3kN, and 3.5kN for DA.

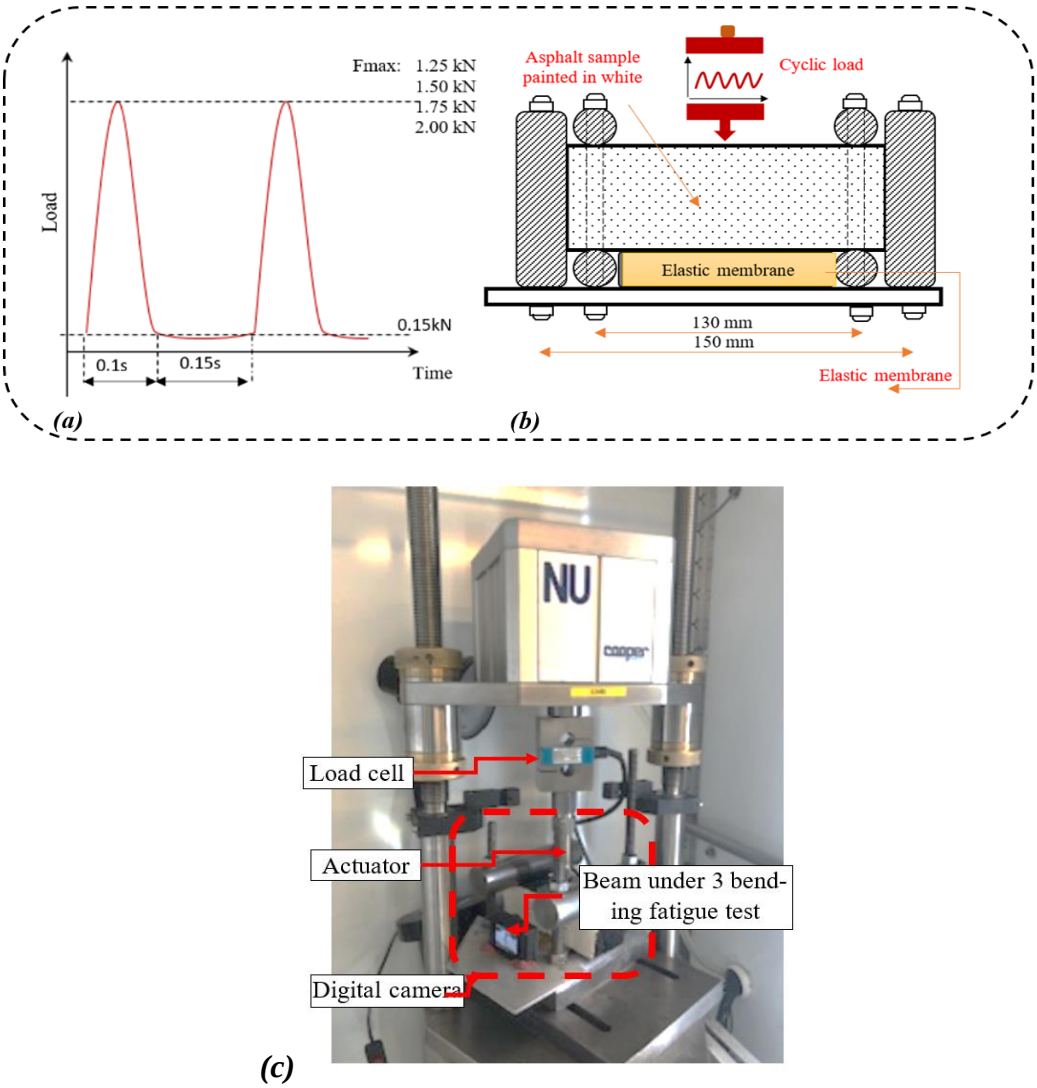


Figure 3.3: (a) Configuration setup of Loading , (b) Scheme representation of the modified 3-point bending test used. (c) Universal machine used.

The crack formation on the painted side of the beams (see Figure B.4a in Appendix B) was continuously monitored by a static camera with f/2.8 aperture and 12 Megapixels of resolution that took one picture every 40 loading cycles. By using the image processing software ImageJ, the total length of emerging cracks could be accurately measured in each picture until the sample split in half. This Thesis arbitrarily adopted failure

criterion was the number of cycles at which the crack length reached 20% of the total crack length registered at the end of the test as shown in Figure 3.4.

The reason why 20% was chosen is simply because, from the experience of the author, this is one of the first moments when cracks were surely present, without a doubt, in the asphalt. Also, Figure 3.4 shows point 1 and point 2 for the same sample but analysis by using image j , there are two point, point 1 represented the sample tested after several number of cycles for this the crack did not appeared, however in point 2 the sample broken for this the crack appeared clearly.

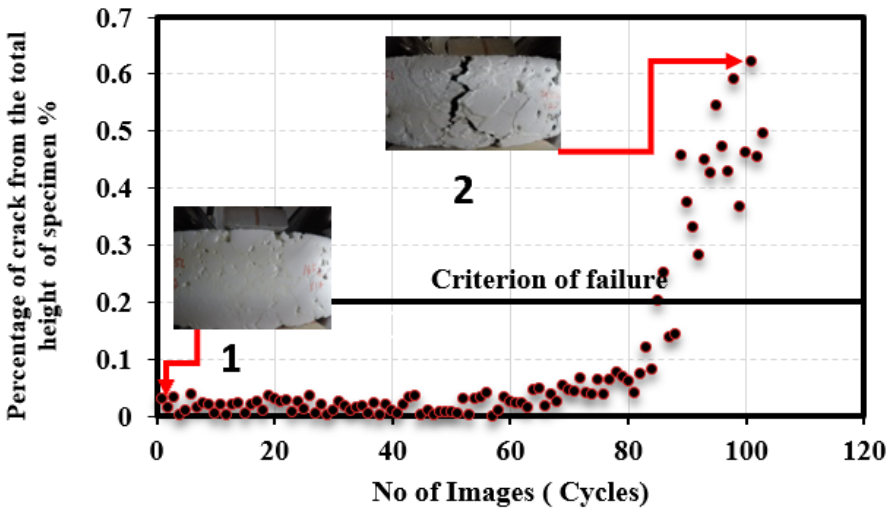


Figure 3.4: Criterion of failure analysis by using Image J software. 1. The sample tested after several cycles (but before failure). 2. The specimen tested until failure.

In addition, Figure 3.5 below shows an example for 21% air void before test and after test analysed by using free image J software (other materials in with before and after testing can be found in the Appendix B, Figure B.4b). To determine the fatigue life of

each studied material, 5-15 samples per material were subjected to the test until failure, and a Weibull distribution function was fitted to the data.

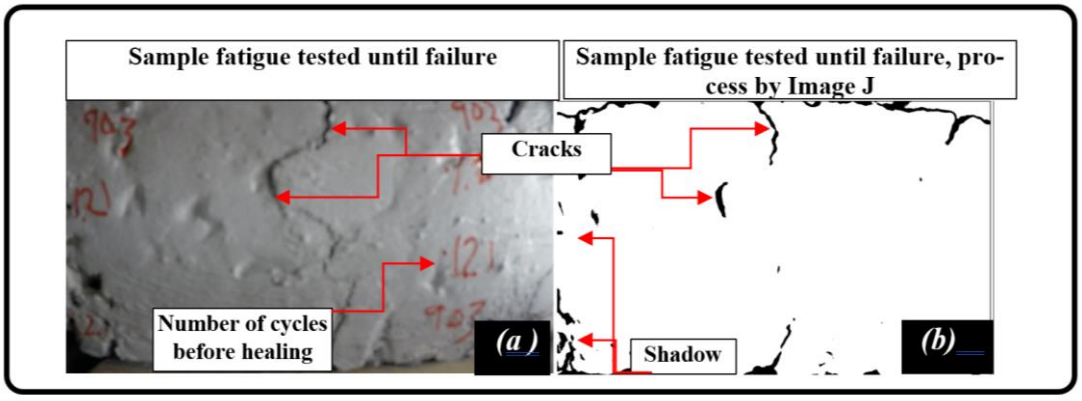


Figure 3.5: An example of an asphalt beam with 21% air voids content, a) the beam after three point bending fatigue test, and b) the beam processed in image J.

This probability distribution was selected considering that fatigue damage is produced by the progressive accumulation of mechanical energy on each applied cycle [156].

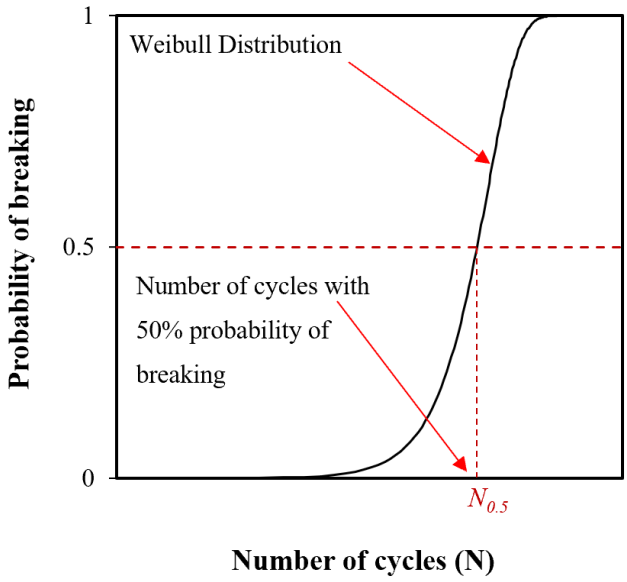


Figure 3.6: Scheme of how the number of cycles with 50% probability of breaking can be obtained based on Weibull probability distribution.

The samples' average lifetime was estimated as the number of cycles whose probability of breaking the specimens is 50%. This number of cycles will be referred to hereafter as $N_{0.5}$, see Figure 3.6.

The service life extension for each sample was assessed through the concept of the Healing Index (HI) according to [75], which compares the total number of cycles resisted (N_f) and the reference number ($N_{0.5}$), as shown in Figure 3.7.

$$HI = \frac{N_f - N_{0.5}}{N_{0.5}} \tag{3.1}$$

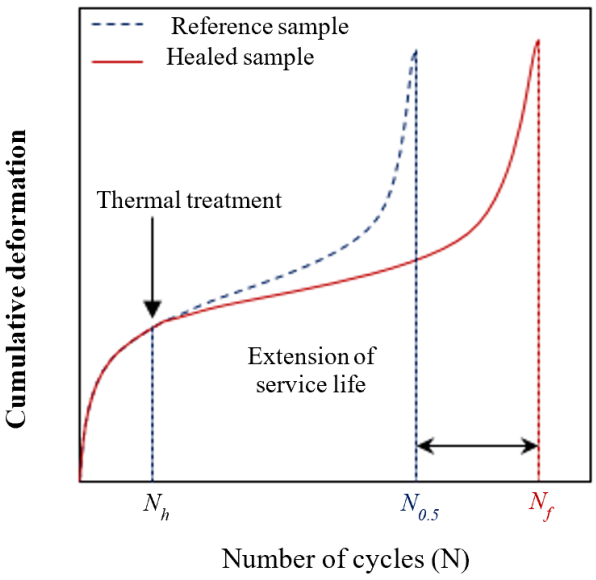


Figure 3.7:Scheme of how the number of cycles and service life extension can be evaluated.

3.6 Methods to induce self-healing

3.6.1 **Self- healing by infra-red heating**

In order to evaluate asphalt mixes' capacity, to extend their service life, when subjected to thermal treatment by using infrared heating, a series of 40 samples for each material was manufactured and tested, as described above. In this case, each fatigue test was paused at a different number of cycles; then, the healing treatment was applied. The samples were embedded in white sand, with the exception of the top surface, and placed for 200 min under a set of four 250 W infrared lamps, which simulated the Sun's heating effect Figure 3.8.

The white sand allowed only the upper surface of the samples to be heated by radiation (similar to field conditions) and also provided a confining medium, which prevents samples from deforming during the heating process.

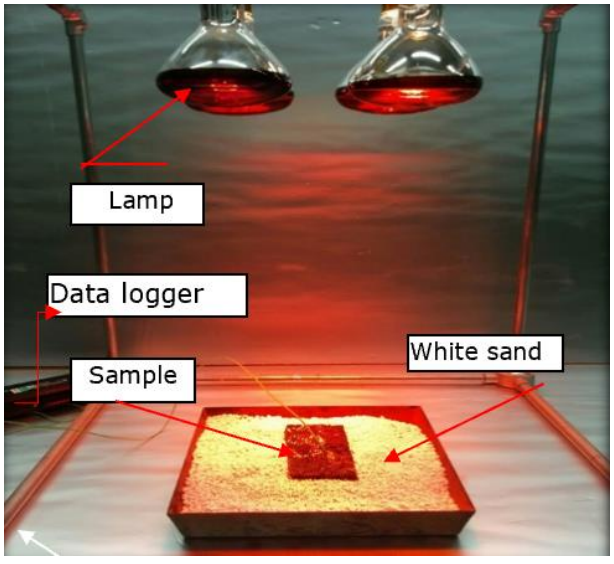


Figure 3.8: Infrared Heating setup.

The heat source contained four 250-Watt intra-red lamps built-up in two rows above asphalt surface.

The lamps were connected to the steel frame pipes constructed in a Nottingham Transportation Engineering Centre (NTEC). The centre-to-centre distance between lamps was 280 mm and the distances between lamps and samples' top surface were 300,700, and 1100 mm see Figure 3.9 (to obtain the optimum healing). Later, the samples were conditioned at 20 ± 1ºC for 24 h and returned to the test until reaching failure.

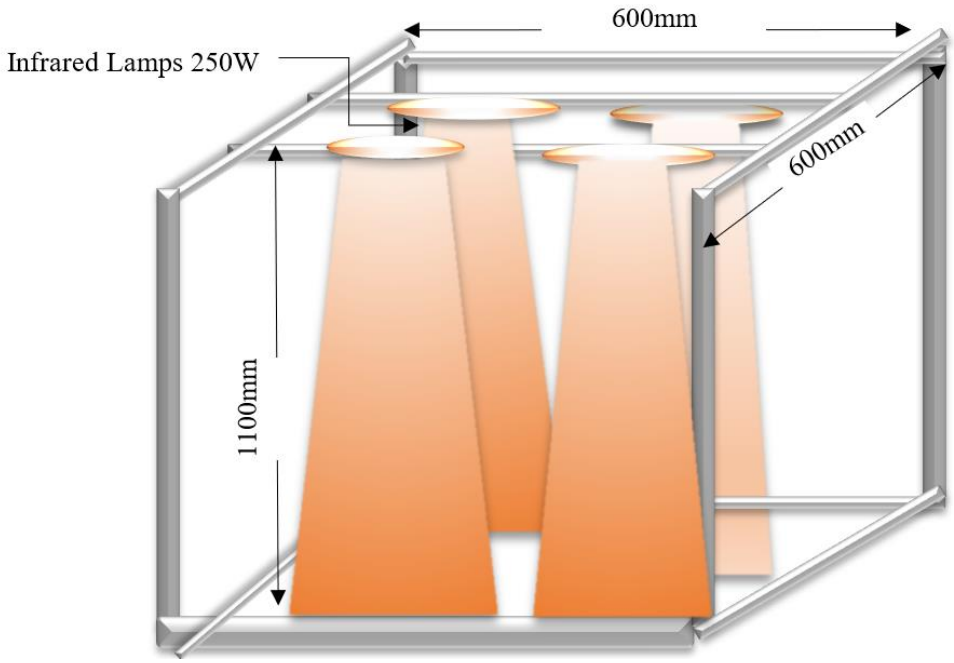


Figure 3.9: Scheme of infrared lamps setup for farm.

3.6.2 **Self-healing by induction heating**

Healing of asphalt samples was carried out by applying 90s of electromagnetic induction on the samples containing steel wool fibres. This process induced electric microcurrents along the conductive fibres, heating them by the Joule effect and, therefore,

heating the bitumen too. Consequently, the viscosity of the bitumen reduces, and at the same time, its volume increased due to thermal expansion, which contributed to its drainage through internal cracks and cavities[157].

After heating, the temperature of asphalt reverted to that of the environmental, and the cracks remained full of bitumen, therefore, the fatigue life of the samples could be extended [157] as shown in Figure 3.7.

The distance between the coil and the samples was set to 2 cm and the samples were embedded in sand to prevent permanent deformations while heating them. The heating temperature was continuously monitored by a full-colour infrared camera with a resolution of 320 x 240 pixels as shown in Figure 3.10.

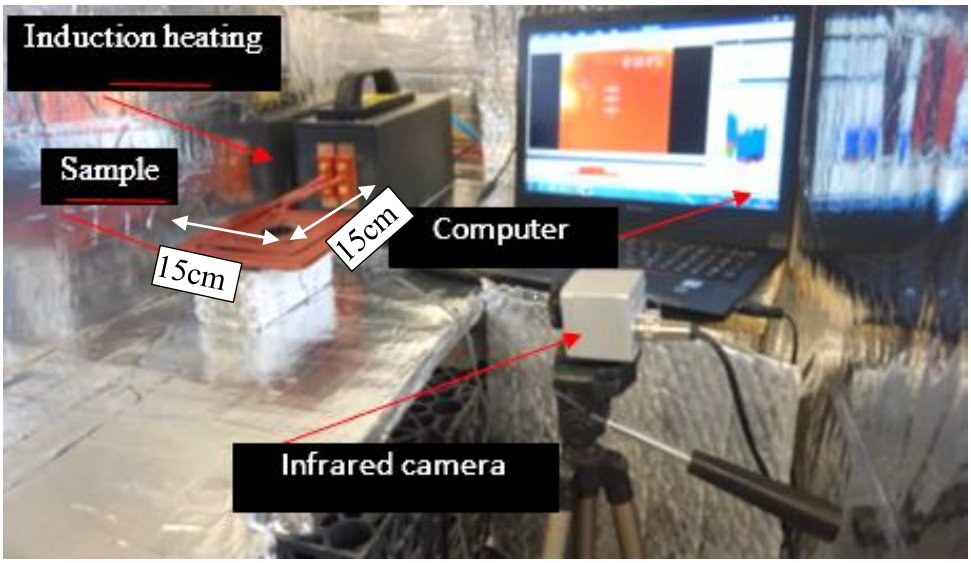


Figure 3.10: Self-healing under induction heating.

Electromagnetic induction was applied by a 15x15 cm^2 square coil connected to a 6-kW induction generator with a power configuration of 2.8 kW and a working frequency of 348 kHz. A new series of 10 samples were tested but, this time, stopping the test at a number of cycles N_h, which represents different damage levels, applying the induction treatment and resuming the test until the beam cracked. The total life of the test samples, including the cycles before the heating treatment, N_h, and until cracking was defined as N_f. The healing index was defined as the percentage extension of fatigue life with respect to the reference $N_{0.5}$, as described in the previous Section (3.5) and using the same formula.

3.6.3 **Encapsulated rejuvenators**

The amount of oil released by the capsules to the mixture was measured according to the methodology defined in Micaelo [159], developed by Al-Mansouri et al [154]. This methodology is based on the idea that the sunflower oil has a distinct absorption peak at ~1,745 cm^{-1}, which bitumen does not have. To have a reference to determine the amount of oil released by the capsules, sunflower oil was mixed with bitumen in the mass percentages 1.0 %, 1.5 %, 2.0 %, 3.0 %, 5.0 %, 6.7 %, 8.0 %, 9.0 %, and 10.0 % and the normalized area under the FTIR curve calculated, as shown in reference [154].

In addition, asphalt mastic samples had to be obtained to determine the amount of oil released by the capsules. To do that, asphalt mixture was heated to 100 ^oC, broken in small pieces by hand and mastic samples were collected from the surface of coarse aggregates using a hot knife. The FTIR curve of the mastic was obtained and the normalized area under the curve for the mastic specimens was compared to the values obtained from mixing bitumen and sunflower oil.

Mastic was extracted from mixtures that had been just compacted, at different stages of cyclic loading, and after the resting period that was used to allow the cracks to self-heal.

- Capsule production

The polymer capsules was a composite of calcium-alginate with water and oil at a ratio of 0.1 and they were produced by ionotropic gelation of alginate In the presence of calcium see Figure 3.9 at 20^{o}C.according to [154]. A scheme of the manufacturing process of the capsules is illustrated in Figure 3.11. To manufacture the capsules, firstly, 150ml of a sunflower oil was added into 1500ml of deionized water and mixed into a lab beaker of capacity 2000 ml and stirred to make a stable emulsion.

The mix (sunflower and water) was blended utilizing a laboratory gear drive mixer for 1 min at 400rpm as shown in Figure 3.11(a). Secondly, an addition (55 g) of sodium alginate was introduced to the laboratory beaker and stirred until complete solution at 400 rpm for 10 min, (see Figure 3.11(b)).

The third step is mixing 36 gm of calcium chloride solution into 2% water (1800 ml), blended together into a 5000 ml beaker container. The advantage of using calcium alginate, according to Tabaković [160] is its low-cost and that it is strong enough to carry the oil. Finally, the mixture was introduced into a 2000 ml capacity piece of glassware containing a calcium chloride solution. Capsules were formed by dropping from a funnel with a 3mm diameter as shown in Figure 3.11c.

During formation of the capsule, the calcium chloride solution was gently agitated using a magnetic stirrer at 60 rpm. In this research, 2-3 hours approximately was the

time taken for the capsules manufacturing process. After finishing processing, the capsules were dried in an oven at 40 ^{o}C for 72 h after being washed with deionised water

Finally, these capsules were stored in a freezer at -18 ^{o}C. The encapsulation procedure allowed the manufacture of capsules with an average diameter 2.5 mm as shown in Figure 3.2 with contents 75% and 25% by volume of sunflower oil and calcium-alginate polymer, respectively. 5 kg of capsules were manufactured in this study.

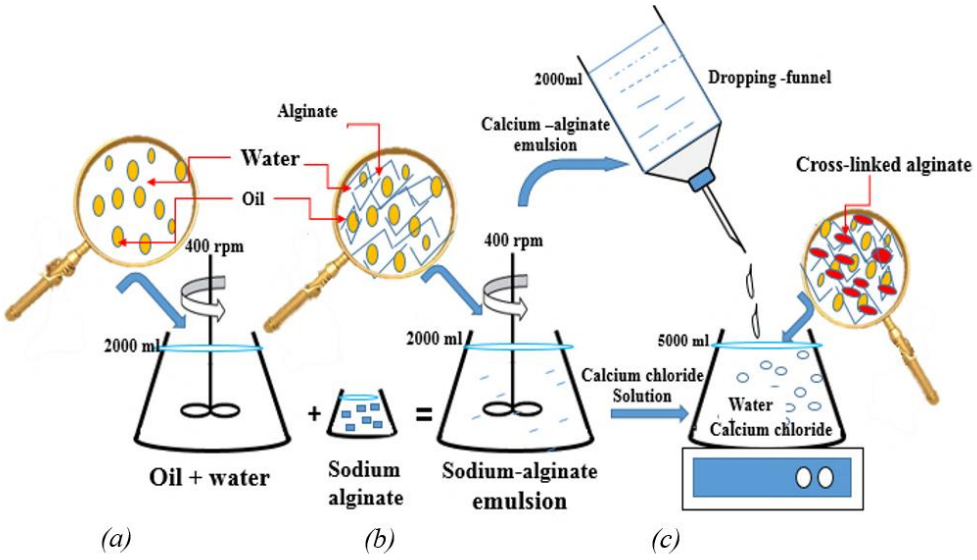


Figure 3.11: Schematic diagram of the manufacturing process of capsules by ionotropic gelation of alginate Capsule presentation, based on [140].

3.7 X ray Computed Tomography (CT) Scans

To examine the air voids of the test samples, a XRadia Versa XRM-500 scanner operating at 80 kV and 120 µA was used see Figure 3.12. The machine that used in University of Nottingham available.

The beams were mounted on a rotational table at a distance of 11.8 mm from the X-ray source and the distance between the X-ray source and the X-ray detector was 1155 mm. It was ensured that the focal spot size of the X-ray tube was about 2 μm and therefore, a spatial resolution of 4 μm was achieved see Figure 3.13.

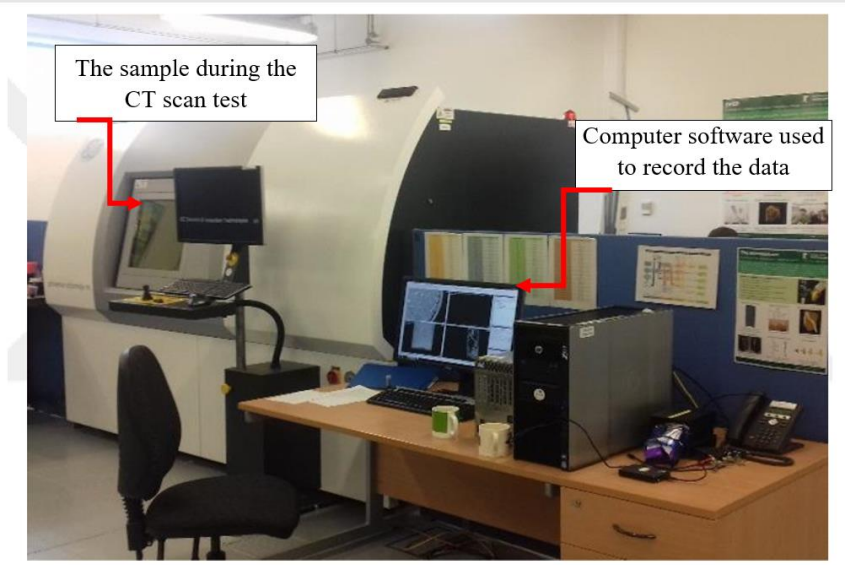


Figure 3.12: XRadia Versa XRM-500 scanner machine in Sutton Bonington campus.

Finally, the air void volumes and diameters in the test samples were analysed using the software Image. 3-dimnission representations of the air voids were made using MeshLab.

The reconstruction and corrections of scans were performed using Phoenix Datos X2 Reconstruction software. Once reconstructed into 3D volumes, 2D image slices were exported in TIFF format along the XY axis.

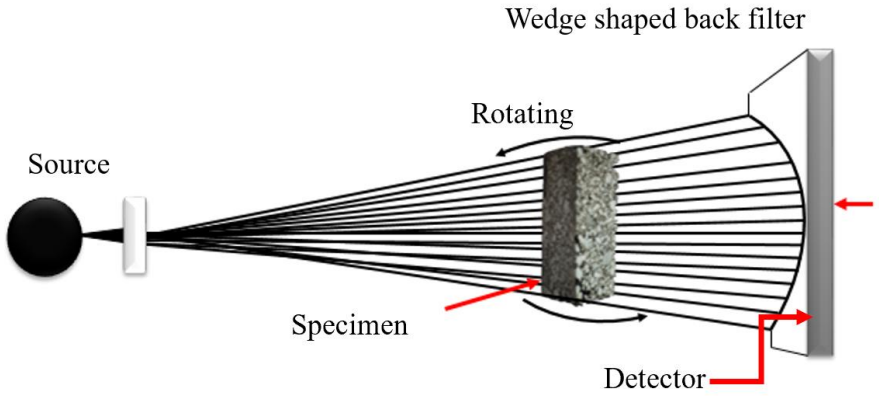


Figure 3.13: The X-ray scanning (plan view) illustration after [161].

3.7.1 Connectivity of pore network test

In Chapter 4, the connectivity of the pore network was required in order to analyse its effect on the heating/healing of asphalt. The air voids were digitally isolated using ImageJ, and the interconnectivity was evaluated based on the Euler number (χ) [162], which is a function of the number of isolated air voids (N), number of redundant connections in the air paths or genus (C) and the number of completely enclosed cavities (H), as follows:

$$\times = N - C + \mathrm{H} \tag{3.2}$$

These parameters were obtained using the BoneJ particle analyser plugin (version 1.3.11) in ImageJ. According to [163] negative values of χ indicate that the air voids have percolated, forming effective hydraulic conducts between the material's opposite surfaces as shown in Figure 3.14.

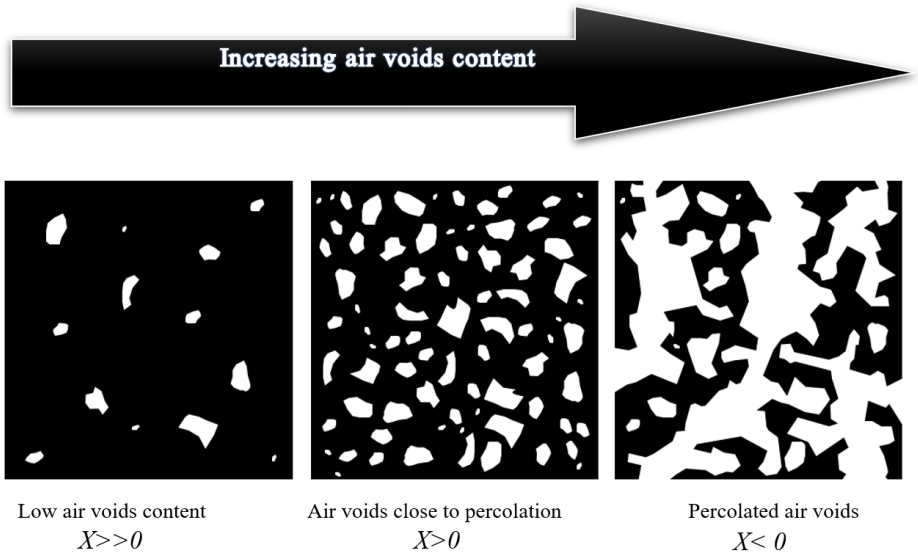


Figure 3.14: Binary 2D images of pore networks with a range of air void content and their correlation to the Euler number (χ).

3.7.2 Use of CT scans to determine the percentage of cracks healed

In order to quantify the width of cracks and the percentage of cracks that had healed in the asphalt, the test samples were fatigued up to a certain percentage of $N_{0.5}$, using the same procedure described in Section 3.4; then, prisms of 40 mm x 40 mm x 40 mm width were selected from the central part of each test sample (see Figure B.5 in Appendix B), to capture the most damaged area, and from the extreme of the test samples, to capture an undamaged area, and CT scanned. The total volume of air voids of the undamaged area (V_n) and the damaged area (V_d) were determined. These values were used to calculate the total volume of cracks in the test sample, as $V_d - V_n$.

$$Change\ of\ air\ voids\ due\ to\ loading\ = (\frac{V_d\ -\ V_n}{V_n}) \times 100 \ldots\ldots\ldots\ldots\ldots\ldots (3.2)$$

Next, the damaged prisms were induction-heated for 90 s, using the same procedure as explained above, allowed to rest for 2 h, to reach the ambient temperature and CT scanned immediately after. The total volume of air voids in the healed sample, (V_h), was determined.

$$Change\ of\ air\ voids\ to\ induction\ heating\ = \left(\frac{V_d - V_h}{V_d}\right) \times 100 \ldots\ldots\ldots\ldots (3.3)$$

3.8 Bulk density and air void content

The bulk density of the test specimens was determined according to [166] by dividing the dry mass between the volume of the test specimens, calculated as the dry minus submerged mass. The maximum density (ρ_m) of asphalt mixture was determined mathematically according to [167]. The mathematically method is calculated as the (dry mass divided by the measured volume of loose test samples). The maximum and bulk densities were used to calculate the Air Void Content (AVC) according to the following equation:

$$AVC = \frac{(\rho_m - \rho_b)}{\rho_m} \times 100\% \quad (3.4)$$

where ρ_m [168] is the theoretical maximum density of the mixture without voids in g/cm^3, ρ_b the bulk density in the mixture in g/cm^3, and AVC is the air void content in the mixture, in %.

3.9 Thermal expansion test

In order to measure the thermal expansion experienced by the material under temperature changes, prismatic 150mm × 60mm x 50 mm beams were first placed into a steel frame to avoid horizontal deformations due to consistency reductions during heating. Then, the samples and frames were conditioned into a temperature-controlled cabinet for 4 hours at 20 ± 1ºC.

Before starting the test, a Linear Variable Differential Transformer (LVDT) was set and zeroed at the upper surface's midpoint as shown in Figure 3.15. The test was carried out in a Universal machine at Nottingham university. Finally, the temperature was increased at a rate of 1.25ºC/min until reaching 60ºC, and the upper surface was continuously monitored.

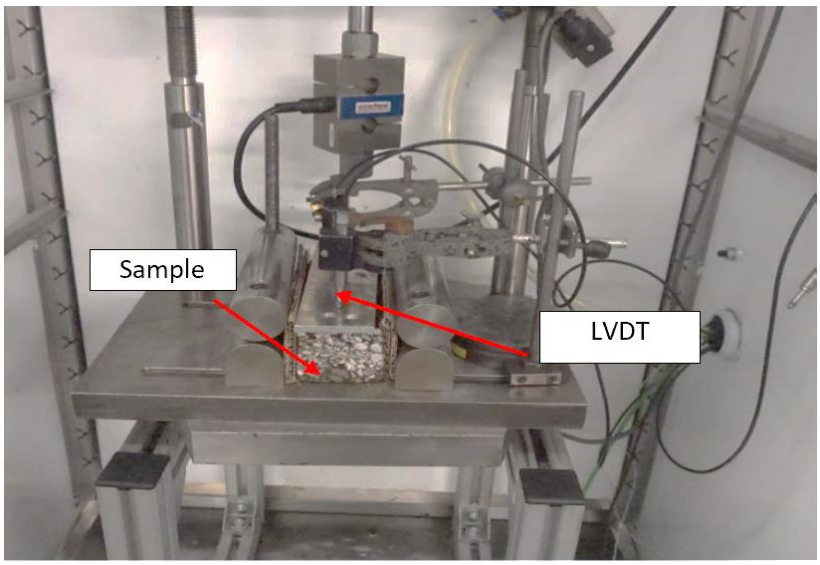


Figure 3.15: Setup for thermal expansion for mixture.

3.10 Indirect tensile stiffness modulus (ITSM)

In Chapter 5, to assess the effect of ageing due to induction heating on the stiffness of asphalt, the indirect tensile stiffness modulus (ITSM) of cylinders was calculated. This test was used, due to its being related to the capacity of the material to distribute traffic loads. The ITSM is a non-damaging and deformation-controlled test defined by BS EN [155]. Knowledge of stiffness modulus for any layer in a pavement is required for adequate structural design.

The ITSM was carried out using the Cooper's Nottingham Asphalt Tester (NAT) Machine, as shown in Figure 3.16. The configurations of the test are summarized in Table 3.5 below:

Table 3.5: ITSM test configuration depending on [155].

Item	Range
Specimen diameter	100±2 mm
Transient peak horizontal deformation	5±2 μm
Rise time	124±4 ms
Poisson's ratio (assumed)	0.35
Test temperature	20°C
Specimen thickness	40-80 mm

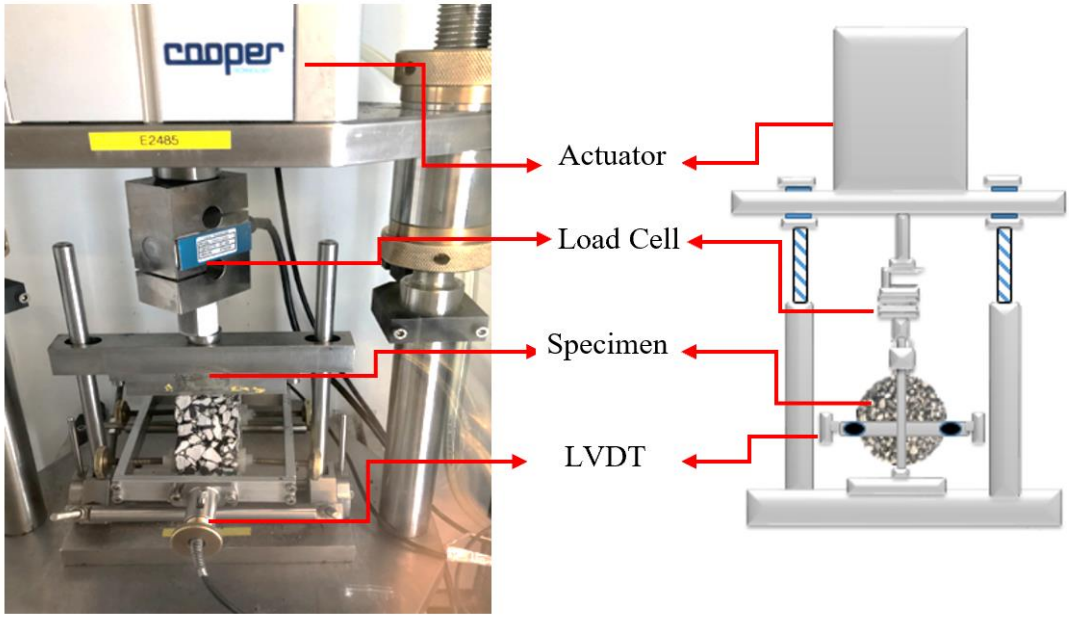


Figure 3.16: Indirect tensile stiffness test setup.

3.11 Fourier Transform Infrared Spectroscopy (FTIR)

FTIR is the technique utilized to measure the oil release from the capsule. A Fourier Transform Infrared Spectroscopy (FTIR) spectrum model Bruker Tensor 27 was used, as shown in Figure 3.17.

The FTIR test was used spectrum model Bruker Tensor 27 see Figure 3.17. The process was set in the absorption mode, in the wavenumber band range of 400 to 4000 cm^{-1} at a resolution of 4 cm^{-1}. The oil influence on the bitumen was assessed by changes in the optimum absorbance between wavenumbers 1700 and 1800. The selection of these wavenumbers is recommended by methodology of [159].Vegetable sunflower oils have a distinct peak at ~1745 cm^{-1} , while the bitumen has zero index in this range as seen in Figure 3.18.

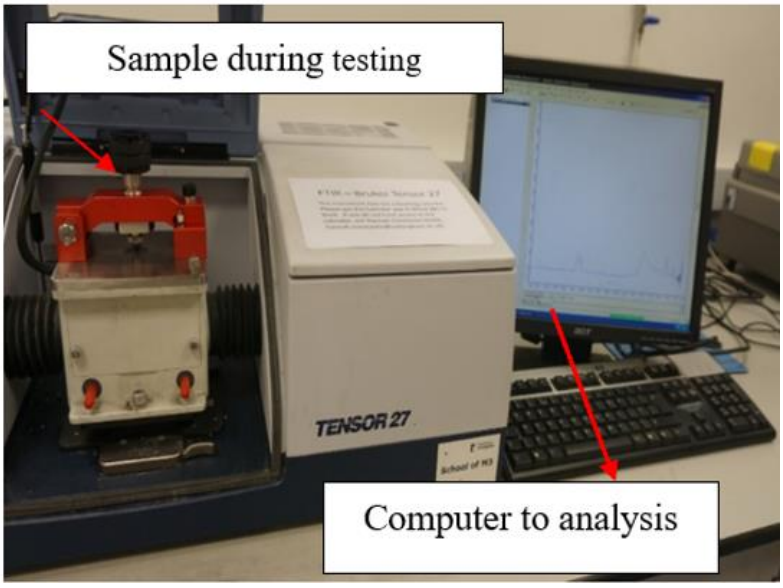


Figure 3.17: Fourier Transform Infrared device.

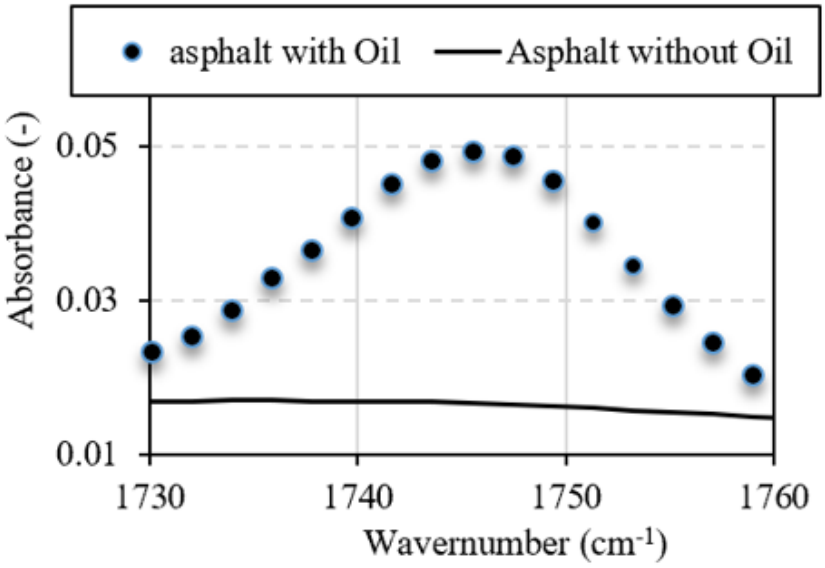


Figure 3.18: FTIR curves for asphalt mixture samples with and without oil.

3.12 Summary

In this chapter, the different asphalt materials and self-healing agents that could fulfil the project's aims and objectives have presented. These materials have consisted of Dense Asphalt (DA) (also called 5% because of its air void content) and mixtures with 10%, 13%, 21%, and 26% air void contents. They have been selected because of their variety of air voids (to know the influence of air voids on the self-healing). Also, porous asphalt (PA), stone mastic asphalt (SMA) have utilized as well. These mixtures have selected because of the most commonly used surface courses in Europe.

In addition, to promote the self-healing,1.1% of fibre has added to PA, which is an optimum amount of fibre that maximizes the healing and does not affect the mechanical properties, and 0.5% of capsules has added to DA, PA, and SMA to evaluate the effectiveness of using encapsulated oil in order to improve the self-healing properties of asphalt mixture with a range of gradations .

Mechanical test to quantify the self-healing has evaluated when the samples tested to fatigue under modified three-point bending fatigue configuration at 20±2^{o}C which ensured the formation of vertical cracks at the midpoint. Additionally, three methods to induce a self-healing namely infrared heating, induction heating and encapsulate rejuvenator have used. X-Ray Computed Tomography (CT Scans) has used to evaluate air void distribution before and after healing. However, there are additional testing have used namely thermal expansion, stiffness modulus, Also Fourier transformed Infrared Spectroscopy (FTIR) has used to evaluate oil release in the asphalt mixture. Finally, the main objectives for this thesis, are studied in the next chapters

Chapter 4: Effect of porosity on infrared healing of fatigue damage in asphalt

4.1 Introduction

This chapter aims to understand the effect of air void content on the healing capacity of asphalt mixtures by using infra-red healing. In Chapter 2 it was shown that asphalt mixture is a self-healing material, and there are different artificial healing techniques that have been studied by many researchers previously. However, the healing phenomenon related to fatigue damage has not been yet been studied in depth. Hence, the first objective of this Chapter is to understand, at a fundamental level, the effect of air voids content on the healing capacity of fatigue damage in asphalt mixes.

For that, the natural heating effect, produced by the Sun on asphalt roads and simulated by means of infra-red heating was considered and parameters, such as (i) extension of fatigue life; (ii) optimum number of cycles at which to apply the thermal treatment

(N_{opt}); (iii) evolution of internal pore structure during both damaging and healing processes; and (iv) material thermal expansion, have been studied experimentally for a wide range of asphalt mixes with different air voids contents.

4.2 Experimental summary

In this Chapter, infrared heating has been used as the self-healing technique, to simulate the heating by solar radiation as described in Section 3.6.1. This Chapter was described tests on asphalt mixture samples using five different air void contents, 5%, 10%, 13%, 21% and 26% as can be seen in Figure 4.1, with corresponding gradations in Table 3.4 in Chapter 3. Air void content may play a key part in determining the self-healing properties of an asphalt mixture [11]. The methodology of the Chapter is summarized in Figure 4.1.

All the specimens used had dimensions 150 mm x 60 mm x 50 mm beams obtained by cutting 306 mm x 306 mm x 50 mm slab into eight beams see (Section 3.4 in Chapter 3 and Figure B.3 in appendix B). The test was carried out at a constant temperature., the asphalt beams were subjected to dynamic cyclic loading under 3-point bending at 20 ± 1ºC, see Section 3.5, with maximum loading value 2.5 kN, minimum 0.15 kN to insure an attached the actuator with the sample, and resting period of 0.15 s included between consecutive loads.

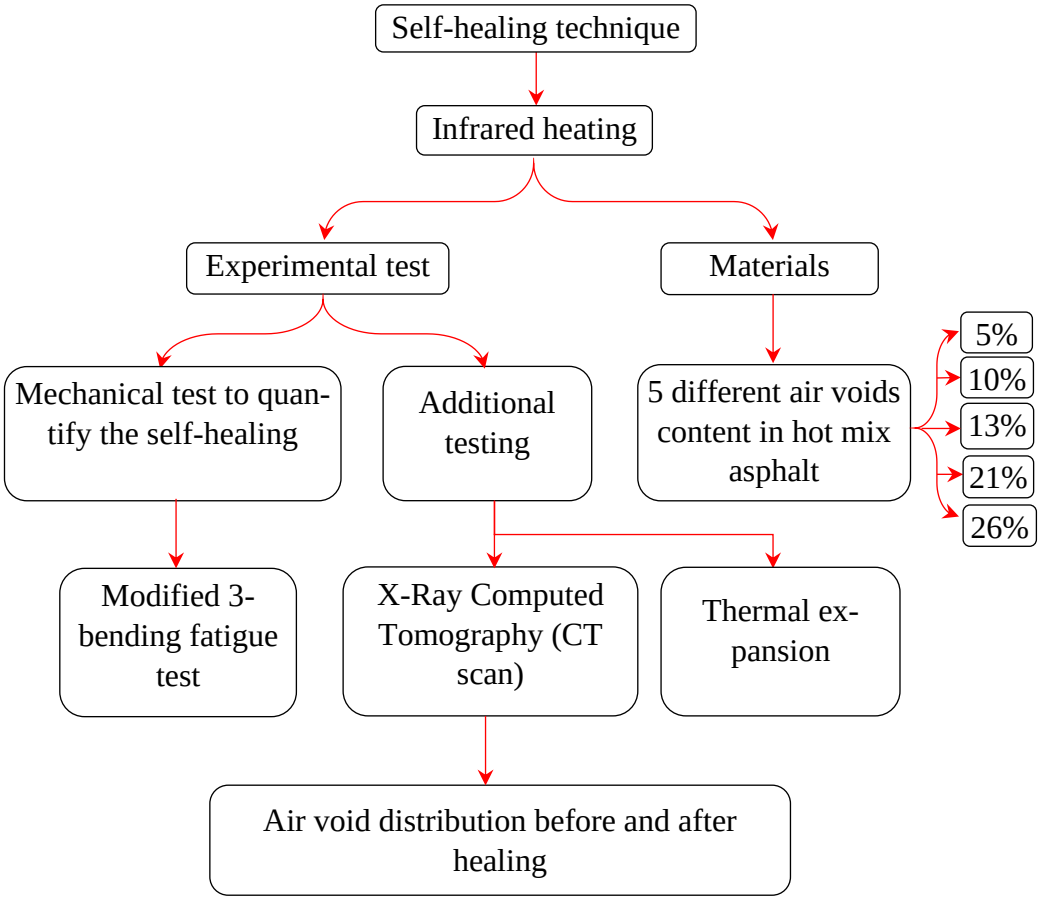


Figure 4.1: Experimental methodology used in Chapter 4.

Finally, in order to detect small cracks during the fatigue tests, a uniformly white marking spray paint was applied to one of lateral 150 mm x 50 mm sides (see Figure B.4 in appendix B).

4.3 Results and Discussion

4.3.1 **Service life of asphalt samples**

In order to evaluate an asphalt mixture's capacity to extend its service life when subjected to a thermal treatment, many samples were manufactured and tested as described in Sections 3.4, and 3.5. The results of the probability for breaking the test samples is presented below in Figure 4.2, which shows a certain number of loading cycles fitted by the Weibull distribution and depending on the air void content. The reference number of cycles value $N_{0.5}$. As can be seen, the curves tend to get shifted to the left for asphalt with higher air voids. In other words, the probability of breaking the material at a certain number of cycles increases.

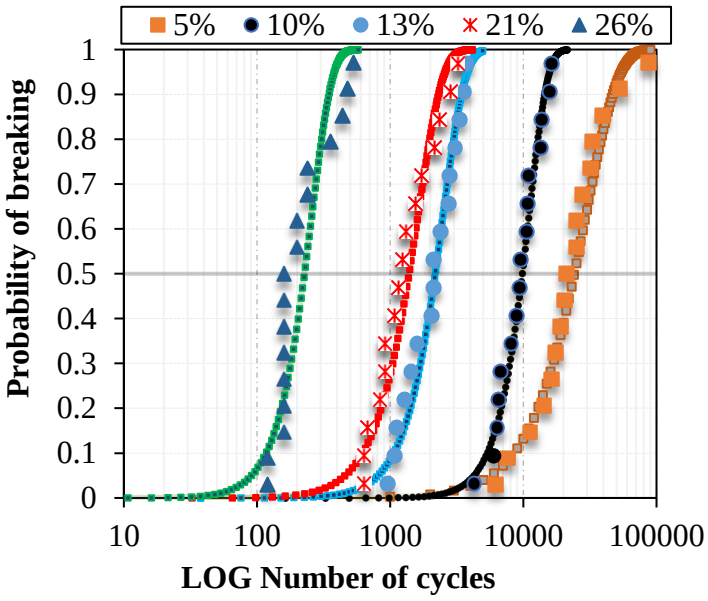


Figure 4.2: Probability of breaking and number of cycles for a probability of 0.5.

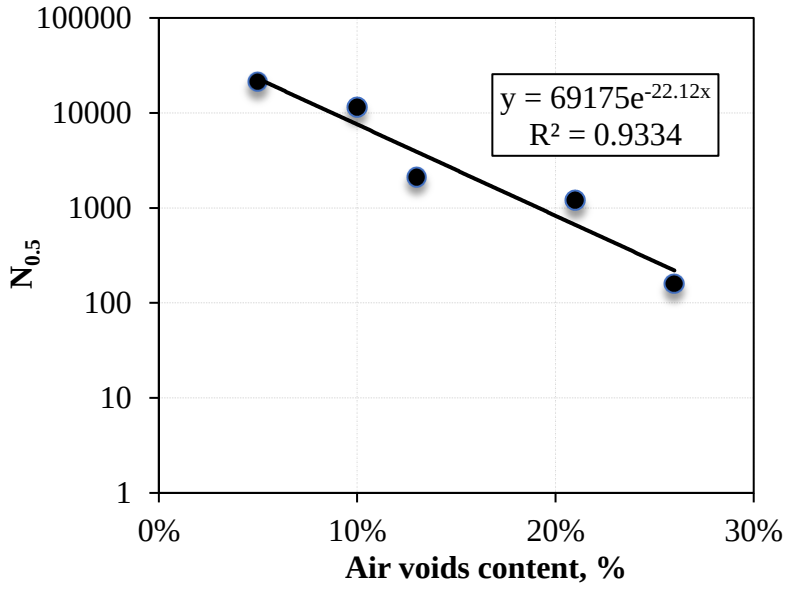


Figure 4.3: Probability of breaking obtained for the studied materials with different air voids contents.

At the 0.5 probability, the reference number of cycles $N_{0.5}$ was obtained (21160 cycles for 5%, air void content, 11440 for 10%, 2120 for 13%, 1200 for 21%, and 227 for 26%). This reference value is also shown in Figure 4.3, for the different materials, and, as can be seen, it is inversely related to air voids content through an exponential function. Hence, the best mechanical performance was obtained for mixes with the lowest air void content (5%), but small increases in the air void content produced sharp reductions in the asphalt life durability, e.g. $N_{0.5}$ reduced by 45.9% when the air voids content was increased from 5% to 10%.

4.3.2 **Asphalt test sample temperatures during the heating treatment**

In this Section the temperature effect during the heating treatment was studied by repeating for the mix with 5% air voids content, the same tests as described in Section 3.6.1. The results in Figure 4.4 below show the surface temperature evolution of asphalt with 5% air voids content when placing the lamps at 30 cm, 70 cm and 110 cm over the test samples.

The maximum temperatures reached by the samples are considerably different and they vary with the distance between lamp and surface (93ºC at 30 cm, 71 ºC at 70 cm, and 51 ºC at 110 cm). Also, significant differences between the temperatures of top and bottom surfaces were observed.

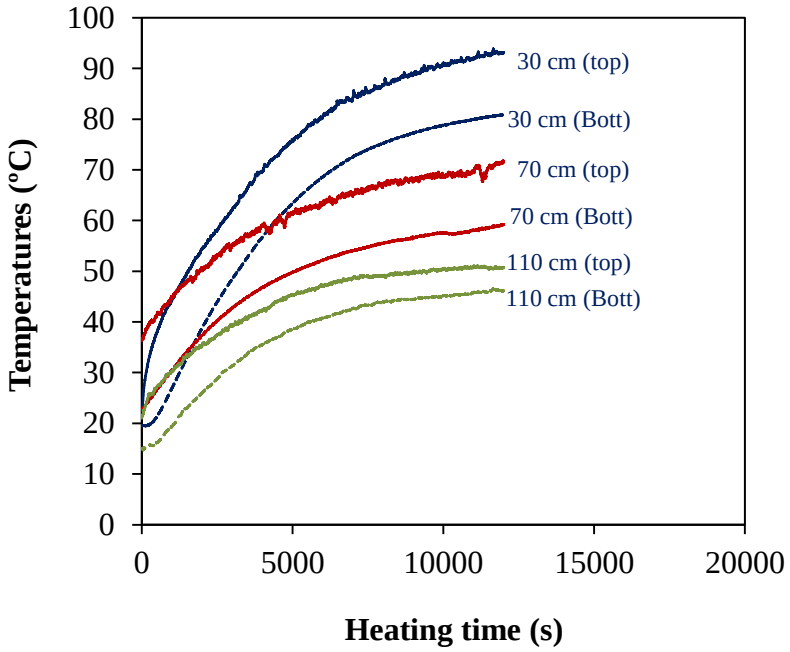


Figure 4.4: Evolution of temperature with the heating time for different distances between sample and lamps.

These differences were around 12ºC when the samples were placed at 30 and 70 cm, but approximately 5ºC when the distance was 110 cm. This indicates that when the energy applied is very high, the dissipated energy produced by the differential temperature between sample and ambient air is higher than the energy that the material can transmit downwards by conduction.

Below a threshold temperature of approximately 60ºC, both surfaces reached a steady-state equilibrium where the top and bottom temperatures were not excessively dissimilar. Figure 4.5 shows, for samples with different air voids contents, the steady-state temperature reached by the upper and lower surfaces during a heating period of 200 min with the lamps placed at 110 cm above the specimens.

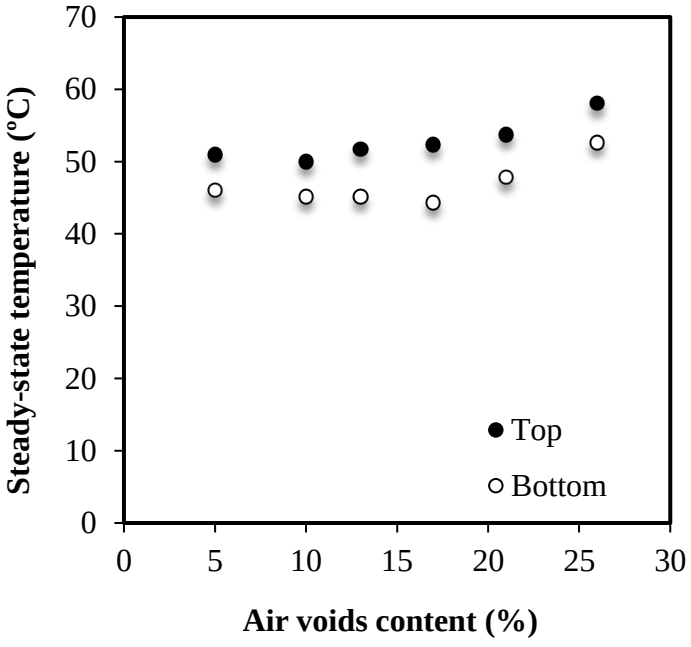


Figure 4.5: Steady-state temperatures reached by samples with different air voids.

As can be seen, all the test samples reached similar temperatures, within the range of 50 ºC – 58 ºC for the upper surface and 44 ºC 52 ºC for the lower. Both, top and bottom temperatures tended to slightly increase with the air voids content, due to the greater exposed surface that air voids produce. The analysis of how temperature variations, due to changes in infrared energy and air voids content, affect the healing of cracks and the consequent service life extension is detailed in Section 4.3.3.

4.3.3 **Service life extension by infrared heating**

To show the extension of service life, the asphalt mixtures were subjected to a thermal treatment represented by infrared heating as shown in Section 3.6.1. The results are showed in Figure 4.6. The healing index is obtained after applying 200 min of thermal treatment, (determined as the time required to achieve a steady state) after various numbers of cycles.

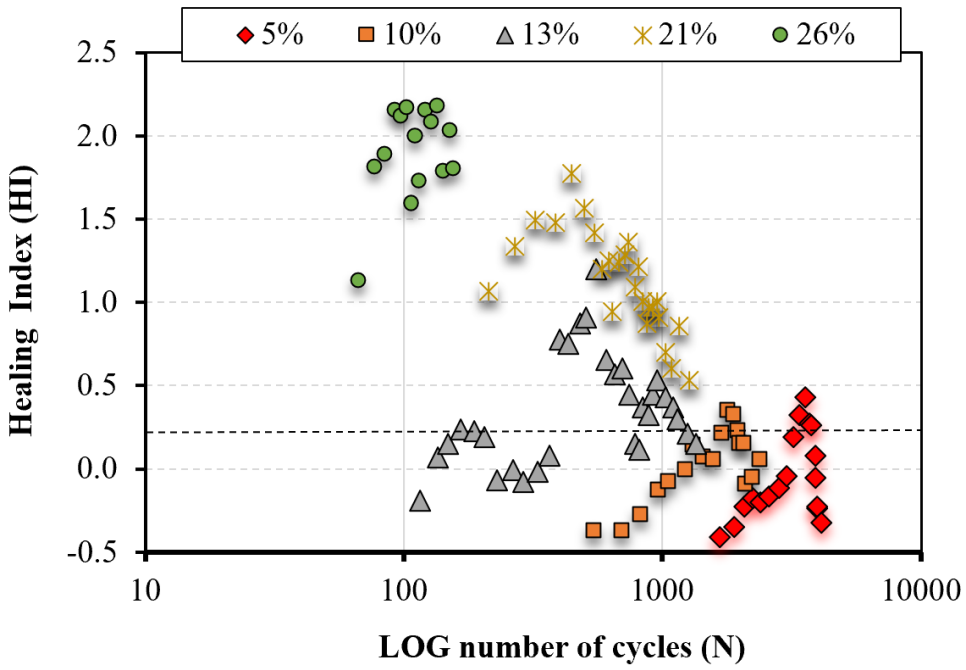


Figure 4.6: Healing index obtained for samples with different air voids content.

The first fact that can be observed is that all the curves present an approximate bell shape, see Figure 4.6, which indicates that when the cracks are still small, the service life cannot be significantly extended, while when the cracks are too wide, the healing becomes more difficult see Figure 4.7.

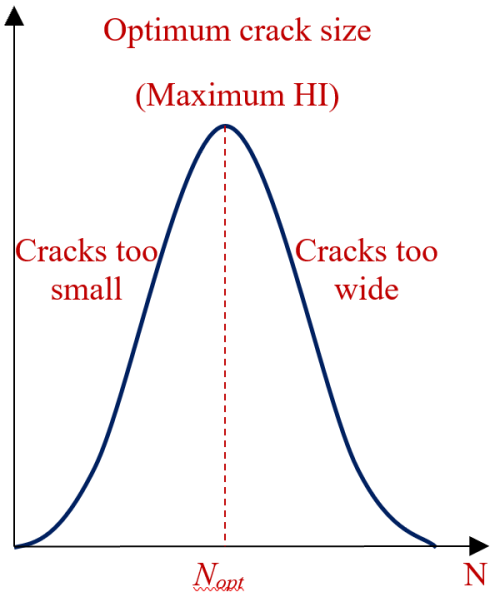


Figure 4.7: Schematic simplification of obtained curves subjected to thermal heating at different numbers of cycles.

Therefore, there is an optimum number of cycles (N_{opt}) for each material, at which the healing index is maximised. These values were 3562, 1802, 476, 445 and 136 for mixes with 5%, 10%, 13%, 21% and 26%, respectively see Figure 4.8. N_{opt} decreases as the air voids content increases in the mix. Figure. 4.8, also shows this sharp decrease in the optimum number of cycles when the air voids increase.

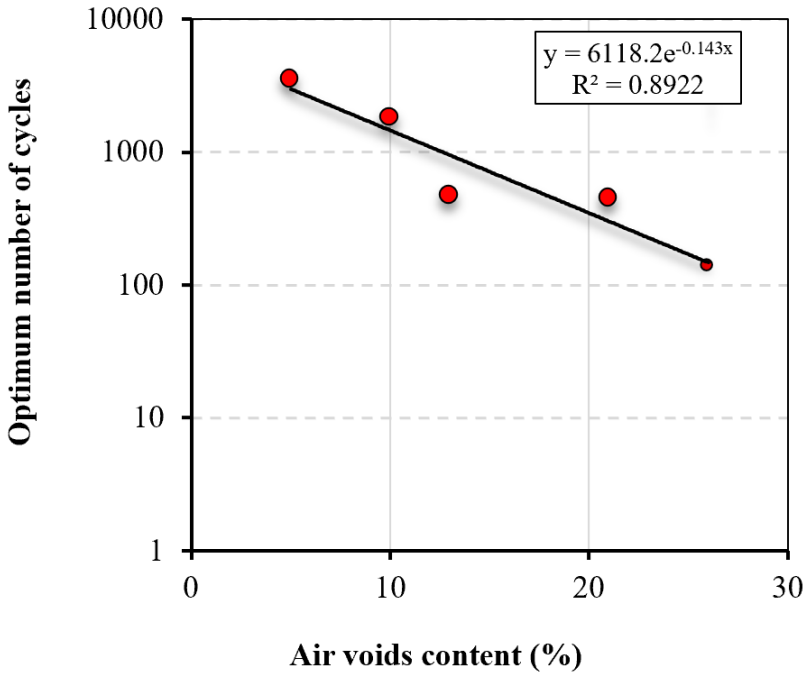


Figure 4.8: Optimum number of cycles and healing index.

Another aspect, which can be observed in Figure 4.6 and is summarised in Figure 4.9, is that the healing index tends to increase linearly with the air voids content (correlation coefficient R^2=0.938).

Nevertheless, although the service life of porous asphalt test samples can be extended by up to 200% due to the thermal treatment, their original fatigue life was noticeably shorter, as has been explained in Section 4.3.1. Therefore, despite the thermal treatment, the fatigue life of dense asphalt mixes is still significantly longer than that of porous asphalt mixtures, see Table 4.1.

Table 4.1: Comparison between the numbers of cycles resisted by test samples without thermal treatment ($N_{0.5}$) and total number of cycles resisted by test samples after applying a thermal treatment.

Air void content	Fatigue life without thermal heating ($N_{0.5}$)	Longest fatigue life with thermal treatment	Increase
5%	21160	30218	42.80%
10%	11440	15419	34.80%
13%	2120	4657	119.70%
21%	1200	3333	177.80%
26%	227	721	217%

In Figure 4.9 it can also be seen that samples wth high air voids content may reach HI-values that are higher than 2.

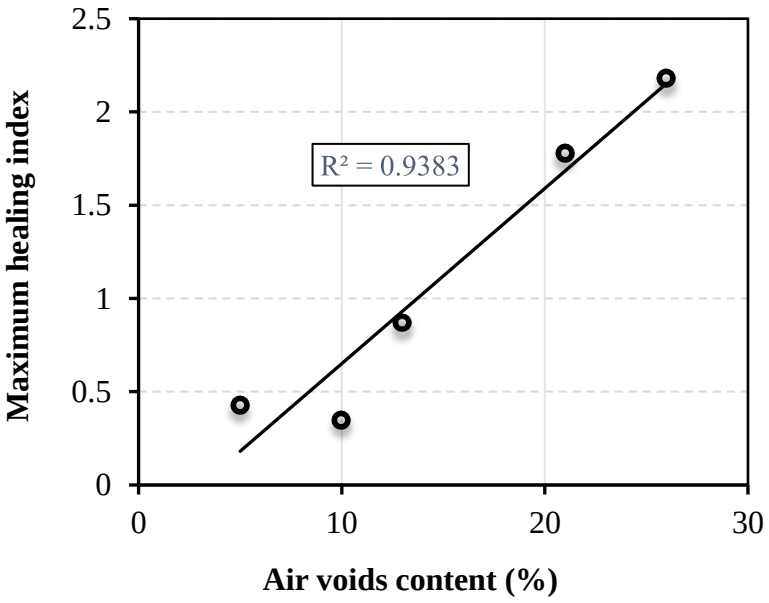


Figure 4.9: Optimum number of cycles obtained for samples with a range of air void contents.

That HI values are higher than 1 (see formula 3.1 in Section 3.5 in Chapter 3), means that not only were cracks healed, restoring the original service life, but also that the material's properties must have been modified obtaining samples with improved fatigue resistance. The reasons behind this behaviour will be studied in Section 4.3.5.

On the contrary, most of the test samples with air void content lower than 13% registered lower healing indexes, such as averaging 0.43 and 0.35 for test samples with 5% and 10% air voids content, respectively. This means that the healing capacity of dense asphalt mixes is limited. The reason for this could be that porous asphalt test samples may reach slightly higher temperatures than denser asphalt types [40].

Consequently, in porous asphalt, the viscosity of bitumen and the density of the air inside cavities would be slightly lower, which improves the capillary flow of bitumen through cracks. However, it is believed that the small temperature differences between dense and porous asphalt materials would only marginally contribute to the significant differences observed in the healing results.

Another explanation is that cracks in porous asphalt are more prone to happen through the mastic connecting the aggregates (weak points) while a higher packing level of particles in dense asphalt produces more cracks through aggregate particles. These cracks could be filled with bitumen, but the final strength would never be as high as the original aggregate.

Additionally, it must be noticed that the bell-shape curves, in dense mixes, are very sharp. Hence, when the healing treatment is applied at a number of cycles slightly higher or lower than the optimum, dense asphalt samples will not recover their fatigue

resistance. Thus, it could be very difficult to design an effective maintenance plan that meets the optimum number of cycles and obtains a significant service life extension.

Moreover, the values can even become negative, which means that the samples could be damaged instead of healed. Read [8], explained that the coefficient of thermal expansion of bitumen ($6 \cdot 10^{-4}$/ºC) is more than one order of magnitude higher than the coefficient of thermal expansion of the asphalt mixture ($3 \cdot 10^{-5}$/ºC).

According to Gámez et al [11] this differential expansion, together with reductions in bitumen viscosity during heating, plays an important role in asphalt healing by forcing the melted bitumen to drain through large cracks. However, fatigue cracks produced during the early stages have reduced dimensions. Thus, in dense mixtures, the internal pressure generated by bitumen may damage the asphalt mixture and reduce its fatigue life see Figure 4.10.

In this healing-damaging process, the content of fine particles in the mix (e.g. filler) might also play an important role, although it is not clear whether positive or negative. For instance, higher contents would reduce the interstitial space between aggregates, increasing capillary forces and consequently improving the flow of bitumen through cracks. On the other hand, the mastic would be denser and with higher viscosity, which would produce a detrimental effect on healing capacity.

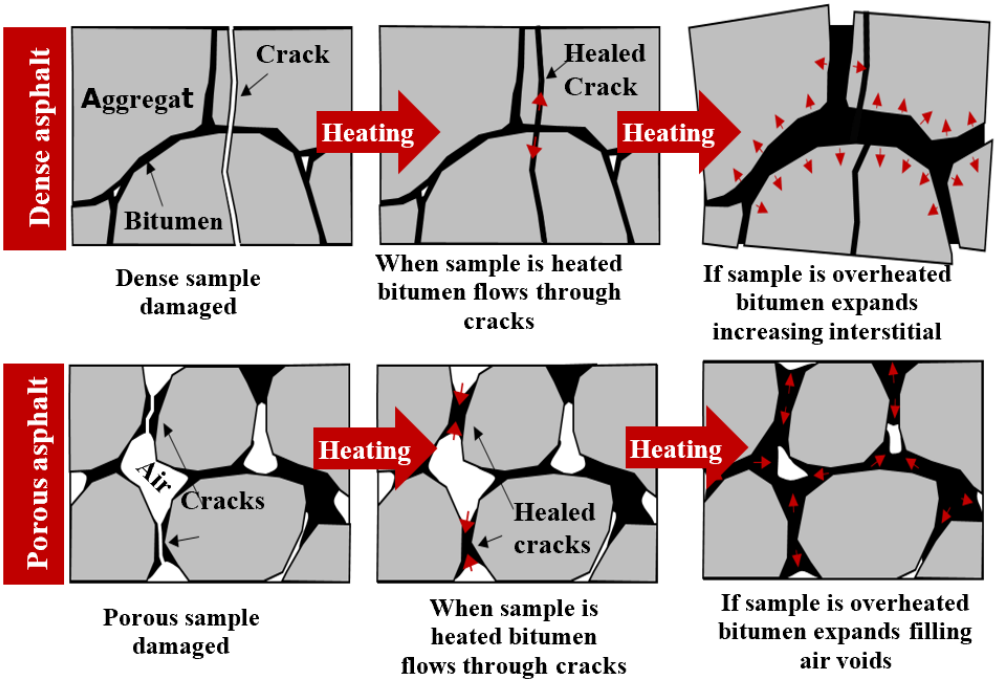


Figure 4.10: Phenomena happening inside dense (top) and porous asphalt (bottom) during heating.

In the present investigation the content of bitumen was reduced with the content of fine particles, so the effect could not be properly identified, leaving it as a feasible hypothesis to be confirmed or rejected in future investigations.

4.3.4 Effect of temperature on asphalt self-healing

To observe the temperature and heating rate's influence on asphalt self-healing, (see Figure 3.6 Section 3.6.1 for the setup using infra-red heating), different distances of the lamps from the surface were used to achieve the different temperatures, and the results are shown in Figure 4.11. As the distance between sample and lamp was reduced from 110 cm to 70 and 30 cm, this increased the steady-state temperature from 51ºC to 71ºC and 93ºC respectively. The tests were repeated for samples with 5% air

voids content. As seen in Figure 4.11, the curves observed at 51ºC and 71ºC were very similar, although the peak value result at 71ºC (HI=0.43) was 55.4% lower than at 51ºC (HI=0.24). On the other hand, when the temperature was increased to 93ºC, the results became significantly lower, with a peak value of -0.02, which is 104.7% lower than at 51ºC and negative, and means that the treatment produced more damage than, healing. This suggests that it is not possible to extend dense asphalt's service life by applying a thermal treatment at that temperature.

This may be because bitumen drainage through pores and cracks grows with the heating rate and temperature and, if these are too high, internal pressure increases may damage the material.

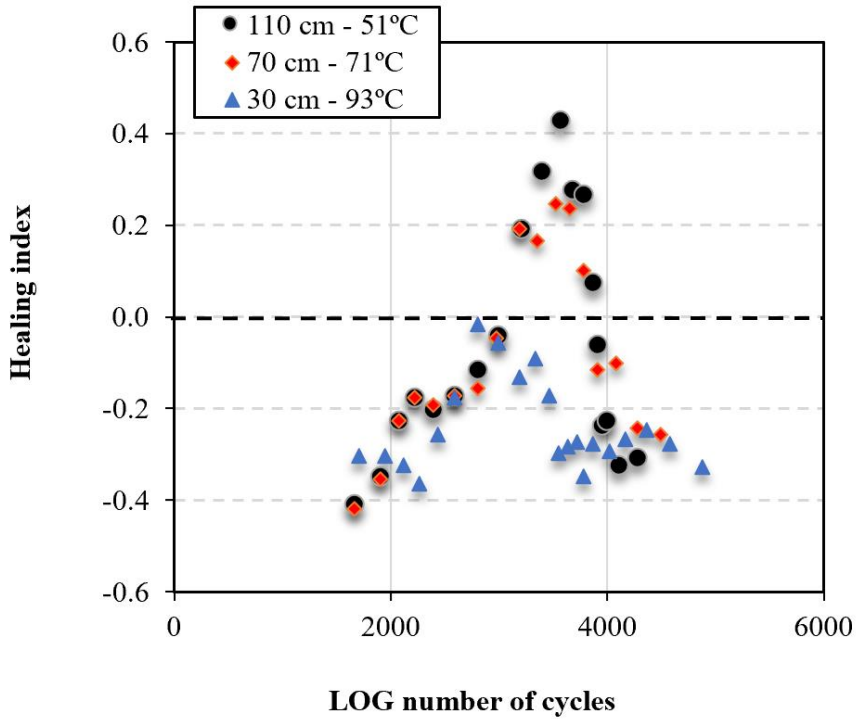


Figure 4.11: Healing index obtained for samples with 5% air voids content that have been subjected to thermal heating at different numbers of cycles and temperatures and different distances (110cm, 70cm, and 30cm).

4.3.5 Evolution of internal air voids distribution after heating

Air void content is considered a key parameter in understanding the thermal healing of asphalt. As explained in Section 3.7, the CT scan test was used to observe the distribution of the air voids within the materials on samples with 5% and 21% air voids content. Results are shown in Figure 4.12. CT-Scans were repeated:

- Before applying any loading cycle to the samples,
- At the optimum number of cycles for thermal heating (3562 cycles for 5% air voids content and 445 cycles for 21%) before, and,
- After applying the heating treatment.

It can be seen, first, that the initial average air void content matches the design content with an error of less than 10%: 4.49% and 21.67% respectively. In both cases, it is also noticeable that the final air void content after applying the heating treatment is significantly lower than the initial: 3.55% and 18.8% (decreases of 20.9 % and 13.24% respectively). Since no compressive loads were applied during the thermal treatment, these air void content reductions match the hypothesis given above that bitumen flows into pores and cracks.

Additionally, the porosity of dense mixtures is reduced by 20% of initial value, which means that the bitumen could be able to flow and close the cracks, for this densification to happen, which could be the reason for the process of self-healing. This hypothesis will be proven in the following chapters.

Finally, it can also be noticed that repeated loading cycles did not significantly densify dense asphalt mixtures or change their air void content distribution. On the other hand,

in porous mixes, the material experienced an internal rearrangement of aggregates and a densification during cyclic loading.

The thermal treatment did not significantly contribute to reducing the air void content of porous asphalt, as in this case the bitumen could expand through a wide network of percolated pores. However, once the material cooled down, the new mix was rearranged of the sample and, as a result, the extension of its service life went further than simply 100%, as described in Section 4.3.3.

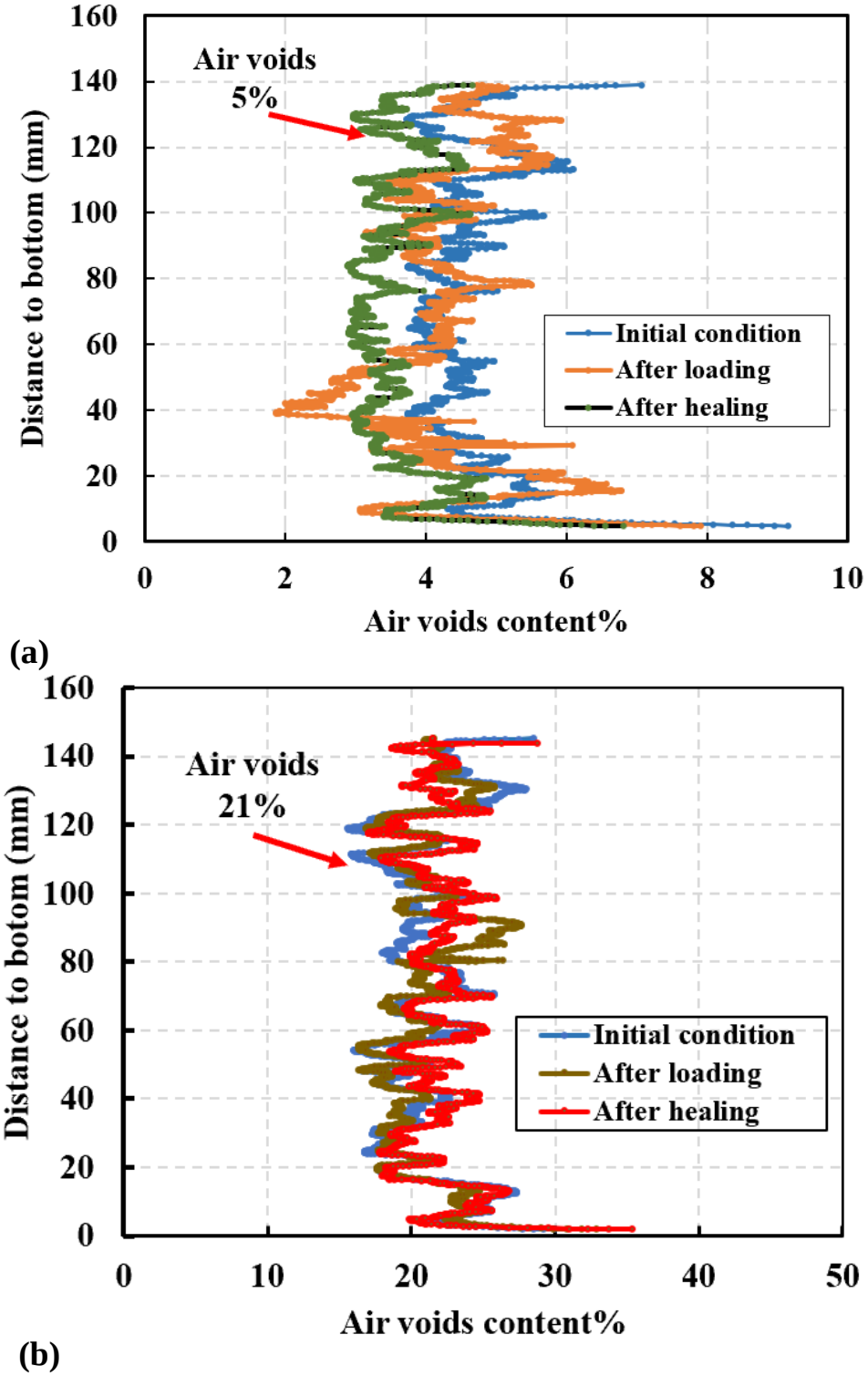


Figure 4.12: Air voids distribution for samples with 5% (a) and 21% (b) after production (new) and at the optimum number of cycles before (optimum) and after applying thermal heating (healing).

4.3.6 **Thermal expansion of asphalt during the heating treatment**

Moving to another key parameter that affects self –healing, thermal expansion was measured using by a Universal machine at the University of Nottingham as shown in Chapter 3 Section 3.9. The results of test can see below in Figure 4.13. To support the hypothesis of bitumen expanding inside the internal pore network, thermal expansion tests were carried out. It can be noticed that the height of asphalt samples increased in with increasing temperature during the first stage of the test. Then, at around 40ºC, the viscosity of the binder reduced to allow the sample to collapse. Additionally, it was found that:

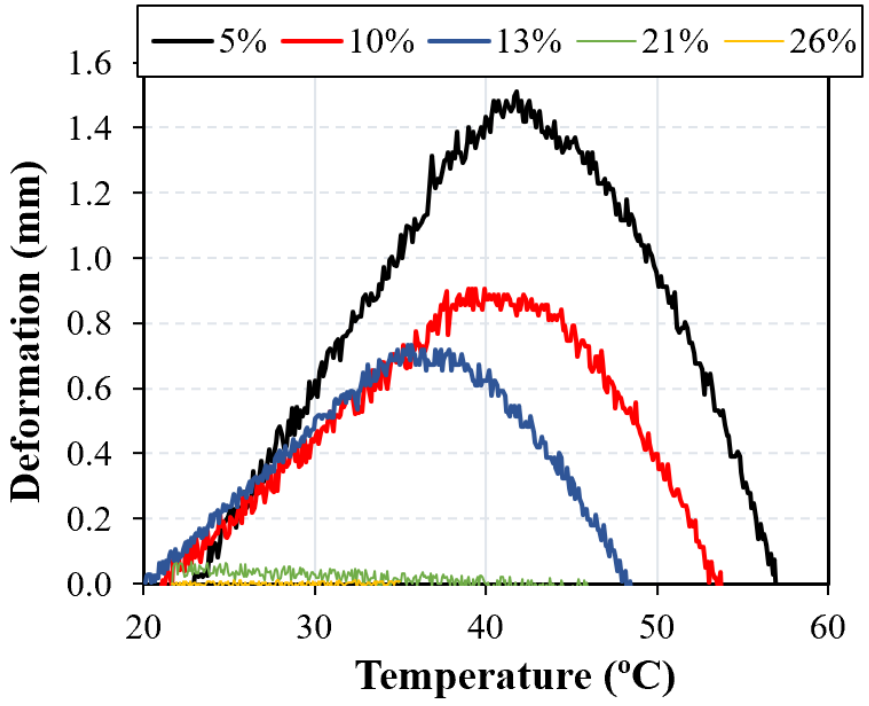


Figure 4.13:Thermal expansion of asphalt samples with different air voids contents and at different temperatures.

I. Only test samples with air void content up to 13% experienced significant thermal expansion, and.

II. The magnitude of expansion is inversely related to the air void content in the mixture,

Test samples with air void content lower than 13% presented low healing levels (HI<0.5), where HI is derived shown in formula 3.1 in Section 3.5 in Chapter 3. Additionally, the air void content tended to 0 after the heating treatment. Finally, asphalt mixtures with air void content lower than 13% experienced thermal expansion when the temperature was increased.

On the other hand, asphalt mixtures with air void content higher than 13%, presented optimum number of cycles to apply the heating treatment lower than that of asphalt test samples with air void content lower than 13%.

It is therefore demonstrated that the reduced interconnectivity of pores of dense asphalt mixture, and its consequent reduced capacity to allow bitumen flow during heating, is the most feasible explanation for the reduced healing capacity of dense asphalt mixture.

4.3.7 **Influence of pore network connectivity on asphalt self-healing**

Connectivity is another aspect that affects self- healing in asphalt as broadly explained in Section 3.7.1. The results can see below in Figure 4.14. The pore network connectivity of asphalt samples with various air void contents was evaluated through the Euler number. The air void content at which the Euler number passes from positive to negative, is the minimum content that produces the percolation of air cavities and creates effective conducts able to transport fluids such as air, moisture or bitumen, between

sample surfaces. As seen in Figure 4.14, the percolation of air voids happened at around 13% air void content.

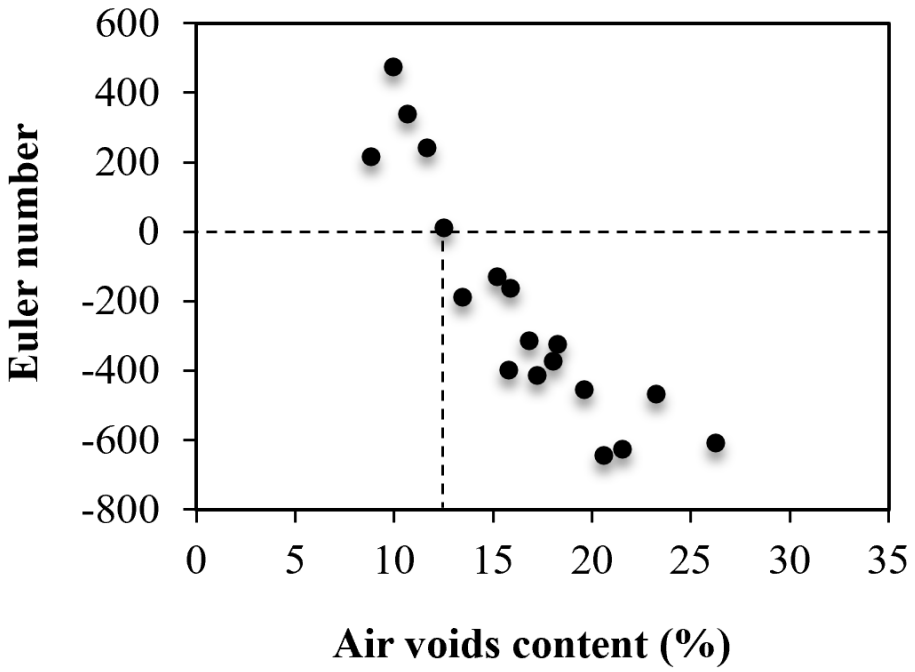


Figure 4.14: Euler number obtained for test samples with different air voids content.

4.4 Summary of Chapter

This chapter has explored the effect of air voids content and their interconnectivity on the capacity of asphalt mixtures to heal fatigue cracks when a thermal infrared treatment has applied. Results have shown that the percolation of air voids is required to optimise healing results. In samples with a lower content, the thermal expansion of bitumen and its flow through cracks can exceed the pore network's capacity. As a consequence, the internal pressure can increase enough to produce material damage instead of healing. The optimum moment in porous asphalt when healed the crack is studied in the next chapter.

Chapter 5: Optimum moment to heal cracks in asphalt roads by means electromagnetic induction

5.1 Introduction

The main aim of this chapter is to provide an indication of the best moment to heal an asphalt road in order to repair cracks, something which has not been tested before. In Chapter 4, it was concluded that porous asphalt was the mixture with highest natural self-healing capacity. Furthermore, it was found that there is an optimum moment when the application of heat causes the highest life extension. The limitation was that the duration of the heating applied by means of infra-red lamps was unrealistically high to get benefits from the self-healing.

For this reason, Chapter 5 will focus on using induction heating to accelerate the self-healing of asphalts and the study will be done on porous asphalt (PA), since it is the type of mixture with the highest healing capacity. Induction heating consists of mixing electrically conductive particles, such as steel wool fibres, into the asphalt mixture and heating them when the road surface starts developing cracks.

By doing this, the temperature of the bitumen around the metallic particles will increase, which will contribute to reducing the viscosity of bitumen, and the bitumen will expand, which will push it into empty spaces, such as cracks or air voids.

5.2 Experimental program

This Chapter makes used of induction heating, which has been described in Section 3.6.2. The porous asphalt had 20 % air void contents and was composed of crushed limestone aggregates, bitumen and steel wool fibre as shown in Table 3.4, see Section 3.2. The aggregate had maximum size 20 mm and density 2,596 kg/m^3, the gradation is shown in Table 3.4. Figure 5.1 shows a summary of all the tests done in this chapter.

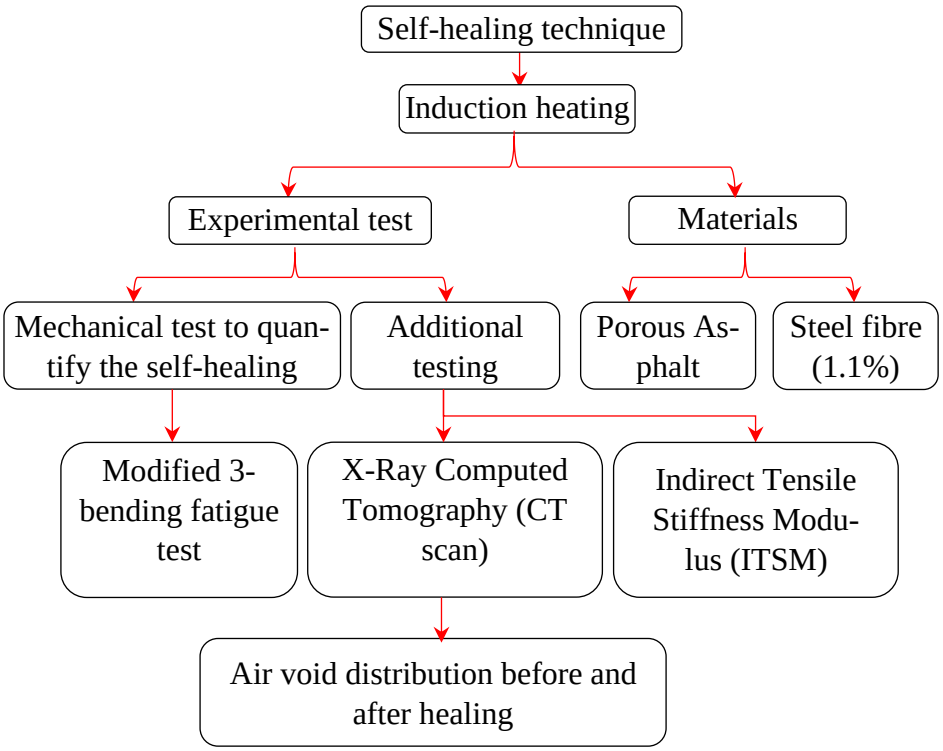


Figure 5.1: Summary of the methodology used in Chapter 5.

The different sample geometries used in this chapter were (i) 150 mm x 60 mm x 50 mm, (ii) 150mm x 40mm x 40mm, and (iii) 100 mm(diameter) x 40 mm (see the geometries in Section 3.4) for 3-point bending fatigue (see Section 3.5), Computed Tomography scans (see Section 3.7), and Indirect Tensile Stiffness modulus tests (see Section 3.10), respectively. The loads were 1.25kN, 1.50kN, 1.75kN, 2kN, for the 3-point bending fatigue and 0.7kN, 0.5kN for CT scan tests (see Figure B.5 in Appendix B), which have been described in Section 3.5.

Finally, the percentage of steel wool fibres has been shown in Table 3.3. The steel wool had an average length of 1.4 mm and a diameter 40 μm. Its content was 1.1 % by mass of mix as shown in Table 3.4, in Chapter 3.

5.3 Results and discussion

5.3.1 Fatigue durability of asphalt samples

The loading levels that were used in this chapter are: 1.25kN, 1.50kN, 1.75kN, and 2kN, see Section 3.5. The results are presented in Figure 5.2, which shows the Weibull distribution of the number of cycles resisted by the test samples under the action of a range of load levels.

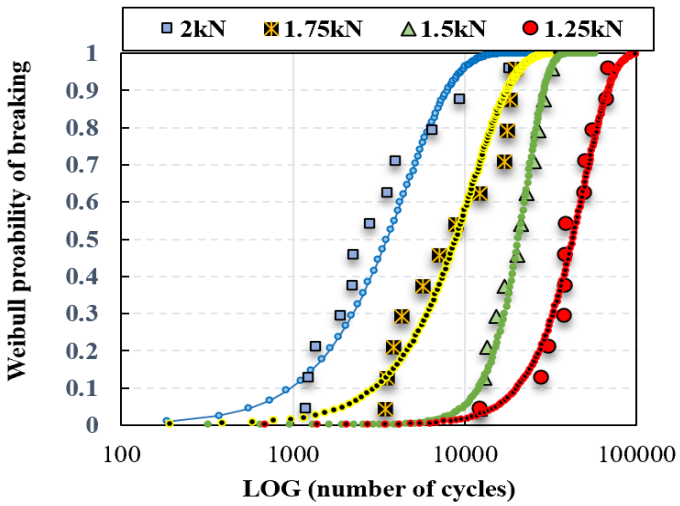


Figure 5.2: Probability of breaking the test samples at the load levels studied.

these curves represent the cycles resisted without resting periods. As in the previous chapter, these curves have been used to find $N_{0.5}$, which is the number of cycles when the probability for breaking is 0.5.

Figure 5.3 shows the relationship between $N_{0.5}$ and the maximum dynamic loads. This is the Wöhler curve. Increases in the load level produced exponential reductions in the fatigue life.

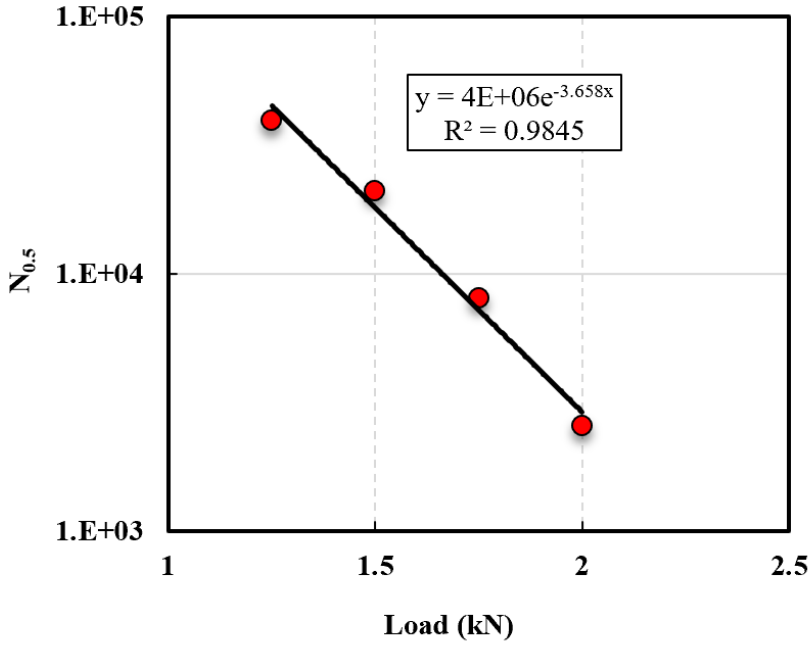


Figure 5.3: Wöhler curve for $N_{0.5}$ probability.

Hence, the $N_{0.5}$ values for 150x60x50 mm^3 specimens were applied in different loads as shown in Table 5.1, respectively. Furthermore, the $N_{0.5}$ values for 150x40x40 mm^3 specimens were 5503 and 602 when 0.5 kN and 0.7 kN were applied.

Table 5.1: Number of Cycles ($N_{0.5}$) with different loads applied.

Loads (kN)	Number of Cycles ($N_{0.5}$)
1.25	39240
1.50	20840
1.75	8020
2.00	2560

5.3.2 **Temperatures of asphalt test samples during the heating treatment.**

Heating treatment by means of induction heating for self-healing is shown in section 3.6.2. The protocol of induction heating is seen in Figure 3.8 and analysis data represented in Figure 5.5.

The temperature of the samples was continuously monitored during induction heating by using an infrared camera (see Figure 3.8 Section 3.6.2 and Figure 5.4 shows the sample under induction heating test). Figure 5.4 shows the temperature evolution of an asphalt sample containing 1.1% of steel after being heated for 2 min at the top, centre and bottom of the sample. So, for example, in Figure 12 in reference[11], which represents a test sample that was heated using an infrared light, the surface temperature was higher than the bottom temperature.

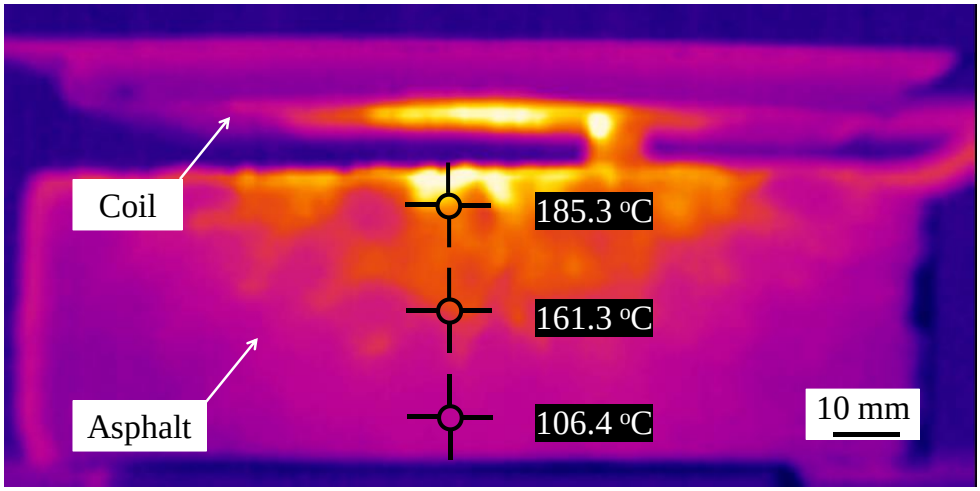


Figure 5.4: Infrared image of asphalt sample containing 1.1 % steel wool under induction heating.

It was found that the increase of temperature was approximately linear at any point of the asphalt's surface, see Figure 5.5. The temperature reached by the surface of the test samples after 90 s heating was at least 100 ^{o}C. Based on previous research by the author, this difference of temperature between parts of the test samples does not affect the healing of the cracks as soon as the temperature increases in every point of the test sample.

Despite that, the healing of the crack seemed to be uniform over the whole height of the sample. Furthermore, when the temperature reaches the steady state equilibrium, the bitumen will flow to the bottom of the sample due to gravity[11].

The reason for this is because if the temperature increases at the rates that are typical for asphalt induction heating, bitumen will expand and drain into the cracks [170]. It is still unclear which is the minimum heating rate required for asphalt self-healing.

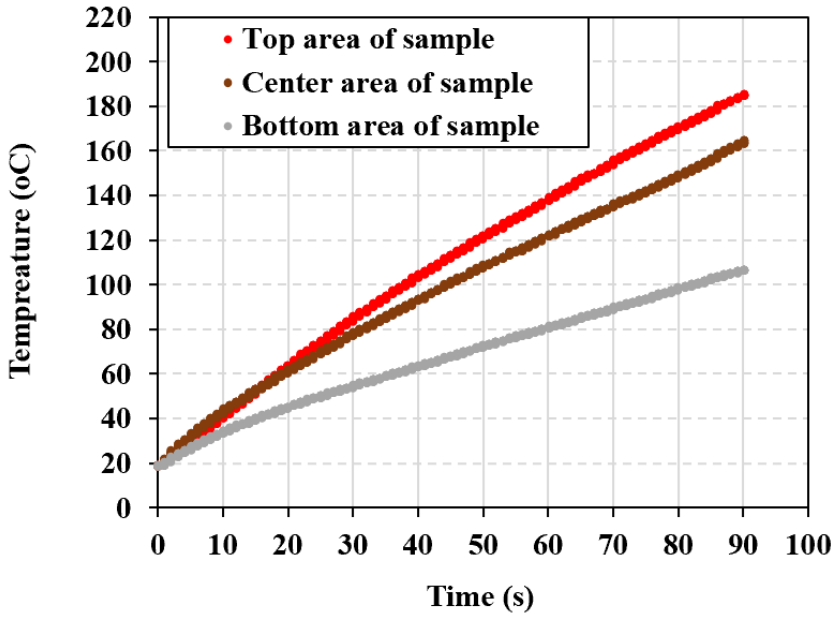


Figure 5.5: Evolution of the asphalt's surface temperature over heating time.

5.3.3 **Effect of induction heating on the healing index.**

Healing index was calculated by using Formula 3.1 in Section 3.5, and the result of healing index is shown in Figure 5.6 and Figure 5.7, which represents the extension of fatigue life, for the loading levels 1.25 kN, 1.50 kN, 1.75 kN, and 2.00 kN, when the healing is applied after N_h cycles. As can be seen in the figure, the healing index follows a bell-shaped distribution in all cases, which means that there is an optimum moment to apply the healing treatment, at which the obtained extension of fatigue life is a maximum.

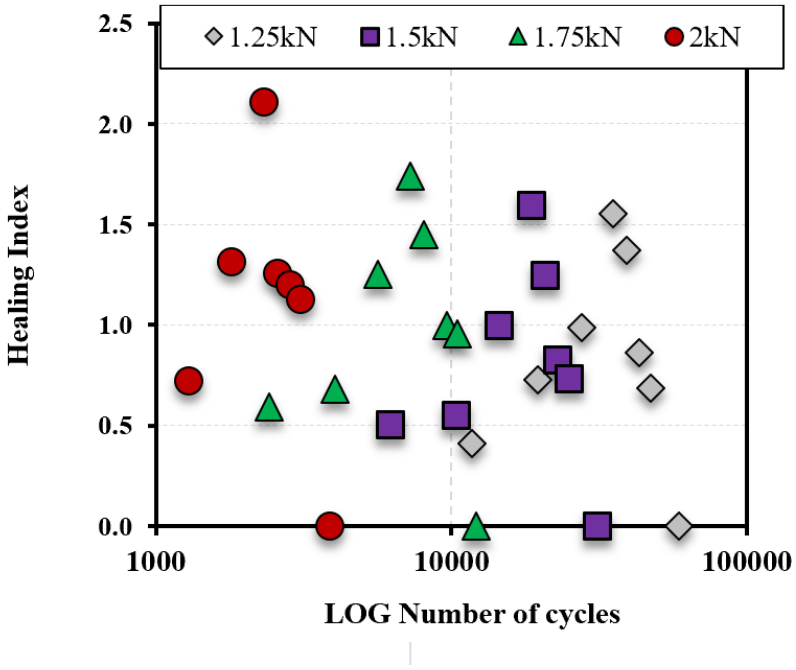


Figure 5.6: Healing index versus the number of cycles (Nh) for porous asphalt with 1.1% of steel wool.

This occurred in all cases at approximately 35% of the total life of the asphalt, independent of the applied load, see Figure 5.7. When the induction heating treatment is applied too early, the number of cracks is not enough to produce a significant fatigue life extension.

On the other hand, when the induction heating treatment is applied too late, the cracks are so big that the treatment stops being effective. Similar results had been reported in references [176] and [75], for different types of asphalt, loading modes, and healing treatments.

The optimum number of cycles at which the extension of fatigue life is a maximum reduces with the load, can be seen in Table 5.2. Thus, in a road with a shorter design life, healing treatment should be carried out more frequently, at 35% of the time envisaged for the life of the road.

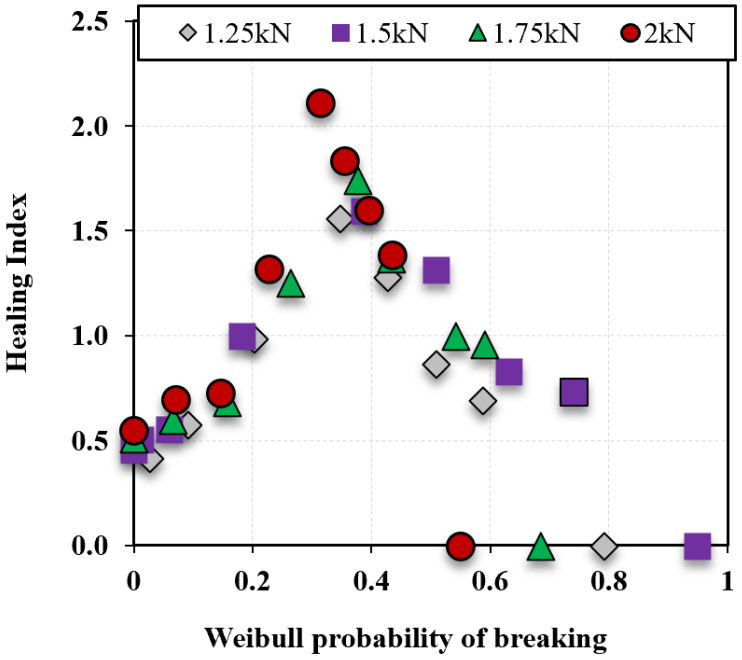


Figure 5.7: Healing index versus the Weibull probability for breaking the test samples.

It is also noticeable that the extension of fatigue life obtained can be higher than 100% (HI > 1) and for the case of 2 kN, even higher than 200% see Figure 5.8.

Table 5.2: $N_{0.5}$ cycles for different Load.

Load, kN	Number of cycles life extension after healing
1.25	35316
1.50	18760
1.75	7236
2.00	2318

When the HI value is higher than 1, it can be concluded that cyclic loading and induction heating introduces changes in the asphalt that go beyond simply closing the existing cracks.

It is possible that the reason for this is the stiffening of the test samples, either due to ageing of the bitumen, or to a densification of the solid skeleton. These changes in the asphalt due to cyclic loading and self-healing will be investigated in the next sections.

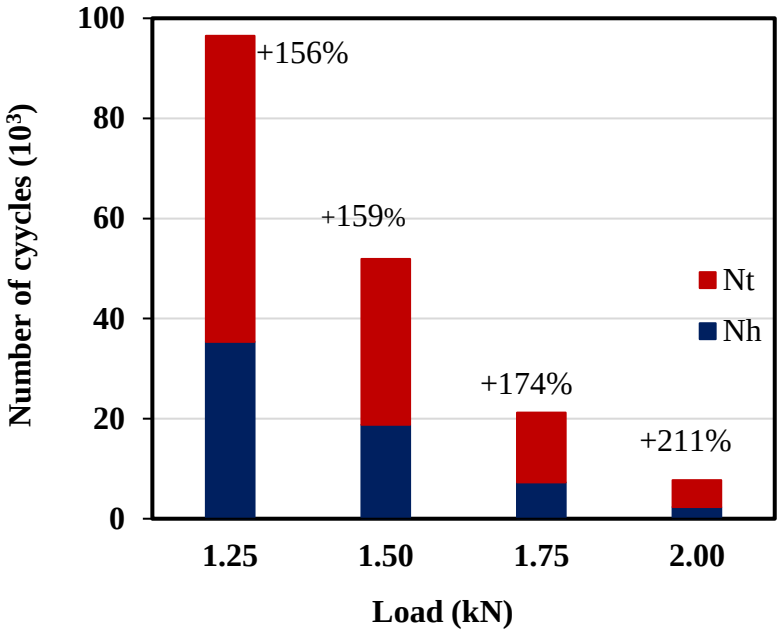


Figure 5.8: Optimum number of cycles to apply healing treatment (Nh) and extra number of cycles survived after induction heating (Nt).

5.3.4 **Effect of natural healing on extension to service life.**

Figure 5.9 represents the probability for breaking of the sample at a certain number of loading cycles fitted by the Weibull distribution. The healing index was obtained from the percentage of reference number $N_{0.5}$, after the samples had been subjected to natural healing at 20°C during a 24 h rest period. It can be observed that there is a certain number of cycles after which the damage is very high, and the test sample cannot be healed any more. In this thesis the number of cycles representing the optimum moment for healing is 2314. At this optimum moment the sample reaches the maximum healing level of 22%, after this point the sample does not heal so effectively.

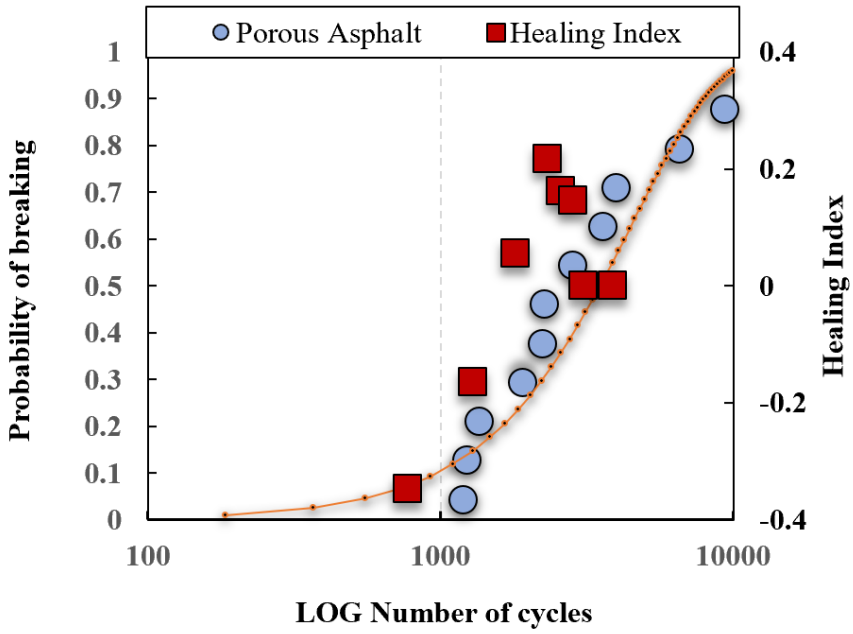


Figure 5.9 : Number of cycles versus healing index and probability for breaking versus number of cycles subjected to 2 kN repeated loading.

In Figure 5.10, shows the results of healing index against number of cycles, comparing the healing index induced by induction heating and the healing index induced by natural heating.

All samples were fatigued at 2kN maximum loading and tested at 20ºC ±1ºC. These samples were fatigued to different proportions of reference number of cycles ($N_{0.5}$), namely, 0, 30%, 50%, 90%, 100%, 120% and 150%.

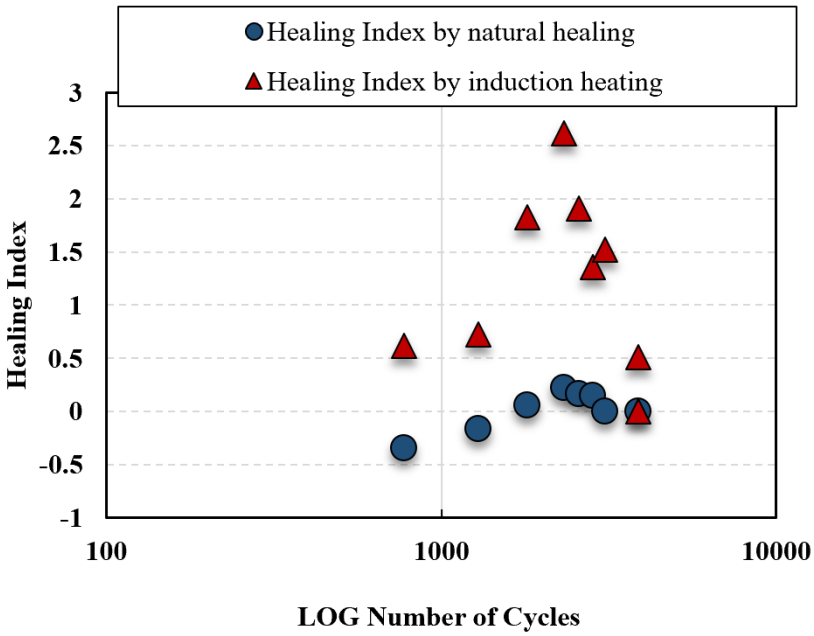


Figure 5.10: Healing index of beams under both- natural and induction healing

After the pair's samples had been tested, one was healed naturally for 24 h in a cabinet at 20ºC, and the second one was healed by 90s of induction heating for healing. After 24 h the two samples were fatigued again. It was found that the maximum extension of service life was only 20% under natural healing, but over 200 % with induction heating.

Based on Chapter 4, it might seem that healing could be improved by increasing the temperature. Some researchers have stated that healing can occur at relatively low temperature or even by leaving the samples at ambient temperature.

However, this hypothesis was rejected, as previous investigations[157], [176] showed that there is a minimum temperature (between 40ºC and 60ºC) necessary to develop the healing process in an effective and efficient way. When heating the samples below

such a critical temperature, some healing can be obtained but more slowly and never reaching the same healing levels.

5.3.5 **Hypothesis for the healing mechanism of damage caused by cyclic loading.**

The air voids content is a key parameter in self-healing has been shown in Figure 5.6,5.7 and 5.11during fatigue loading and induction heating. Figure 5.11, shows an example of the evolution of air voids of an asphalt section with 0.5 cm width (selected from the scan of a 150x40x40 mm^3 test sample), before testing, after loading at 0.5 kN, until 35% of $N_{0.5}$ (optimum moment), and after 90s induction heating, obtained using CT Scans and reconstructed using ImageJ and Meshlab. Air voids are represented by the dark area in this image.

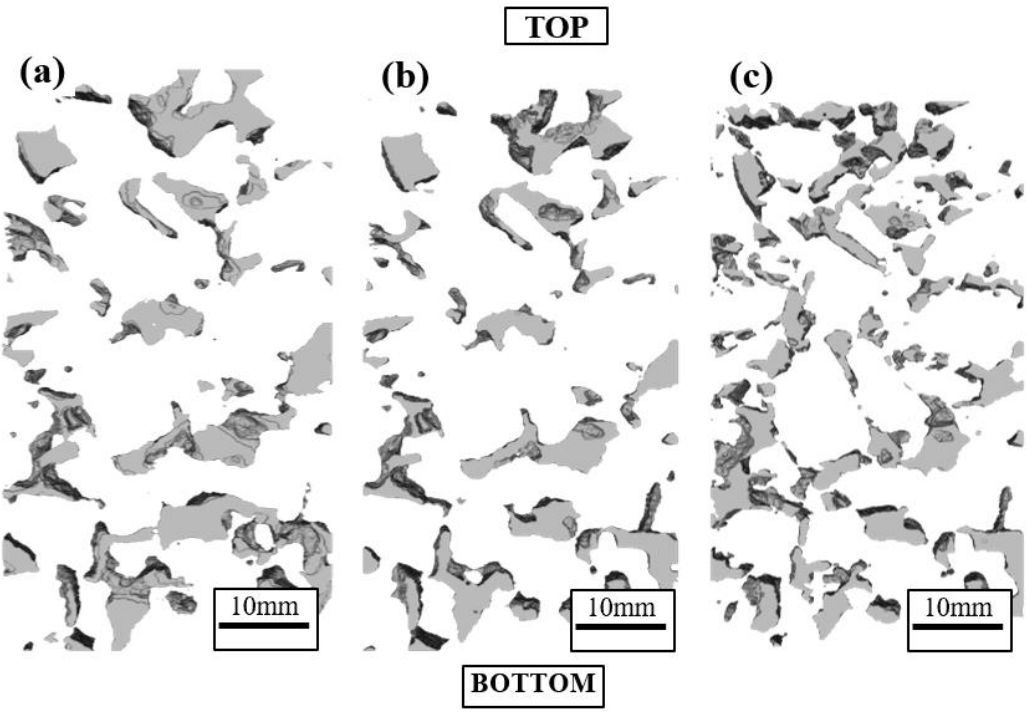


Figure 5.11: Air voids of a 0.5cm width test section (a) before testing, (b) after cyclic loading, (c) after induction heating.

In this figure the reader can appreciate at first sight that, while cyclic loading may affect the size and amount of air voids, the biggest change happens due to induction heating, because the air voids size seems to reduce. Changes in the air void content due to cyclic loading and induction heating have been quantified in Figure 5.12. Figure 5.12 shows the changes in the air voids when the cyclic loading is 0.5 kN,

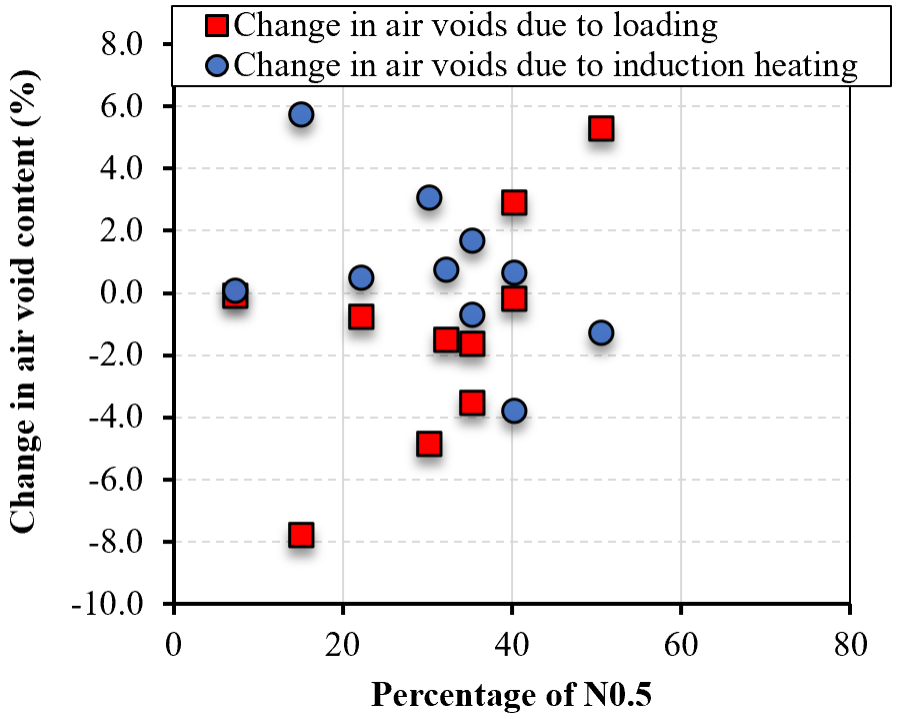


Figure 5.12: Change of air void content with the percentage of $N_{0.5}$. when the load is 0.5 kN

Figure 5.13 shows the changes in the air void content when the cyclic loading is 0.7 kN. From the change in air voids due to cyclic loading, it can be observed (from Figures 5.12 and 5.13) that it produces a reduction in the air void content of between 6% and 8% in the first 15% - 20% cycles. This may be due to compaction caused by cyclic

loading. After wards, the air void increased steadily, which may be due to cracks and aggregate movements occurring in the material due to cyclic bending.

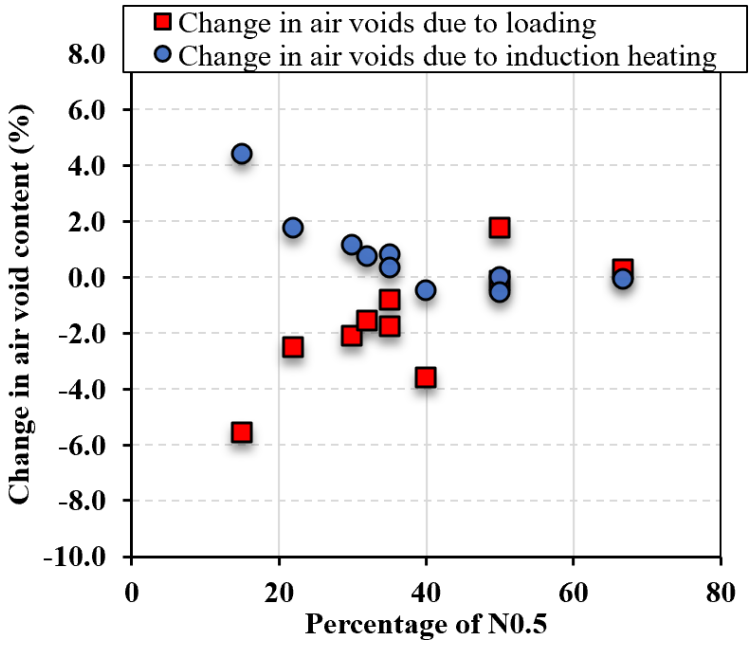


Figure 5.13:Change of air void content with the percentage of $N_{0.5}$. when the load is 0.7 kN.

When the cyclic loads were higher than approximately 0.35 $N_{0.5}$ the densification disappeared, and the air void content became higher than the original one. These are new phenomena reported in asphalt mixtures and from the opinion of author, they can only explained easily by means of numerical simulation.

Induction heating increased the air void content in the asphalt when it was applied very early in the lifetime of the test samples, in asphalts that had been densified due to cyclic loading. The reason for this is unclear

It may be due to the generation of gases in the mixture, due to the high temperatures reached by the steel fibres, or to the drainage of the binder to the external zones of the test samples. In general, induction heating tends to revert the air void content back to what it was before cyclic loading was applied.

In addition, stiffness modulus tests were conducted before and after induction heating in order to evaluate the effect of the air voids increase caused by induction energy on the mechanical properties of new asphalt. It was found that the stiffness modulus reduced by 32 % (see Table 5.3), which may be due to the increase in air voids due to induction heating.

Also, Figure B.6 in Appendix B shows another results of the relationship between all the stiffness modulus values measured by the indirect tensile test (ITSM) on the PA specimens in the longitudinal (A-A') and cross (B-B')direction , these results for PA specimens test measured in longitudinal (Y) and cross (X) directions, it can be observed that the stiffness modulus measured in both directions were very similar .

Table 5.3: Stiffness Modulus (SM) before and after induction heating

SM before induction heating (GPa)	2.43
Standard deviation (GPa)	0.31
SM after induction heating (GPa)	1.65
Standard deviation (GPa)	0.51

This could show that the increase in life is mainly caused by the densification due to cyclic loading and that induction heating simply corrects any crack or defect that may appear during the densification process.

Furthermore, in test samples damaged by cyclic loading at 0.5 kN, when cyclic loading created air void content higher than the original one, at cycles higher than 0.35 $N_{0.5}$, induction heating reduced the air void content. The reason for this is unclear and may be due to crack closing or thermal expansion during heating.

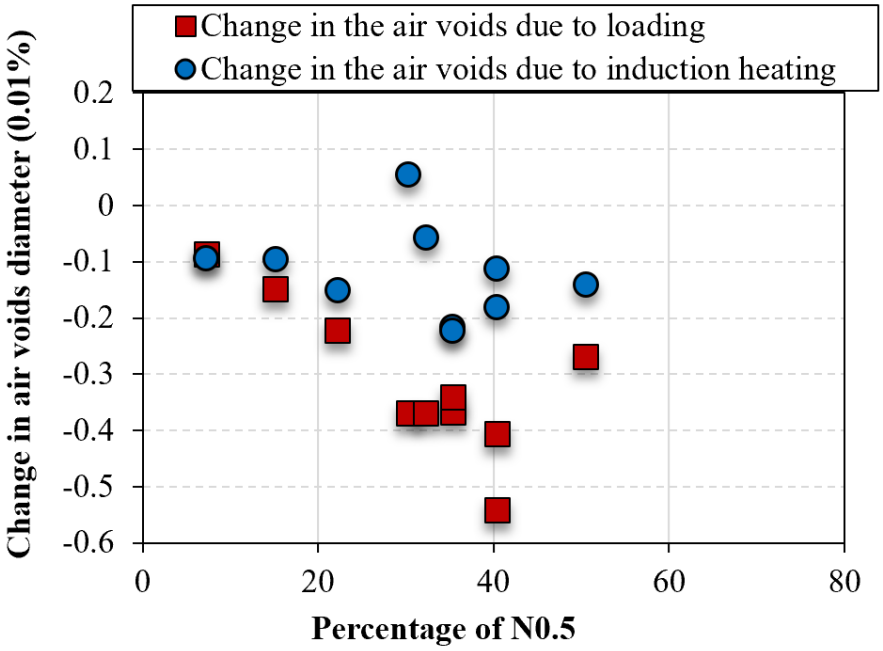


Figure 5.14: Change of air void size with the percentage of $N_{0.5}$. when the load is 0.5 kN.

According to the observations of this study, induction heating closes the cracks and alters the internal configuration of the test samples, as can be observed in Figure

5.11(c), including the position of the air voids and the distribution of aggregates. After applying induction heating to an asphalt, its air void structure transforms.

Finally, in both Figure 5.12 and Figure 5.13 it can be observed that 0.35 $N_{0.5}$, the optimum moment for self-healing, corresponds to the moment when the mixture is most densified, which shows that there may be a relationship between the increase in life due to induction heating and the compaction of asphalt due to induction heating. Cyclic loading reverses this densification due to cracking and aggregate movements.

At that moment, induction heating does not affect the air void content. One can conclude that the reason for the increase of air voids due to induction heating does not affect the asphalt at this level of damage. The binder redistributes in the asphalt, closing the cracks, and the aggregates remain densified. Therefore, the Healing Index can be higher than 1.

It was mentioned before that the air void diameter changes also during cyclic loading and induction heating. The average air void diameter of new test samples is 3.91 mm with standard deviation 0.41 mm. In Figure 5.14 and Figure 5.15 it can be observed that the air void size reduced steadily with the cycles by up to 40% or 50% of the original size, depending of the maximum load applied, until approximately 0.35 $N_{0.5}$.

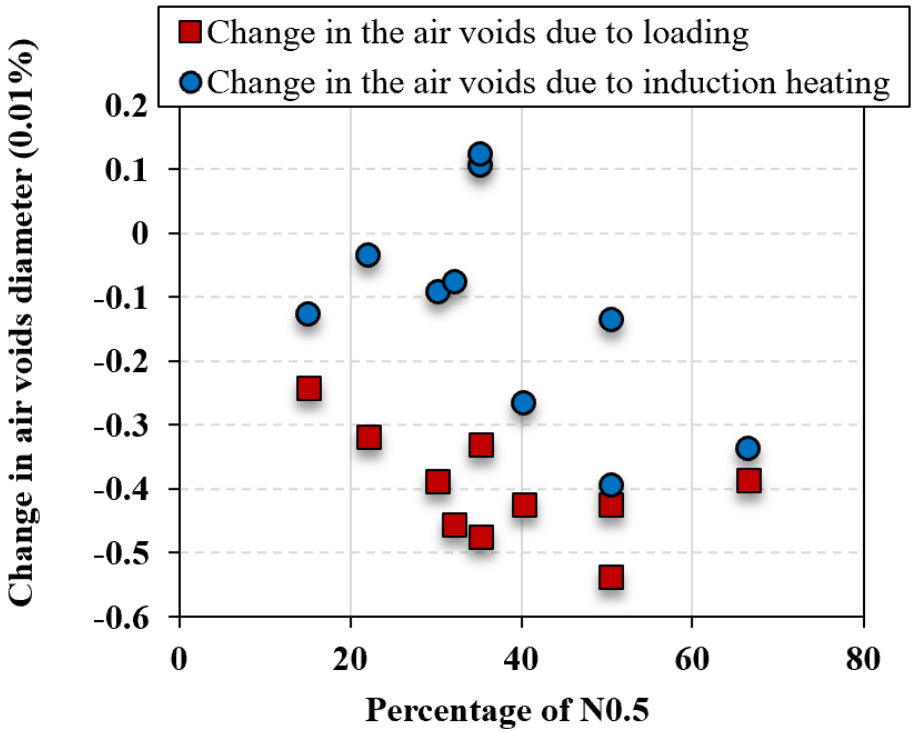


Figure 5.15: Change of air void size with the percentage of $N_{0.5}$. when the load is 0.7 kN.

From that moment, the air void diameter remained constant. Based on this, it can be inferred that the densification continued until 0.35 $N_{0.5}$ and from that moment, cracks started appearing, which may be the reason for the rapid decline of the healing index observed in Figure 5.6 and Figure 5.7. This big reduction of air voids content may correspond to the closer of the smaller pore due to the pressured exerted during cyclic loading.

Unfortunately, the resolution of the CT Scans used did not allow to observe the cracks directly and this hypothesis will have to be validated in the future. Moreover, in Figure 5.14 and Figure 5.15 it can be observed that induction heating reduces the size of the air voids further.

The reason for this is unclear and the author are not able to offer an explanation without further testing and numerical modelling. In a porous asphalt, this may make the material more prone to clogging. This phenomenon occurs with higher intensity before 0.35 $N_{0.5}$, while the size of the air voids rate of change reduces after.

5.4 Summary of Chapter 5

To achieve the aims and objectives of this study, this chapter has given a reader a method to understand the accelerate the self-healing in asphalt, it has called induction heating. Metal fibre has added to the asphalt and, once the road is cracked, it has heated by applying an alternating electromagnetic field, which melts the bitumen and contributes to repair the cracks. The chapter has explored by experimental work the optimum moment to apply the induction heating. To do that, cyclic loading tests have been used and the extension in the number of cycles have quantified. Furthermore, the physical properties of the air voids in the asphalt before and after cyclic loading, and after induction heating have been quantified using Computed Tomography Scans. It has observed that the macro porosity of asphalt and diameter of air voids changes with the tests and the induction heating. The Influence of aggregate gradation on self-healing of asphalt enhanced with capsules is studied in the next chapter.

.

Chapter 6: Influence of mixture type on self-healing of asphalt enhanced with capsules

6.1 Introduction

This chapter aims to evaluate the effectiveness of using encapsulated oil in order to improve the self-healing properties of asphalt mixture with a range of gradations, namely dense asphalt, porous asphalt, and stone mastic asphalt. In Chapters 4 and 5, self-healing was applied by means of infrared heating and induction heating. These methods were used to extend service life and to treat the asphalt at the optimum moment; however, neither method can actually reverse pavement ageing, or work autonomously. To overcome this barrier, this chapter will investigate the use of microcapsules containing sunflower oil to promote self-healing and rejuvenation of aged asphalt mixtures.

For this purpose, three different hot asphalt mixes, a dense asphalt mixture, a porous asphalt mixture and a stone mastic asphalt, have been selected since these materials are the most commonly used asphalt types in Europe. These mixtures have been studied with and without addition of capsules in order to evaluate the relative effectiveness of capsules in different mixture types. In this chapter the self-healing properties of cracks caused by repeated loading in these three asphalt mixtures will be measured

determining the optimum time when the capsules should break to maximise the self-healing. Finally, this will give an insight into the type of cracks that are healed and the breaking mode of the capsules due to repeated loading.

6.2 Experimental summary

The encapsulated rejuvenator has been described in Section 3.2.3. This capsule was added into three types of asphalt: Dense Asphalt (DA), Stone Mastic Asphalt (SMA), and Porous Asphalt (PA), see Section 3.3. The gradations were shown in Table 3.4. Different amounts of bitumen were used for the three mixtures, see Table 3.4, based on laboratory experience. Different loadings were also used, see in Section 3.5.

The average air void contents were 20%, 5.5% and 5% for PA, SMA and DA, respectively, see Table 3.4. Test samples with and without capsules were manufactured. In each case the capsule content was 0.5% by total mass of the mixture.

This amount of capsules was proposed by Al-Mansouri et al. in[140], as the amount that maximised the self-healing and did not affect the functionality of the asphalt mixture, such as skidding resistance, or rutting properties. All the mixtures were manufactured with crushed limestone aggregate, with nominal maximum size 20mm for PA and DA, 14mm for SMA and 50/70 pen bitumen see Table 3.4.

The amount of oil released by the capsules to the mixture was measured according to the methodology defined in [159], developed by [164]. This methodology is based on the idea that the sunflower oil has a distinct absorption peak at ~1,745 cm^{-1} base on FTIR test (Fourier Transform Infrared Spectroscopy,) see Section 3.12, which bitumen

does not have. To have a reference to determine the amount of oil released by the capsules, sunflower oil was mixed with bitumen in the mass percentages 1.0 %, 1.5 %, 2.0 %, 3.0 %, 5.0 %, 6.7 %, 8.0 %, 9.0 %, and 10.0 % and the normalized area under the FTIR curve calculated as shown in section 3.5.6 , as in Figure 3.4 of reference[140]. To determine the amount of oil released by the capsules in asphalt mastic, asphalt mixture was heated to 100 ^{o}C, the sample broken in small pieces by hand and mastic samples were collected by from the surface of coarse aggregate by using a hot knife. The FTIR curve of the sample was obtained, see Section 3.12, and the normalized area under the curve for the specimens was compared to the values obtained from mixing bitumen and sunflower oil. The samples were extracted from mixtures that had been just compacted, at different stages of cyclic loading, and after the resting period that was used to allow the cracks to self-heal. The tests programme is summarized in Figure 6.1.

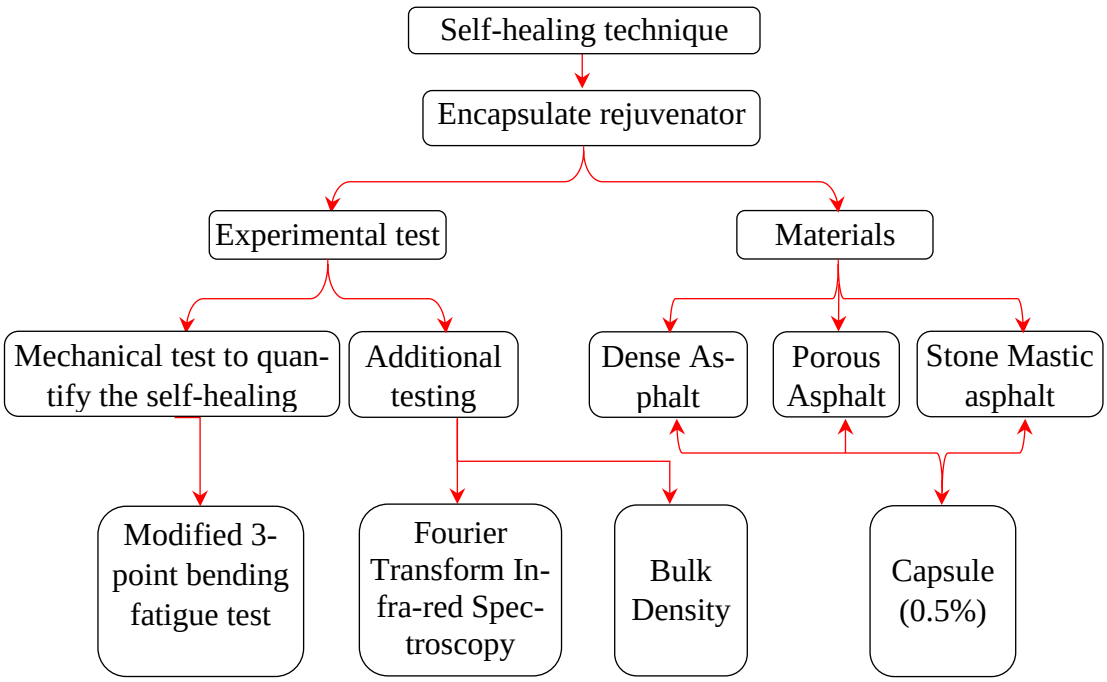


Figure 6.1: Summary of test programme in Chapter 6.

6.3 Results and Discussion

6.3.1 Density and air void properties of asphalt mixture with capsules.

The details of the density test can be found in Section 3.8, and the results are presented in Table 6.1. Fatigue durability of an asphalt is directly related to its air void content Ma et al [141] . It was therefore important to guarantee that the capsules did not affect the air void content of the mixture and that every variation in the fatigue life was caused by the rupture of the capsules. Table 6.1 shows the bulk density of the three types of asphalt studied, with and without capsules. As can be observed, the difference in bulk density and air void content between mixtures with and without capsules is negligible, which implies that capsules survived mixing and compaction.

Table 6.1: Bulk density and air void content of the asphalt mixtures studied (W/C: with capsules; WO/C: without capsules).

Asphalt type		Bulk Density, ton/m^3 (BD)	Air Void Content, % (AVC)	Standard Deviation	
				BD	AVC
SMA	W/C	2.2	5.64	0.01	0.46
	WO/C	2.2	5.67	0.01	0.44
PA	W/C	2.01	19.62	0.01	0.48
	WO/C	2.01	19.94	0.01	0.49
DA	W/C	2.35	4.91	0.49	0.49
	WO/C	2.35	4.96	0.49	0.49

6.3.2 Repeated loading durability of asphalt mixture with capsules.

This section shows the effect of repeated loading on fatigue life in different mixtures with and without adding capsules. Figure 6.2 shows the cumulative probability of breaking of SMA without capsules, loaded at 1.25 kN, 1.5 kN, 1.75 kN, and 2 kN, as an example. Also, results for PA and DA materials with and without capsules are presented in Appendix (C) (Figure C.1, Figure C.2, and Figure C.3); 5 to 10 samples each were used to calculate the probability of breaking with and without adding capsules. These probabilities were obtained for the three types of asphalt studied, SMA, PA, and DA, with (W/C) and without capsules (WO/C) and were used to calculate $N_{0.5}$. As would be expected, the number of cycles resisted by the asphalt decreased with increases in the load applied.

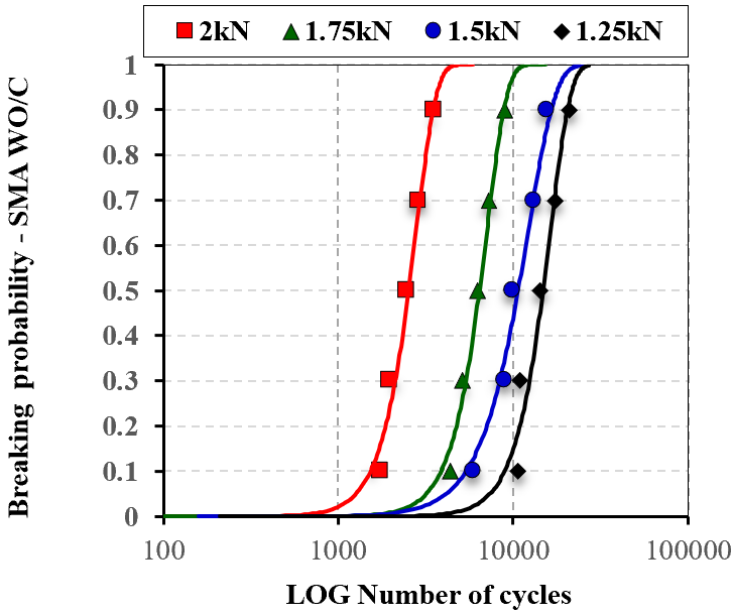


Figure 6.2: Distribution functions of the number of cycles resisted by SMA without capsules (WO) at different loading levels

Figure 6.3 shows the Wöhler curves for the three types of asphalt studied, at the probability level 0.5. DA has higher fatigue durability than SMA, and SMA, has higher fatigue durability than PA. It is not possible to compare in any simple numerical way the durability of the three types of asphalt, because the three Wöhler curves are not parallel.

The main conclusion that can be obtained from Figure 6.3 is that, without resting periods, the capsules reduced the number of cycles resisted by the asphalt by 21 %, 33 %, 29 %, for DA, SMA, and PA, respectively.

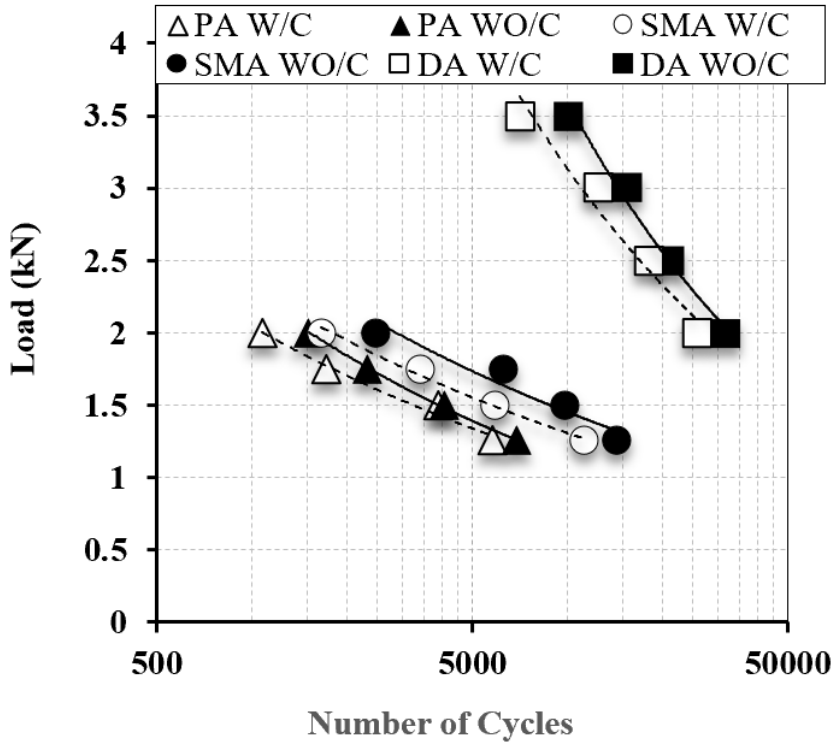


Figure 6.3: Wöhler curves for dense asphalt (D), Stone Mastic Asphalt (SMA), and Porous Asphalt (PA), with (W/C) and without (WO/C) capsules.

This effect had been reported in previous research [143] , where it was found that capsules reduced the fatigue durability of SMA by approximately 74%, Figure 7.2a in Reference[143]. The durability reduction of asphalt with capsules is 2%, 5%, and 5%, for DA, SMA, and PA, respectively, while in reference [143], the durability reduction of SMA with capsules is 15% by using logarithm scale.

In this study, the ratio between sodium alginate and oil in the capsules was 25:75, while the capsules in reference[140], were at ratio of 15:85. Consequently, the toughness of the capsules was higher, and the fatigue durability of the asphalt increased. This result suggests that if the strength of the capsules increases, the fatigue durability of the asphalt with capsules will eventually equal that of asphalt without capsules.

On the other hand, increasing the strength of capsules may delay their rupture to a point when the cracks are too big for healing. This suggests the opinion that, when these capsules break slightly before macro-cracks appear in the asphalt, they are ideal to repair the fatigue damage in the road. To validate this point, future research must evaluate the fatigue durability and self-healing performance of asphalt that contains capsules with a range of strengths.

6.3.3 Oil released from the capsules during the repeated loading tests.

Figure 6.4 shows the results of mixing various percentages of oil in bitumen versus the area under the FTIR curve. A similar figure can be found in Norambuena-Contreras et al. [140] albeit for a different type of bitumen. The linear fitting has been used as a reference to determine the amount of oil in the mixture.

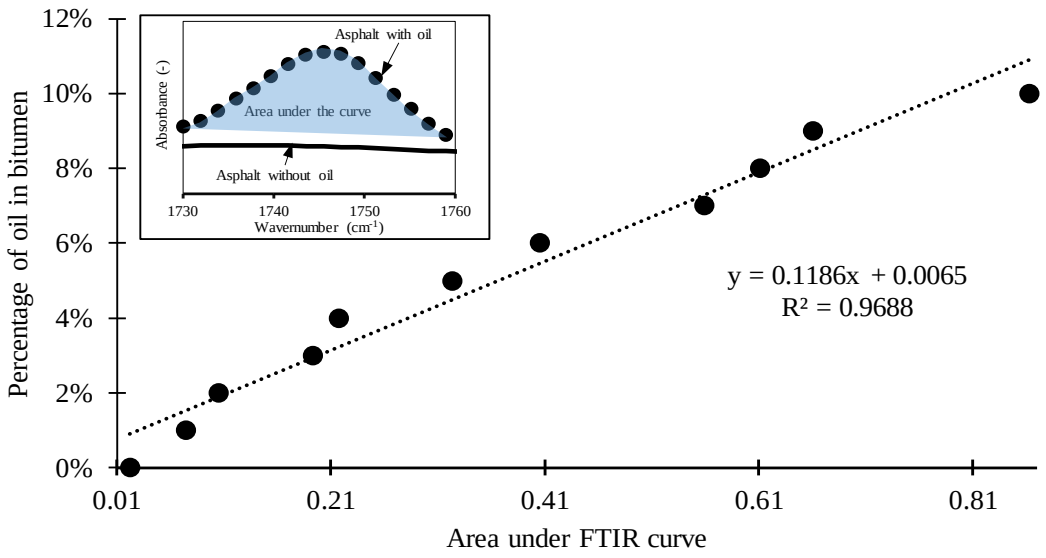


Figure 6.4: Area under the FTIR curve for bitumen modified with various percentages of sunflower oil.

The percentage of capsules broken during mixing and compaction could be estimated from the amount of oil in the asphalt and this was found to be 10.85 %, 8.27 %, and 8.78 %, for SMA, PA, and DA, respectively. The standard deviations were 0.52 % (SMA), 0.81 % (PA), and 0.55 % (DA). These values indicate that most of the capsules resisted mixing and compaction. There is no significant difference in the percentage of capsules broken between the three different types of asphalt studied. For that reason, it can be concluded that the aggregate gradation does not affect the breakage of capsules during mixing and compaction.

Figure 6.5 shows the oil released by the capsules in SMA see Appendix C Figure C.10 for DA, and PA mixes. It can be observed that the amount of oil released by the capsules tends to a maximum of around 75 % - 80 % of the total oil available in the capsules. Since 10.85 % of the oil had been released after compaction of the mixture, this

suggests that the capsules resist relatively intact for a certain number of cycles and that they start to break when cracks appear in the asphalt.

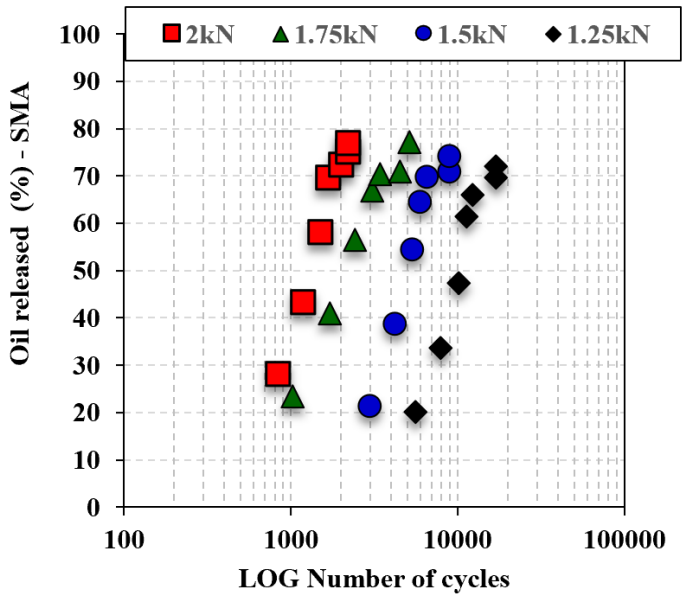


Figure 6.5: Oil released from the capsules embedded in SMA.

To prove this, Figure 6.6 shows the release of oil from the capsules compared to the probability of breaking of the SMA. It can be seen that all the trends obtained from different load levels are approximately coincident. If the probability of breaking is related to the growth of cracks in the asphalt, this graphic shows how the capsules in the mixture become gradually damaged until a maximum, which is independent of the load level.

From Figures 6.2, Figure 6.3, Figure 6.5, and Figure 6.6, it is obvious that there is a range of number of cycles when the asphalt cracks and that the capsules break at the same time. The author believes that this is the ideal situation to reach maximum healing efficiency.

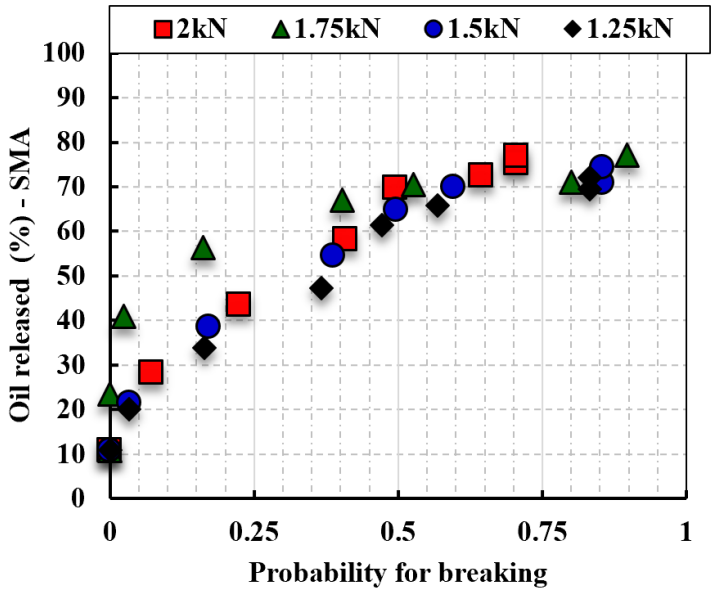


Figure 6.6: Oil released from the capsules embedded in SMA beams versus the probability of breaking the beams.

Figure 6.7 shows how the oil is released from the capsules during the cyclic loading tests for SMA, PA, and DA, tested at 2kN. As in the case of SMA, the capsules in PA and DA break gradually with the cyclic loading. Since 10.85%, 8.27%, and 8.78% of capsules were broken during mixing and compaction, for SMA, PA, and DA, respectively, one can intuitively understand from the curves in Figure 6.7 that there is a moment when a significate steep increase in the release of oil happens.

By comparing the breaking probability results from Figure 6.2 for SMA , to the oil release results from Figure 6.7, one can conclude that this step increase in the oil release corresponds to the number of cycles when macrocracks started forming in the mixture. Similar results occur for PA and DA. The author considered that this could be proof that the capsules that used in this study remained dormant until the moment when macrocracks appeared.

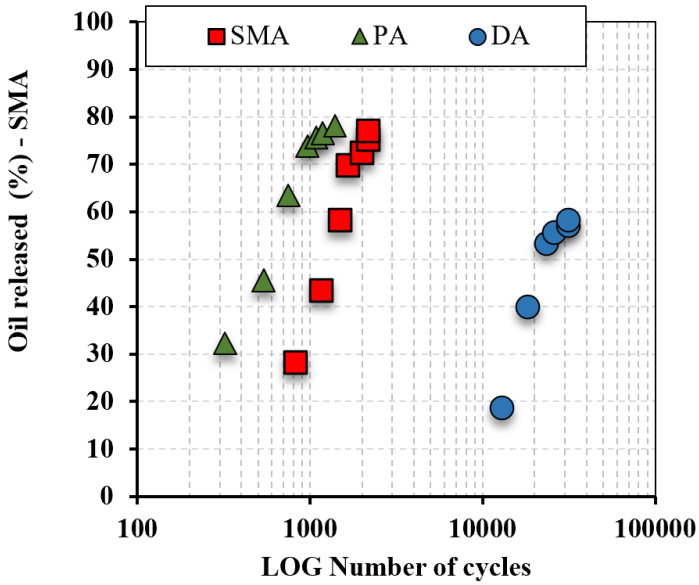


Figure 6.7: Oil released from the capsules embedded in PA, SMA, and DA subjected to 2 kN repeated loading

At this point of the thesis, the difference in behaviour between capsules in PA and DA can be explained only because of the aggregate gradation, and the reason is that capsules in rockier mixtures tend to get damaged by the aggregates during cyclic loading, while capsules in denser mixtures tend to float in the mastic and are damaged only under the high stresses caused by the asphalt cracking.

An indication of this may be the lower maximum amount of oil released by the capsules in DA% 58%, compared to PA, 78%, which reflects the fact that capsules far from the maximum bending moment area may have remained undamaged. However, this is a hypothesis and must still be proven with detailed experiments with capsules in DA and PA.

6.3.4 Self-healing of crack in PA, DA, and SMA by the action of encapsulated oil

Figure 6.8 shows the Healing Index of SMA without capsules for the range of loading levels studied, as an example, and other materials are presented in the (Appendix. C) similar graphic has previously been reported in [75]. With the number of cycles, the healing level increases up to a maximum and then, it decreases. Menozzi et al.[75], considered this to be an indication that there is an optimum moment to apply the healing treatment.

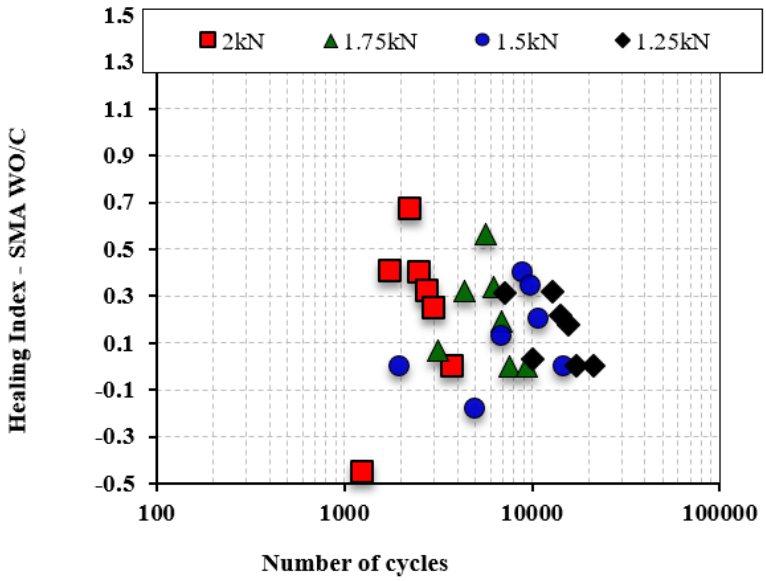


Figure 6.8: Healing index vs number of loading cycles for SMA without capsules.

It is also obvious that the optimum moment for self-healing will depend of the loading level, as can be seen in the figure and that the maximum healing level decreases with load reduction, probably due to less capsules being broken. There are samples with healing Index below to 0 due to the natural scatter of cyclic loading results between

test samples. Figure 6.9 shows the Healing Index of SMA versus the probability of the test samples breaking. The data is represented in this way to show the similarity between the curves obtained with different loading levels, and it shows the optimum moment for healing at a similar probability for breaking, approximately 0.34.

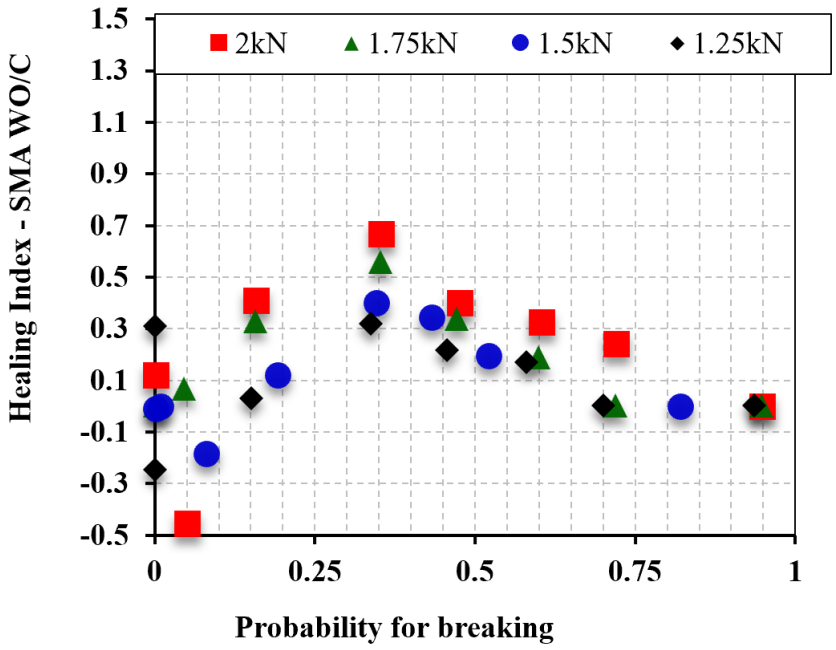


Figure 6.9: Healing index vs probability of cracking for SMA without capsules.

Figure 6.10 shows the maximum healing level reached by all the types of asphalt studied. At 2kN, the capsules increase the healing level of SMA, PA, and DA by 35%, 30%, and 19%, respectively. The author hypothesizes that the maximum healing level reached by the different types of asphalt is related to the number of capsules broken and the type of damage in the mixture at the maximum healing level. Table 6.2 shows the number of repeated loading cycles, percentage of oil released, and healing level at the optimum healing time in test samples loaded at 2kN. Figure 6.10 shows the maximum healing level reached by healing level at the optimum healing level time at 2kN.

Table 6.2: Number of repeated loading cycles, percentage of oil released, and healing level at the optimum healing time at 2kN.

Type of mixture	Number of cycles at the optimum	Oil released at the optimum (%)	Healing level (%)
SMA	1494	58.22	35
PA	972	73.76	30
DA	23220	53.3	19

It is evident that cracks in DA do not heal to the same high level as the other mixtures studied and the reasons are, firstly the lower number of capsules broken, as has been mentioned above and secondly, the higher bending and rutting that DA samples suffered during the cyclic loading, which may have led to densification and reduction in the bitumen's capacity to flow between the aggregates and drain into the cracks.

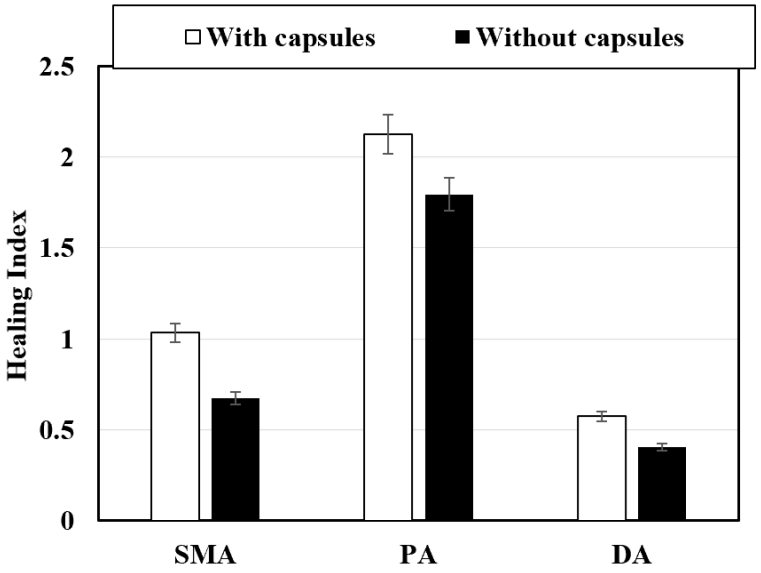


Figure 6.10: Healing index of all the types of asphalt studied at 2kN.

This is a noteworthy point that must be studied in the future, as it is probable that the rutting and trafficking of asphalt mixture reduces its self-healing ability, and consequently, the durability of the road.

Figure 6.11 shows the average probability for fracturing the asphalt test samples at the point of highest self-healing. From this figure, what is remarkable is that the probability for breaking to give maximum healing is always higher in test samples with capsules than in test samples without capsules, which may be a prove of the self-healing despite there being no resting period, although this will have to be proven in future research.

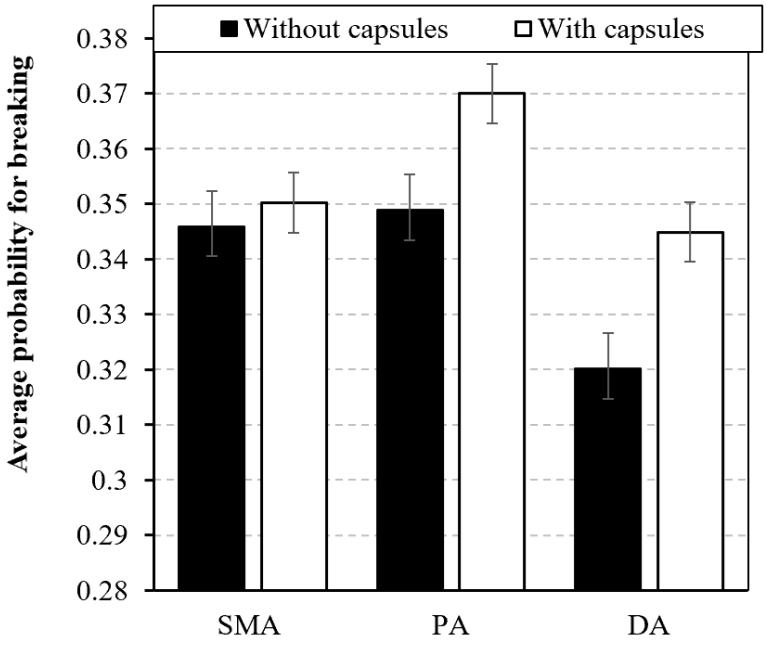


Figure 6.11: Average probability for breaking the asphalt test samples at the highest heading index.

6.4 Summary of Chapter 6

This chapter has shown a study of the self-healing in asphalt mixtures with capsules. It has then examined the self-healing properties of cracks due to repeated loading in Dense Asphalt (DA), Porous Asphalt (PA), and Stone Mastic Asphalt (SMA) asphalt mixtures, which are the most commonly used asphalt types worldwide. The chapter has determined the optimum time when the capsules should break to maximise the self-healing. Finally, it has given an insight into the type of cracks that already heal and the breaking mode of the capsules due to repeated loading. Important findings from this and all other chapters, obtained from the different experimental tests carried out, is summarised in the next chapter.

Chapter 7: Conclusions and Recommendations

This chapter reviews the main elements of the thesis. The aims and objectives are then summarised, including the level of success and what could be done in the future to improve the results. In addition, a list of recommendations for future work has been included.

7.1 Review of Aims and Objectives

Chapter one included the aims and set objectives for the project. The aims were stated as follows:

- To investigate the optimum moment in the life of an asphalt, where a self-healing technique can be applied, and the self-healing is maximised. Three different self-healing techniques will be investigated, namely infrared heating, induction heating, and encapsulated healing agents.

- To investigate differences in the self-healing performance of asphalt using infrared, induction heating, and encapsulated rejuvenators to accelerate the self-healing.
- To investigate differences in the self-healing performance in different types of asphalt.

- To give an insight into the asphalt properties that most affect the self-healing.

In order to given specific objectives of this study, but are not limited to the following:

The research objectives:

Objective 1: Effect of porosity on infrared healing of fatigue damage in asphalt.

Objective 2: Optimum moment to heal cracks in asphalt roads by means of electromagnetic induction.

Objective 3: Influence of aggregate gradation on self-healing of asphalt enhanced with capsules.

These are now discussed in the context of what was achieved and what could be improved upon. Following this, recommendations for further work are made.

Major topics relevant to the project were explained in Chapter 2 which also referenced definitive sources for further information and state of the art research concerning the different materials used in this project. Firstly characteristices of fatigue damage are described then the concept of self-healing togther with the most significant agents that impact on the self-healing phenomenon. In addition, the methods of artificial self-healing were presented in detail and the response of the materials added to mixtures to accelerate healing. Finally, a critical evaluation was made of previous studies concerned with the self-healing phenomenon in order to find the limitations that need to be overcome on this topic.

7.2 Conclusions of Chapter 4: "Finding of Using infrared healing to assess the porosity in fatigue damage"

This aspect was investigated using five different types of hot mix asphalt, these were 5%10%, 13%,21% and 26% air void contents with correspondingly different amount of asphalt contents respectively. The type of bitumen was 40/60 pen for all the mixes and the aggregate was crushed limestone with maximum size 20 mm. The fatigue test was carried out by subjecting asphalt beams to dynamic cyclic loads under modified 3-point bending fatigue conditions. This test configuration was selected to produce clean vertical cracks at the midpoint of the specimens.

To determine the fatigue life of each studied material, 15 samples per material were subjected to testing until failure, and the Weibull Distribution was fitted to the data. This probability distribution was selected considering that fatigue damage is produced by the progressive accumulation of mechanical energy on each applied cycle. The samples' average lifetime was estimated as the number of cycles at which the probability of breaking the specimens was 50%.

In order to evaluate the asphalt mixes' capacity and extend their service life, when subjected to a infra-red heating, a series of 40 samples for each material was manufactured and tested, as described in section 3.4 in Chapter 3.

The results suggest that:

1. There is an optimum number of cycles at which to apply the heating treatment in an asphalt mixture, below which there is not enough damage in the test samples and

healing does not happen; and after which, the material is too damaged and cracks cannot be repaired.

2. Asphalt test samples with non-contiguous air cavities present:

- longer fatigue life.
- lower healing capacity (HI<0.5);
- Negative HI-values when the thermal treatment is applied too early or too late, meaning that test samples experience damage instead of healing
- Strong reductions occur in the optimum number of cycles at which to apply the thermal treatment when the air void content is slightly increased. In other words, more frequent treatments would be needed.
- Strong reductions in the air void content were found after the healing treatments and.
- Thermal expansion when the material's temperature is increased.

3. In contrast, asphalt mixtures with contiguous air void content achieved higher fatigue life extensions than denser asphalt mixtures, to the point of tripling their lifetime. This was produced by a combined effect of densification during repeated loading testing and consolidation during heating, resulting in denser samples with enhanced durability.

4. The temperature reached by the samples during the thermal treatment depended on the distance between lamps and test samples and on the material's air void content. However, increasing the temperature is not a solution to improve asphalt self-healing

with non-contiguous air voids. On the contrary, internal damage can be produced, reducing the fatigue life. Asphalt self-healing can be maximised by designing an asphalt mixture with an air void content that produces contiguous pores.

7.3 Conclusions of Chapter 5: "Finding the optimum moment to heal asphalt roads by means electromagnetic induction"

The aims of the second element of the work was to provide an indication of the best moment to induction heat an asphalt road in order to repair cracking, something, which has not been tested before. This study was carried out on porous asphalt because, based on earlier testing, this is the type material where asphalt self-healing may be most successful. Also, it is prone to ravelling, which may be delayed using induction heating, and it does not tend to suffer rutting. The mix had 20% air voids content and was composed of crushed limestone aggregate, 4.5% bitumen and 1.1% of steel wool was used as well.

The extension of fatigue life obtained in porous mixes, when these are subjected to electromagnetic induction, was studied. Based on the results of laboratory fatigue tests, carried out at different loading levels, the main conclusions that could be extracted are listed, as follows:

1. The number of cycles, whose Weibull probability of breaking the material is 0.5 ($N_{0.5}$) was considered as the reference fatigue life that can be expected from the material. This value decreases exponentially when the applied load increases.

2. The current was induced by a 15x15 cm^2 square flat coil with 4 turns, connected to an induction generator of 6 kW with a power of 2800 W and a working frequency of 348 kHz at a distance of 2 cm from the surface. The 1.1% of steel wool was enough to increase the surface temperatures of the asphalt above 120ºC after 60s.

3. For all the stress levels applied in this investigation, it was found that there is an optimum number of cycles at which, when the healing is applied, the obtained extension of fatigue life is maximum. This optimum number of cycles reduces when the load increases. Furthermore, the maximum healing index obtained at the optimum number of cycles increases with the load.

4. The optimum number of cycles to apply the healing occurs at approximately 35% of the expected life, independent of the loading level. This is the moment that must be included in a pavement management system for application of induction heating treatments.

5. Cyclic loading produces a densification of the test samples in approximately the first 15% - 20% of cycles. After this, the air void content increases steadily, which may be due to the growth of cracks.

6. Cyclic loading produces a reduction of the air void diameter in the test samples up to 40% and 50% of the original size until 0.35 $N_{0.5}$. After this, the air void diameter remains constant.

7. Induction heating produces an increase of the air void content until 0.35 $N_{0.5}$. The reason for this is unclear. Induction heating reverts the densification caused by cyclic loading. Induction heating did not affect the air void content after 0.35 $N_{0.5}$.

8. Induction heating reduces the diameter of the air voids. The reason for this is also unclear and further testing and modelling will have to be carried out in the future to explain this point. It is also unclear how this will affect to the performance of the road.

7.4 Conclusions of Chapter 6: "Using capsules to induce self-healing of cracks in asphalt mixture"

The third objective explores the delay of cracking in dense, porous, and stone mastic asphalt using encapsulated healing agents embedded in the asphalt. The rate at which the oil is released from the capsules when the asphalt is exposed to cyclic loading was investigated, together its capacity to improve the natural self-healing of the asphalt.

Most of the capsules resisted asphalt mixing and compaction. In porous asphalt, the oil is released. This is an indication that the gradation of the asphalt is a critical parameter to affecting the design of the strength of capsules for asphalt self-healing. Furthermore, the self-healing efficiency of capsules is higher in porous and stone mastic asphalt than in dense asphalt.

The results suggest that:

1. The capsules manufactured in this thesis did not affect the air void content or bulk density of the asphalt mixture.

2. Without including rest periods in the laboratory tests, the capsules reduced the number of cycles resisted by the three types of asphalt mixtures studied SMA, PA and DA. These capsules reduced the durability of the asphalt mixtures less than those capsules used in previous studies. This shows that in future developments it will be possible to develop capsules that do not

reduce the durability of the asphalt mixtures in the laboratory by increasing the strength of the capsules.

3. The capsules did not break during testing; instead, the healing agent just can leak out by the pressure acted on the capsules. This point must be validated in future research, as the oil was released differently in porous and dense asphalt mixtures, which may be a reflection of the different gradations.

4. In the lifetime of an asphalt pavement, there is an optimum moment to do its maintenance, which is at approximately 35% of the cycles to rupture (with 50% probability). This point seems to be independent of the loading level, and the air void content. The reason for this is still unknown but it is probably related to the size of cracks in the asphalt. In the future, it is of the foremost importance to design test methods to identify the optimum maintenance.

5. The encapsulated oil increased the durability of stone mastic asphalt, porous asphalt, and dense asphalt in 35%, 30%, and 19%, respectively because of self-healing and additional compaction. The reason for the difference between materials may be due to the amount of mastic in the asphalt mixture, which influences the way in which the asphalt gets deformed due to cyclic loading and the flow of mastic.

6. The cyclic compaction of asphalt with, and without, capsules caused an immediate decrease of the air void content (densification) of the material, which continued up to 35% of the cycles to rupture (with 50% probability). Afterwards, the air void content increased, which may be due to the growth of crack and defects.

7. During the resting period the asphalt mixture with capsules saw the air void content increased, which may be due to the local reduction of viscosity.

7.5 Suggestions and recommendations for future work

The following items are drawn from the discussion points which, indicate that further research may be useful and perhaps lead to significant results:

The present study regarding the effect of air voids was focused on a fundamental understanding of how the air voids content affects the healing of fatigue damage in asphalt materials. In order to study that, the same test conditions were applied to samples with different air voids contents. However, in a real case, porous and dense mixtures would normally be used in the surface course and base layers, respectively. So, the loading configuration would be also different, and it is recommending that the effect of this is studied.

- In this research, only one type of binders (40/60) was studied in some specific asphalt mixtures. Nonetheless, many other gradations such as AC10 and small stone mastic size SMA are in use, together with various type of binders, such as polymer modified binders. Fatigue behaviour of these different mixes will need to be investigated to provide a complete picture of fatigue performance and healing.

- Based on findings related to the second objective, it would be useful to incorporate self - healing within a road maintenance plan to improve sustainability by reducing the cost and time.

- Regarding DA for which the healing capacity was low. Moreover, the sample suffered higher bending during cyclic loading that led to runout the bitumen and reducing capacity for flow between the aggregates and drainages into the cracks. This is a noteworthy point must be studied in future. Rutting and trafficking may reduce the self-healing ability of DA and thus, reduce the durability of the road.

- Regarding the self-healing test methods developed in this thesis, further research is needed to validate and implement these methods into practice. The test methods can be

used for ranking the self-healing capabilities of different types of binders and modifications in relation to the physical-chemical, rheological and micro-structural properties. More variables should also be considered including aging, moisture and so on. In addition, it is also recommended to apply these developed methods to evaluate the crack-sealing capability of sealants and joint materials.

References

[1] Sultan, S. A. and Guo, Z., (2016). Evaluating life cycle costs of perpetual pavements in China using operational pavement management system. International Journal of Transportation Science and Technology 5(2): 103-109.

[2] García, A., Schlangen, E., Van de Ven, M., and Van Vliet an Vliet, D., (2011). Induction heating of mastic containing conductive fibers and fillers. Materials and structures 44(2): 499-508.

[3] Loizos, A., Scarpas, T. and Al-Qadi, I.L., 2008.Pavement cracking: CRC Press. mechanisms, modeling, detection, testing and case histories.

[4] Fakhri, M., Hassani, K. and Ghanizadeh , A. R. ,(2013). Impact of loading frequency on the fatigue behavior of SBS modified asphalt mixtures. Procedia-Social and Behavioral Sciences 104: 69-78.

[5] Al-Khateeb, G. G. and Ghuzlan, K. A., (2014). The combined effect of loading frequency, temperature, and stress level on the fatigue life of asphalt paving mixtures using the IDT test configuration. International Journal of Fatigue 59: 254-261.

[6] Rao T., R., Craus, J., Deacon, J.A. and Monismith, C.L., (1990). Summary report on fatigue response of asphalt mixtures. Rep. to Strategic Highway Research Program.

[7] Liu, Q., Schlangen, E., Van de Ven, M., Bochove, G. Van and Montfort, J. Van (2012). Evaluation of the induction healing effect of porous asphalt concrete through four-point bending fatigue test. Construction and Building Materials 29: 403-409.

[8] Read, J. and Whiteoak, D., (2003). The shell bitumen handbook, Thomas Telford.

[9] Harvey, J. and Tsai, B.W., (1996). Effects of asphalt content and air void content on mix fatigue and stiffness. Transportation Research Record: Journal of the Transportation Research Board(1543): 38-45

[10] Igwe, E. and May A., (2016). Investigating the effect of air voids content in fatigue life of hot mix asphalt mixtures: case study of rubberized asphalt concrete. IJISET–Int. J. Innovative Sci. Eng. Technol. 3.

[11] Gómez-Meijide, B., Ajam, H., Lastra-González, P. and Garcia, A., (2016). Effect of air voids content on asphalt self-healing via induction and infrared heating. Construction and Building Materials 126: 957-966.

[12] García, Á., Jelfs, J. and Austin, C., J. ,(2015). Internal asphalt mixture rejuvenation using capsules. Contraction and Building Materials 101: 309-316.

[13] Ahmad, J., Rahman, M., Hainin, M., R. and Hossain, M., (2012). Comparative evaluation of hot mix asphalt design methods, International Journal of Pavement Engineering, 13(2), pp.89-97.

[14] Thom, N., (2006). Asphalt cracking: a Nottingham perspective. Engenaria Civil/Civil Engineering 26: 75-84.

[15] Thom, N. (2008). Principles of pavement engineering, Thomas Telford London.

[16] Mahrez, A. and Karim, M., R., (2010). Fatigue characteristics of stone mastic asphalt mix reinforced with fiber glass. International Journal of the Physical Sciences 5(12): 1840-1847.

[17] Taih, S. A., (2011). The effect of additives in hot asphalt mixtures. Journal of Engineering and Sustainable Development 15(3): 132-151.

[18] Zeiada, W.A., Gudipudi, P.P., Underwood, B.S. and Souliman, M.I., (2018). Effect of Loading Waveform Pattern and Rest Period on Fatigue Life of Asphalt Concrete Using Viscoelastic

[19] Daniel L. tacks, P.E., Director, Maintenance Division. July 09, (2018). Pavement Manual. Pavement Design Group, 512: 416-3196, Continuum Damage Model. Transportation Research Record, 2672(28), pp.451-461.

[20] Roberts, F. L., Mohammad, L. N. and Wang, L., (2002). History of hot mix asphalt mixture design in the United States. Journal of Materials in Civil Engineering 14(4): 279-293.

[21] Garber, N. J. and Hoel, L., A., (2014). Traffic and highway engineering, Cengage Learning.

[22] Leng, Z., (2012). Prediction of in-situ asphalt mixture density using ground penetrating radar: theoretical development and field verification, University of Illinois at Urbana-Champaign.

[23] Gorkem, C. and Sengoz, B., (2009). Predicting stripping and moisture induced damage of asphalt concrete prepared with polymer modified bitumen and hydrated lime. Construction and Building Materials 23(6): 2227-2236.

[24] Brown, E. N.,White, S. R. and Sottos, N. R., (2005). Retardation and repair of fatigue cracks in a microcapsule toughened epoxy composite–Part I: Manual infiltration. Composites Science and Technology 65(15-16): 2466-2473.

[25] Mashaan, N.S., Ali, A.H., Koting, S. and Karim, M.R., 2013. Dynamic properties and fatigue life of stone mastic asphalt mixtures reinforced with waste tyre rubber. Advances in Materials Science and Engineering.

[26] Chen, J.S., Hsieh, W. and Liao, M.C., 2013. Effect of coarse aggregate shape on engineering properties stone mastic asphalt applied to airport pavements. International Journal of Pavement Research and Technology 6(5): 595.

[27] Bellin, P., 1997. Development, principles and long-term performance of stone mastic asphalt in Germany. SCI Lecture Papers.

[28] Muniandy, R. and Huat. B. B., 2006. Laboratory diameteral fatigue performance of stone matrix asphalt with cellulose oil palm fiber. American Journal of Applied Sciences 3(9): 2005-2010.

[29] Rekha, K. and Rao, B.N., (2017). A Stone Mastic Asphalt is Gap Graded by Using Bagasse Fiber (sugar cane). IJARIIE-ISSN(O)-2395-4396.

[30] Mahrez, A. and Karim, M. R., 2010. Fatigue characteristics of stone mastic asphalt mix reinforced with fiber glass. International Journal of the Physical Sciences 5(12): 1840-1847.

[31] Richardson, J., 1997. Stone mastic asphalt in the Uk symposium on stone mastic asphalt and thin surfacing. London, Richter E.

[32] Titus-Glover, Von Quintus, L., Smith,H. L. K. L., Stanley, M. and Rao S., 2006. Life-cycle cost analysis of SMA pavements and SMA application guidelines, Wisconsin Highway Research Program.

[33] Campbell, C., 1999, The Use of Stone Mastic Asphalt on Aircraft Pavements, Submitted in fulfillment of the requirements for SEN713 Research/Professional Practice Projects, School of Engineering and Technology, Deakin University, Geelong, Victoria, Australia, December.

[34] Qiu, YF & Lim, KM., (2006), Design and performance of stone mastic asphalt, Journal of Transportation Engineering, vol. 132, no. 12, pp. 956–963.

[35] Roseen, R.M., Ballestero, T.P., Houle, J.J., Briggs, J.F. and Houle, K.M., (2011), Water quality and hydrologic performance of a porous asphalt

pavement as a storm-water treatment strategy in a cold climate. Journal of Environmental Engineering, 138(1), pp.81-89.

[36] Allan -Alderson, A. T., John Bethune, A. T., John Oliver and John Rebbechi, C. E., (1997). Open Graded Asphalt.Design Guide. Australian Asphalt Pavement Association.

[37] National Asphalt Pavement Association ed., (2002). Design, Construction, and Maintenance of Open-graded Asphal Friction Courses. Asphalt Institute; National Asphalt Pavement Association.

[38] https://ops.fhwa.dot.gov/weather/q1_roadimpact.htm. Accesed in FHWA, 2017.

[39] Miljković, M. and Radenberg, M., 2012. Thin noise-reducing asphalt pavements for urban areas in Germany. International Journal of Pavement Engineering, 13(6), pp.569-578.

[40] Hassan, N.A., Abdullah, N.A.M., Shukry, N.A.M., Mahmud, M.Z.H., Yunus, N.Z.M., Putrajaya, R., Hainin, M.R. and Yaacob, H., (2015). Laboratory evaluation on the effect of clogging on permeability of porous asphalt mixtures. J Teknol, 76(14), pp.77-84.

[41] Gardziejczyk, W., (2016). The effect of time on acoustic durability of low noise pavements–The case studies in Poland. Transportation Research Part D: Transport and Environment, 44, pp.93-104.

[42] Paris, P.C. and Sih, G.C., (1965). Stress analysis of cracks. In Fracture toughness testing and its applications. ASTM International.

[43] Collop, A.C. and Roque, R., (2004). Report on the prediction of surface-initiated longitudinal wheel path cracking in asphalt pavements. Road materials and pavement design, 5(4), pp.409-434.

[44] Lee, H. and Kim,J., (2005). Development of a crack type index.Transportation research record, 1940(1), pp.99-109.

[45] S.C.S.R. Tangella, J. Craus, J.A. Deacon, C.L. Monismith, in: Summary Report on Fatigue Response of Asphalt Mixtures, Transportation Research Board, 1990, p. 147.

[46] Van Dijk, W. (1975),"Practical Fatigue Characterisation of Bituminous Mixes", Proceeding of the Association of Asphalt Paving Technologist, Vol.44. pp.38-74..

[47] Gharaibeh, N.G. and Darter, M.I., (2002). Longevity of highway pavement in Illinois---2000 Update.

[48] Read, J.M. (1996),"Fatigue Cracking of Asphalt Pavements", PhD thesis, University of Nottingham, Department of Civil Engineering.

[49] Lytton, R. L., Uzan , J., Fernando, E. G., Roque, R., Hiltunen, D. and Stoffels, S. M., (1993). Development and validation of performance prediction models and specifications for asphalt binders and paving mixes, Strategic Highway Research Program Washington, DC.

[50] Cao, P., Liu, T., Pu, C. and Lin, H., (2015). Crack propagation and coalescence of brittle rock-like specimens with pre-existing cracks in compression. Engineering geology, 187, pp.113-121.

[51] James, M., (2012). Concepts and lab testing Pre- bid Meeting, Oakland, CA.

[52] Pell, P. and Cooper, K., (1975). The effect of testing and mix variables on the fatigue performance of bituminous materials. Journal of the Association of Asphalt Paving Technologists 44: 1-37.

[53] Huang, Y. H. (2004). "Pavement Analysis and Design", 2nd edition, Prentice Hall, Englewood Cliffs, New Jersey.

[54] Shen, S., Chiu, H.-M. and Huang, H., (2010). Characterization of fatigue and healing in asphalt binders. Journal of Materials in Civil Engineering 22(9): 846-852.

[55] Chou, J.S. and Tu, W.T., (2011). Failure analysis and risk management of a collapsed large wind turbine tower. Engineering Failure Analysis, 18(1), pp.295-313.

[56] Rowe, G., (1993). Performance of asphalt mixtures in the trapezoidal fatigue test. Asphalt Paving Technology 62: 344-344.

[57] Little, D. N., Lytton, R. L., Chairl, B. D. , Williams and lTexas, A. ,(1998). An Analysis of the Mechanism of Microdamage Healing Based on the Application of Micromechanics First Principles of Fraci1jre and Healing.

[58] Roberts, F. L., Mohammad, L. N. and Wang L., (2002). History of hot mix asphalt mixture design in the United States. Journal of Materials in Civil Engineering 14(4): 279-293.

[59] Tabaković, A. and Schlangen, E., (2015). Self-healing technology for asphalt pavements. In Self-healing Materials (pp. 285-306). Springer, Cham.

[60] Schlangen, E.and Sangadji,S.,(2013).Addressing infrastructure durability and sustain ability by self-healing mechanisms Recent advances in self-healing concrete and asphalt.Procedia Engineering,54, pp.39-57.

[61] Johnson,A.M.,2000.Bestpractices handbook on asphalt pavement maintenance.

[62] Bazin, P. and Saunier, J.,(1967). Deformability, fatigue and healing properties of asphalt mixes. Intl Conf Struct Design Asphalt Pvmts.TRID.

[63] Qiu, J., (2012). Self -healing of asphalt mixtures: towards a better understanding of the mechanism

[64] Dry, C., (1994). Matrix cracking repair and filling using active and passive modes for smart timed release of chemicals from fibers into cement matrices. Smart Materials and Structures, 3(2), p.118.

[65] Darabi, M.K., Al-Rub, R.K.A. and Little, D.N., (2012). A continuum damage mechanics framework for modeling micro-damage healing. International Journal of Solids and Structures, 49(3-4), pp.492-513.

[66] García, Á., (2012). Self-healing of open cracks in asphalt mastic. Fuel 93: 264-272.

[67] Castro, M. and Sánchez, J. A., (2006). Fatigue and healing of asphalt mixtures: discriminate analysis of fatigue curves. Journal of transportation engineering 132(2): 168-174.

[68] Al-Rub, R.K.A., Darabi, M.K., Little, D.N. and Masad, E.A., (2010). A micro-damage healing model that improves prediction of fatigue life in asphalt mixes. International Journal of Engineering Science, 48(11), pp.966-990.

[69] García, A., Bueno, M., Norambuena-Contreras, J. and Partl, M.N., (2013). Induction healing of dense asphalt concrete. Construction and Building Materials, 49, pp.1-7.

[70] García, A., Norambuena-Contreras, J., Bueno, M. and Partl, M.N., (2014). Influence of steel wool fibers on the mechanical, termal, and healing properties of dense asphalt concrete. Journal of Testing and Evaluation, 42(5), pp.1107-1118.

[71] García, A., Norambuena-Contreras, J., Bueno, M. and Partl, M.N., (2015). Single and multiple healing of porous and dense asphalt concrete. Journal of Intelligent Material Systems and Structures, 26(4), pp.425-433.

[72] Ajam, H., Lastra-González, P., Gómez-Meijide, B., Airey, G. and Garcia, A., (2017). Self-healing of dense asphalt concrete by two different

approaches: electromagnetic induction and infrared radiation. Journal of Testing and Evaluation, 45(6), pp.1933-1940.

[73] Dunn, S.G., Nenniger, E.H. and Rajan, V.S.V., (1989). A study of bitumen recovery by gravity drainage using low temperature soluble gas injection. The Canadian Journal of Chemical Engineering, 67(6), pp.978-991.

[74] Liu, Q., Tang, J. and He, L., (2016). Thermally Activated Healing of Fatigue Damage in Asphalt Binders. Journal of Testing and Evaluation, 45(2), pp.574-581.

[75] Menozzi, A., Garcia, A., Partl, M.N., Tebaldi, G. and Schuetz, P., (2015). Induction healing of fatigue damage in asphalt test samples. Construction and Building Materials, 74, pp.162-168.

[76] Qiu, J., Van de Ven, M., Wu, S., Yu, J. and Molenaar, A., (2012). Evaluating self -healing capability of bituminous mastics. Experimental mechanics, 52(8), pp.1163-1171.

[77] Deng, G., Tang, C., Li, F., Jiang, H. and Chen, Y., (2010). Covalent cross-linked polymer gels with reversible sol− gel transition and self-healing properties. Macromolecules, 43(3), pp.1191-1194.

[78] Nciri, N., Kim, N. and Cho, N., (2017). New insights into the effects of styrene-butadiene-styrene polymer modifier on the structure, properties,

and performance of asphalt binder: The case of AP-5 asphalt and solvent deasphalting pitch. Materials Chemistry and Physics, 193, pp.477-495.

[79] Lesueur, D., (2009). The colloidal structure of bitumen: Consequences on the rheology and on the mechanisms of bitumen modification. Advances in colloid and interface science, 145(1-2), pp.42-82.

[80] Padmarekha, A. and Krishnan, J.M., (2011). Experimental investigation on sol–gel transition of asphalt. International Journal of Advances in Engineering Sciences and Applied Mathematics, 3(1-4), pp.131-139.

[81] Bonemazzi, F. and Giavarini, C., (1999). Shifting the bitumen structure from sol to gel. Journal of Petroleum Science and Engineering, 22(1-3), pp.17-24.

[82] Wool, R.P., 2008. Self-healing materials: a review. Soft Matter, 4(3), pp.400-418.

[83] García, Á., Schlangen, E., M. van de Ven and Liu , Q., (2012). A simple model to define induction heating in asphalt mastic. Construction and Building Materials 31: 38-46.

[84] Bennert, T., Reinke, G., Mogawer, W. and Mooney, K., (2010). Assessment of workability and compactability of warm-mix asphalt. Transportation Research Record, 2180(1), pp.36-47.

[85] Norambuena-Contreras, J., Yalcin, E., Garcia, A., Al-Mansoori, T., Yilmaz, M. and Hudson-Griffiths, R., (2018). Effect of mixing and ageing on the

mechanical and self-healing properties of asphalt mixtures containing polymeric capsules. Construction and Building Materials, 175, pp.254-266.

[86] Shen, S. and Sutharsan, T., (2011). Quantification of cohesive healing of asphalt binder and its impact factors based on dissipated energy analysis. Road Materials and Pavement Design 12(3): 525-546.

[87] Phillips, M., (1998). Multi-step models for fatigue and healing, and binder properties involved in healing. Eurobitume workshop on performance related properties for bituminous binders, Luxembourg. , p. 115.

[88] Qiu, J., (2012). Self -healing of asphalt mixtures: towards a better understanding of the mechanism, TU Delft, Delft University of Technology.

[89] Porto, M.,Caputo, P., Loise, V., Eskandarsefat, S., Teltayev, B. and Oliviero Rossi, C., (2019). Bitumen and bitumen modification: A review on latest advances. Applied Sciences, 9(4), p.742.

[90] Tang, J., Liu, Q., Wu, S., Q. Ye, Sun, Y. and Schlangen, E. (2016). Investigation of the optimal self-healing temperatures and healing time of asphalt binders. Construction and Building Materials 113: 1029-1033.

[91] Van Dijk, W., Moreaud, H., Quedeville, A. and Uge, P., (1972). The fatigue of bitumen and bituminous mixes. Presented at the Third International

conference on the Structural Design of Asphalt Pavements, Grosvenor House, Park Lane, London, England, Sept. 11-15, 1972.

[92] Molenaar, A., (2007). Design of flexible pavements. Delft University of Technology, Lecture CT4860, Delft.

[93] Williams, D., Little, D., Lytton, R. and Kim ,Y., (2001). Microdamage healing in asphalt and asphalt concrete, Volume 2: laboratory and field testing to assess and evaluate microdamage and microdamage healing, Turner-Fairbank Highway Research Center.

[94] Kim, Y. R., Little, D. N. and Benson, F. C. (1990). Chemical and mechanical evaluation on healing mechanism of asphalt concrete (with discussion). Journal of the Association of Asphalt Paving Technologists 59.

[95] Francken, L. and Clauwaert, C., (1987). characterization and structural assessment of bound materials for flexible road structures. sixth international conference, structural design of asphalt pavements, volume I, proceedings, university of michigan, july 13-17, 1987, ann arbor, michigan. publication of: michigan university, Ann Arbor.

[96] Lee, N. K., Morrison, G. R. and Hesp, S., (1995). Low temperature fracture of polyethylene-modified asphalt binders and asphalt concrete mixes (with discussion). Journal of the Association of Asphalt Paving Technologists 64.

[97] Bahia, H. U.,H., K. and Kose, S., (1999). Non-linear viscoelastic and fatigue properties of asphalt binders. Journal of the Association of Asphalt Paving Technologists 68: 1-34.

[98] Kim, B. and Roque, R., (2006). Evaluation of healing property of asphalt mixtures. Transportation Research Record: Journal of the Transportation Research Board (1970): 84-91.

[99] Little, D.N., Lytton, R.L., Chairl, B., Williams, D. and lTexas, A.M., 1998, August. An analysis of the mechanism of microdamage healing based on the application of micromechanics first principles of Fraci1jre and healing. Lino Lakes, MN: Association of Asphalt Paving Technologists.

[100] Van den Bergh, W. 2011. The effect of ageing on the fatigue and healing properties of bituminous mortars.Deft University of Technology, PhD thesis, 2011.

[101] Liu, Q., Schlangen, E., van de Ven, M., van Bochove, G. and van Montfort, J., (2012). Evaluation of the induction healing effect of porous asphalt concrete through four-point bending fatigue test. Construction and Building Materials, 29, pp.403-409.

[102] Vo, H.V., Park, D.W., Seo, J.W. and Le, T.H.M., 2019. Effects of asphalt types and aging on healing performance of asphalt mixtures using induction heating method. Journal of Traffic and Transportation Engineering (English Edition).

[103] Raithby, K.D. and Sterling, A.B., 1970. The effect of rest periods on the fatigue performance of a hot-rolled asphalt under reversed axial loading and discussion. In Association of Asphalt Paving Technologists Proc.

[104] Bonnaure, F., Huibers, A. and Boonders, A. , 1982. A laboratory investigation of the influence of rest periods on the fatigue characteristics of bituminous mixes (with discussion). association of Asphalt Paving Technologists Proceedings.

[105] Bhasin, A., Bommavaram, D. and Greenfiled, M., 2009. Intrinsic healing in asphalt.

[106] Bhasin, A., Little, D.N., Bommavaram, R. and Vasconcelos, K., 2008. A framework to quantify the effect of healing in bituminous materials using material properties. Road Materials and Pavement Design, 9(sup1), pp.219-242.

[107] Lytton, R. L., Chen, C. W. and Little, D. N. (2001). Microdamage healing in asphalt and asphalt concrete: A micromechanics fracture and healing model for asphalt concrete. Western Research Institute Volume III.

[108] Little, D. N. and Bhasin ,A., 2007. Exploring Mechanism of Healing in Asphalt Mixtures and Quantifying its Impact. Self -healing materials, Springer: 205-218.

[109] Liu, Q., Yu, W., Wu, S., Schlangen, E. and Pan, P., 2017. A comparative study of the induction healing behaviors of hot and warm mix asphalt. Construction and Building Materials, 144, pp.663-670.

[110] Sun, D., F. Yu, Lin, L. Li, T. and Zhu, X., 2017. Effect of chemical composition and structure of asphalt binders on self-healing. Construction and Building Materials 133: 495-501.

[111] Kim, Y.R., Little, D.N., Lytton, R.L., D'Angelo, J., Davis, R., Rowe, G., Reinke, G., Marasteanu, M., Masad, E., Roque, R. and Tashman, L.,(2002). Use of dynamic mechanical analysis (DMA) to evaluate the fatigue and healing potential of asphalt binders in sand asphalt mixtures. In Asphalt Paving Technology: Association of Asphalt Paving Technologists-Proceedings of the Technical Sessions Association of Asphalt Paving Technologist. Vol. 71, pp. 176-206.

[112] Song, I., Little, D.N., Masad, E.A. and Lytton, R., (2005). Comprehensive evaluation of damage in asphalt mastics using X-ray CT, continuum mechanics, and micromechanics (with discussion). Journal of the association of asphalt paving technologists, 74.

[113] Molenaar, A. (2006). APT as a Tool for the Development of Design and Performance Models. 10TH International Conference on Asphalt Pavements-AUGUST 12 to 17, 2006, Quebec City, Canada.

[114] Seo, Y. and Kim, Y. R. (2008). Using acoustic emission to monitor fatigue damage and healing in asphalt concrete.KSCE Journal of Civil Engineering 12(4): 237-243.

[115] Kim YR, Little DN (1990). One-dimensional constitutive modeling of asphalt concrete. Journal of Engineering Mechanics ASCE 116 (4):751-772.

[116] Kim YR, Little DN (1991). SEM analysis on fracture and healing of sand-asphalt mixtures. Journal of Materials in Civil Engineering 3 (2):140-153.

[117] Grant, T. P., (2001). Determination of asphalt mixture healing rate using the Superpave indirect tensile test, University of Florida USA.

[118] Zhang, Z., Roque R., Birgisson,B. and Sangpetngam ,B. ,(2001). Identification and verification of a suitable crack growth law (with discussion). Journal of the Association of Asphalt Paving Technologists 70.

[119] Zhang, Z. (2000). Identification of suitable crack growth law for asphalt mixtures using the Superpave indirect tensile test (IDT), University of Florida.

[120] Qiu, J., M. Van de Ven, S. Wu,J. Yu and Molenaar,A., (2011). Investigating self -healing behaviour of pure bitumen using dynamic shear rheometer. Fuel 90(8): 2710-2720.

[121] Hammoum, F., de La Roche, C., Piau, J. and Stefani, C., (2002). Experimental investigation of fracture and healing of bitumen at pseudo-

contact of two aggregates. 9th international conference on asphalt pavements.

[122] Liu, Q., Schlangen, E., van de Ven, M. F., G. van Bochove and van Montfort ,J. , (2012). Predicting the performance of the induction healing porous asphalt test section. 7th RILEM International Conference on Cracking in Pavements, Springer.

[123] Gallego, J., del Val, M. A., Contreras, V., Páez, A., (2013). Heating asphalt mixtures with microwaves to promote self-healing. Construction and Building Materials 42: 1-4.

[124] Wu, S., L. Mo, Shui, Z. and Chen, Z. (2005). Investigation of the conductivity of asphalt concrete containing conductive fillers. Carbon 43(7): 1358-1363.

[125] Lucas, J.,(2016). What Is Faraday's Law of Induction? Live Science Contributor (University of Texas).

[126] Minsk, L. D., (1968). Electrically conductive asphalt for control of snow and ice accumulation. Highway Research Record (227).

[127] Liu, Q., García, Á., Schlangen, E. and van de Ven, M., (2011). Induction healing of asphalt mastic and porous asphalt concrete. Construction and Building Materials, 25(9), pp.3746-3752.

[128] Francken, L., (1979). Fatigue performance of a bituminous road mix under realistic test conditions.Transportation Research Record (712)

[129] Wool, R.P. and, O'connor, K.M.,1981. Atheory crack healing in polymers . Journal of Applied Physics, 52 (10), pp.5953-5963.

[130] Shao-peng, W., Lian-tong , M., Zhong-he , Dong-xing ,S., X., X. Yong-jie and Wen-feng, Y. , (2002). An improvement in electrical properties of asphalt concrete. Journal of Wuhan University of Technology-Mater. Sci. Ed. 17(4): 69-72.

[131] Wu, S.-p., X.-m. Liu, Q.-s. Ye and Ning, L.,(2006). Self-monitoring electrically conductive asphalt-based composite containing carbon fillers. Transactions of Nonferrous Metals Society of China 16: s512-s516.

[132] Garcia, A., Schlangen, E., Van de Ven, M. & Liu, Q. 2012. A simple model to define induction heating in asphalt mastic. Construction and Building Materials, 31, 38-46.

[133] Chiu, C.-T. and Lee, M.-G., (2006). Effectiveness of seal rejuvenators for bituminous pavement surfaces. Journal of Testing and Evaluation 34(5): 390-394.

[134] Sirin, O., D. K. Paul and E. Kassem (2018). State of the Art Study on Aging of Asphalt Mixtures and Use of Antioxidant Additives. Advances in Civil Engineering 2018.

[135] García, Á., Schlangen, E. and Van de Ven, M., 2011. Properties of capsules containing rejuvenators for their use in asphalt concrete. Fuel, 90(2), pp.583-591.

[136] Garcia, A., Jelfs, J. & Austin, C. J. 2015. Internal asphalt mixture rejuvenation using capsules. Construction and Building Materials, 101, 309-316.

[137] Blaiszik, B., Sottos, N. and White, S. ,2008. Nanocapsules for self- materials. Composites Science and Technology 68(3-4): 978-986.

[138] Brown, E. R., 1999. Designing stone matrix asphalt mixtures for rut-resistant pavements, Transportation Research Board.

[139] Garcia, A., Schlangen, E., Van De Ven, M. & Van Bochove, G. 2012b. Optimization of composition and mixing process of a self-healing porous asphalt. Construction and Building Materials, 30, 59-65.

[140] Al-Mansoori, T., Norambuena-Contreras, J., Micaelo, R. and Garcia, A., 2018. Self-healing of asphalt mastic by the action of polymeric capsules containing rejuvenators. Construction and Building Materials, 161, pp.330-339.

[141] Ma T., Zhang Y., Zhang D., Yan J., Ye Q., Influences by air voids on fatigue life of asphalt mixture based on discrete element method 2016, Construction and Building Materials 126: 785-799

[142] García, Á., Schlangen ,E. and Van de Ven, M., 2011. Properties of capsules containing rejuvenators for their use in asphalt concrete. Fuel 90(2): 583-591.

[143] Yalçin, E., 2018. Development of a self-healing asphalt mixture through the use of encapsulated healing agents/İyileştirici maddeler içeren kapsüller kullanılarak kendini onarabilen bitümlü sıcak karışımların geliştirilmesi.

[144] Liu, Y. and Mahadevan, S., 2010. Probabilistic fatigue life prediction of composite materials. In Fatigue life prediction of composites and composite structures (pp. 220-248). Woodhead Publishing.

[145] Su, J.F., Yang, P., Wang, Y.Y., Han, S., Han, N.X. and Li, W., (2016). Investigation of the self-healing behaviors of microcapsules/bitumen composites by a repetitive direct tension test. Materials, 9(7): p.600.

[146] Zargar, M, Ahmadinia, E, Asli, H. and Karim, M.R., 2012. Investigation of the possibility of using waste cooking oil as a rejuvenating agent for aged bitumen, Journal of Hazardous Materials, 233-234:254-258.

[147] BSI, BS EN 13108-1, 2016. Bituminous mixtures — Material specifications Part 1: Asphalt Concrete, British Standard Institute (BSI), 2016.

[148] BSI, BS EN 13108-7:2016, 2016b. Bituminous mixtures. Material specifications. Porous Asphalt. London, England: BSI: British Standard Institute.

[149] BSI, BS EN 13108-5,2008. Bituminous mixtures — Material specifications Part 5: Stone Mastic Asphalt, British Standard Institute (BSI), 2008.

[150] BSI, BS EN 13108-5, 2016. Bituminous mixtures — Material specifications Part 5: Stone Mastic Asphalt, British Standard Institute (BSI), 2016.

[151] BSI, BS EN 12697-33, 2003. Bituminous mixtures — Test methods for hot mix asphalt — Part 33: Specimen prepared by roller compactor, British Standards Institution, London.

[152] HEALED ROADS 2012. Available at www.healroad.eu

[153] Barrasa, R.C., López, V.B., Montoliu, C.M.P., Ibáñez, V.C., Pedrajas, J. and Santarén, J., 2014. Addressing durability of asphalt concrete by self-healing mechanism. Procedia-Social and Behavioral Sciences, 162, pp.188-197.

[154] Al-Mansoori, T., Norambuena-Contreras, J., Micaelor, R. and Garcia, A., (2018). Self-healing of asphalt mastic by the action of polymeric capsules containing rejuvenators, Construction and Building Materials 161, 330–339.

[155] BSI, BS EN 12697-26, 2012. Bituminous mixtures - Test methods for hot mix asphalt - Part 26: Stiffness, British Standards Institution, London.

[156] Tanaka, S., Ichikawa, M. and Akita, S., (1984). A probabilistic investigation of fatigue life and cumulative cycle ratio. Engineering Fracture Mechanics, 20(3), pp.501-513.

[157] Gómez-Meijide, Breixo, Harith Ajam, Pedro Lastra-González, and Alvaro Garcia. 2016. 'Effect of air voids content on asphalt self-healing via induction and infrared heating', Construction and Building Materials, 126: 957-66.

[158] Asphalt Institute-M2., 2014. Asphalt Mix Design Methods (No. 2). Asphalt Institute. Printed in USA Seventh Edition 2014.

[159] Micaelo, R., Al-Mansoori, T. and Garcia, A., 2016. Study of the mechanical properties and self-healing ability of asphalt mixture containing calcium-alginate capsules, Construction and Building Materials, 123, 734–744.

[160] Tabaković, Xu, S, A X Liu, and Schlangen, E., 2018. Calcium alginate capsules encapsulating rejuvenator as a healing system for asphalt mastic, Construction and Building Materials, 169: 379-87.

[161] Hassan, N.A., Airey, G.D. and Hainin, M.R., 2014. Characterisation of micro-structural damage in asphalt mixtures using image analysis. Construction and Building Materials, 54, pp.27-38.

[162] Vogel, H.J., 1997. Morphological determination of pore connectivity as a function of pore size using serial sections. European Journal of Soil Science, 48(3), pp.365-377.

[163] Aboufoul M., and Garcia, A., 2017. Factors affecting hydraulic conductivity of asphalt mixture, Materials and Structures, 50: 116.

[164] Hassn, A., Aboufoul, M., Wu, Y., Dawson, A. and Garcia, A., 2016. Effect of air voids content on thermal properties of asphalt mixtures. Construction and Building Materials, 115, pp.327-335.

[165] BS EN 13043: 2013 Aggregates for bituminous mixtures and surface treatments for roads, airfields and other trafficked areas.

[166]BS EN 12697 PART 6, 2003, British Standards Institute (BSI), Bituminous mixtures, test methods for hot mix asphalt: Determination of bulk density of bituminous specimens.

[167] BSI, EN 12697-26. 2004. Determination of the Maximum Density,British Standard Institute (BSI),.

[168] BS EN 12697 PART 6, 2012; British Standards Institute (BSI), Bituminous mixtures, test methods for hot mix asphalt: Determination of bulk density of bituminous specimens of bituminous specimens, British Slandered Institute, London.

[169] BSI, BS EN. BS EN. 13043:2002, 2002, Aggregates for bituminous mixtures and surface treatments for roads, airfields and other trafficked areas. London, England: BSI: British Standard Institute.

[170] Grossegger D., Gomez-Meijide B., van Steenkiste S., Garcia A., Influence of rheological and physical properties of heat-induced self-healing of asphalt mastic beams, Construction and Building Materials, 182, 298-308.

[171] Ayar, Pooyan, Fernando Moreno-Navarro, and Mª Carmen Rubio-Gámez. 2016. 'The healing capability of asphalt pavements: a state-of-the-art review', Journal of Cleaner Production, 113: 28-40.

[172] Gómez-Meijide, B, Pérez, I., Nonlinear elastic behaviour of bitumen emulsion-stabilized materials with C&D waste aggregates, Construction and Building Materials, 98,2015, 853-863.

[173] Pan, C., Tang, P., Riara, M., Mo, L., Li, M. and Guo, M., 2018. Effect of Healing Agents on Crack Healing of Asphalt and Asphalt Mortar. Materials, 11(8), p.1373.

[174] Pauli, A.T.,2014, Chemomechanics of Damage Accumulation and Damage-Recovery Healing in Bituminous Asphalt Binders, PhD Thesis 2014, TU Delft.

[175] Xu S., Garcia A., Su J., Liu Q., Tabaković A., Schlangen E., Self-healing Asphalt Review: From Idea to Practice, Advanced Materials Interfaces 2018, 5, 17.

[176] Salih S., Gomez-Meijide B., Aboufoul M., Garcia A., Effect of porosity on infrared heating of fatigue damage in asphalt, Construction and Building Materials 2018, 716-725:167.

[177] Jo SD, Richard KY, .2001. Laboratory evaluation of fatigue damage and healing of asphalt mixtures. Journal of Materials in Civil Engineering 13(6):434-440.

[178] Aguirre, M.A., Hassan, M.M., Shirzad S. Daly, W.H. Mohammad, L.N. 2016 Micro-encapsulation of asphalt rejuvenators using melamine-formaldehyde, Construction and Building Materials, 114, (2016) 29-39.

[179] Ma T., Zhang Y., Zhang D., Yan J., Ye Q., Influences by air voids on fatigue life of asphalt mixture based on discrete element method 2016, Construction and Building Materials 126: 785-799.

[180] Moreno-Navarro, F., Sol-Sanchez, M. Rubio-Gamez M.C.2015, Exploring the recovery of fatigue damage in bituminous mixtures: the role of healing. Road Materials and Pavement Design, 2015, 1-15. http://dx.doi.org/10.1080/14680629.2015.1029706

[181] White, S. R., Sottos, N., Geubelle, P. Moore, J., Kessler, Sriram, M. R., S., Brown, E. and Viswanathan., S.,2001. Autonomic healing of polymer composites. Nature 409(6822): 794.

[182] Brown, E. N., White, S. R. and Sottos, N. R. 2005. Retardation and repair of fatigue cracks in a microcapsule toughened epoxy composite—Part II: In situ self-healing. Composites Science and Technology 65(15-16): 2474-2480.

[183] Brown, E. N., White,S. R. and. Sottos, N . R., 2005. Retardation and repair of fatigue cracks in a microcapsule toughened epoxy composite–Part I: Manual infiltration. Composites Science and Technology 65(15-16): 2466-2473.

[184] García, Á., E. Schlangen, M. van de Ven and G. Sierra-Beltrán, 2010. Preparation of capsules containing rejuvenators for their use in asphalt concrete. Journal of hazardous materials 184(1-3): 603-611.

[185] Zhang, Y., M. F. van de Ven, A. A. Molenaar and S. Wu ,2016. Assessment of effectiveness of rejuvenators on artificially aged mortar. Journal of Materials in Civil Engineering 28(9): 04016079.

[186] Shansky, E.,2005. Synthesis and characterization of microcapsules for self-healing materials.

[187] Boyer, R. E. and Engineer, P. S. D., 2000. Asphalt Rejuvenators Fact, or Fable. Transportation systems 58: l.

[188] Yin, T., Rong, M. Zhang, Z. M. Q and Yang, G. C. 2007. Self-healing epoxy composites–preparation and effect of the healant consisting of microencapsulated epoxy and latent curing agent. Composites Science and Technology 67(2): 201-212.

[189] Mousavi, M., Abdollahi, T., Pahlavan, F. and Fini, E.H., 2016. The influence of asphaltene-resin molecular interactions on the colloidal stability of crude oil. Fuel, 183, pp.262-271.

[190] Loise, V., Caputo, P., Porto, M., Calandra, P., Angelico, R. and Rossi, C.O., 2019. A Review on Bitumen Rejuvenation: Mechanisms, Materials, Methods and Perspectives. Applied Sciences, 9(20), p.4316.

[191]Suresh, S.,1998. Fatigue of Materials, Cambridge University Press. Cambridge, England.

[192] Schlangen, E. and Sangadji, S., 2013. Addressing infrastructure durability and sustainability by self -healing mechanisms-recent advances in self-healing concrete and asphalt. Procedia Engineering 54: 39-57.

[193] Cho, D.-W., Kim, K. and Lee M.-J. 2010. Chemical model to explain asphalt binder and asphalt–aggregate interface behaviors. Canadian Journal of Civil Engineering 37(1): 45-53.

[194] Schapery, R.,1989. On the mechanics of crack closing and bonding in linear viscoelastic media. International Journal of Fracture 39(1-3): 1

[195] Shen, S. and Lu, X., 2013. Fracture healing properties of asphaltic material under controlled damage. Journal of Materials in Civil Engineering, 26(2), pp.275-282.

[196] BSI, BS EN. BS EN 12697-8:2003, 2003a., Bituminous mixtures. Test methods for hot mix asphalt. Determination of void characteristics of bituminous specimens. London, England: BSI: British Standard Institute.

[197] Craven, J. M., 1969. Cross-linked thermally reversible polymers produced from condensation polymers with pendant furan groups cross-linked with maleimides, Google Patents.

[198] BSI, B. S. 2016a. BS EN 13108-1:2016, Bituminous mixtures. Material specifications. Asphalt Concrete. London, England: BSI: British Standard Institute.

Appendix A:

Table A.1: Asphalt maintenance techniques [61].

Technique	Reasons of use							Average Treatment Life (years)	Average Unit Cost
	Friction	Ravel-ling	Rut-ting	Pot-holes	Cracking				
					Low	Med	High		
Crack treatment									
Crack repair with sealing									
Clean and seal					X	X		3	£0.2/lf
Saw and seal								7-10	£1.3/lf
Rout and seal					X	X		3	£0.5/lf
Crack filling						X	X	1-3	£0.2/lf
Full-depth crack repair							X	5	£3.9/lf
Surface treatments									
Fog seal		X						1-2	£0.1/sy
Seal coat	X	X						3-6	£0.4/sy
Double chip seal	X	X						7-10	£1.2/sy
Slurry seal	X	X						3-5	£1.2/sy
Micro surfacing	X	X	X					5-8	£1.3/sy
Thin hot -mix overlay		X	X					5-8	£19.3/sy
Pothole and patching re-pair									
Cold -mix asphalt				X				1	£42.4/ton[a]
Spray injection patching				X				1-3	Not availa-ble[b]
Hot- mix asphalt				X			X	3-6	£19.3/ton[a]
Patching w/slurry or micro-surfecing materials				X			X	1-3	£42.4/sy[a]

[a] Cost for materials only
[b] Price various with conditions

Appendix B:

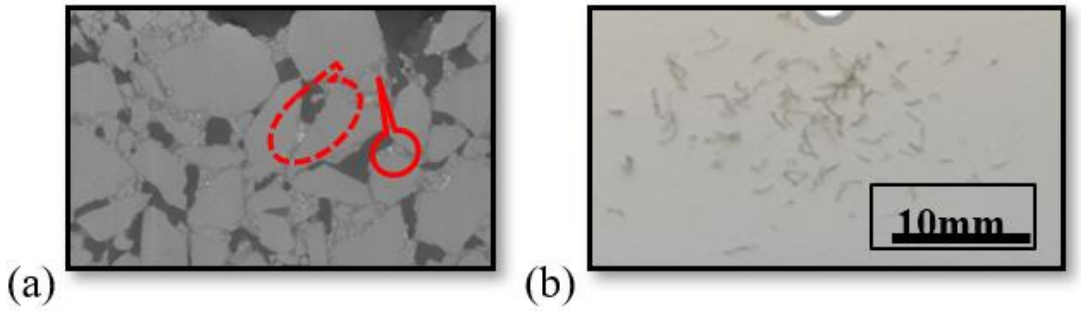


Figure B.1: a Fibre steel, -(a)- distributes steel fibres in sample, (b)- dimeter of steel fibre, in CT scan image

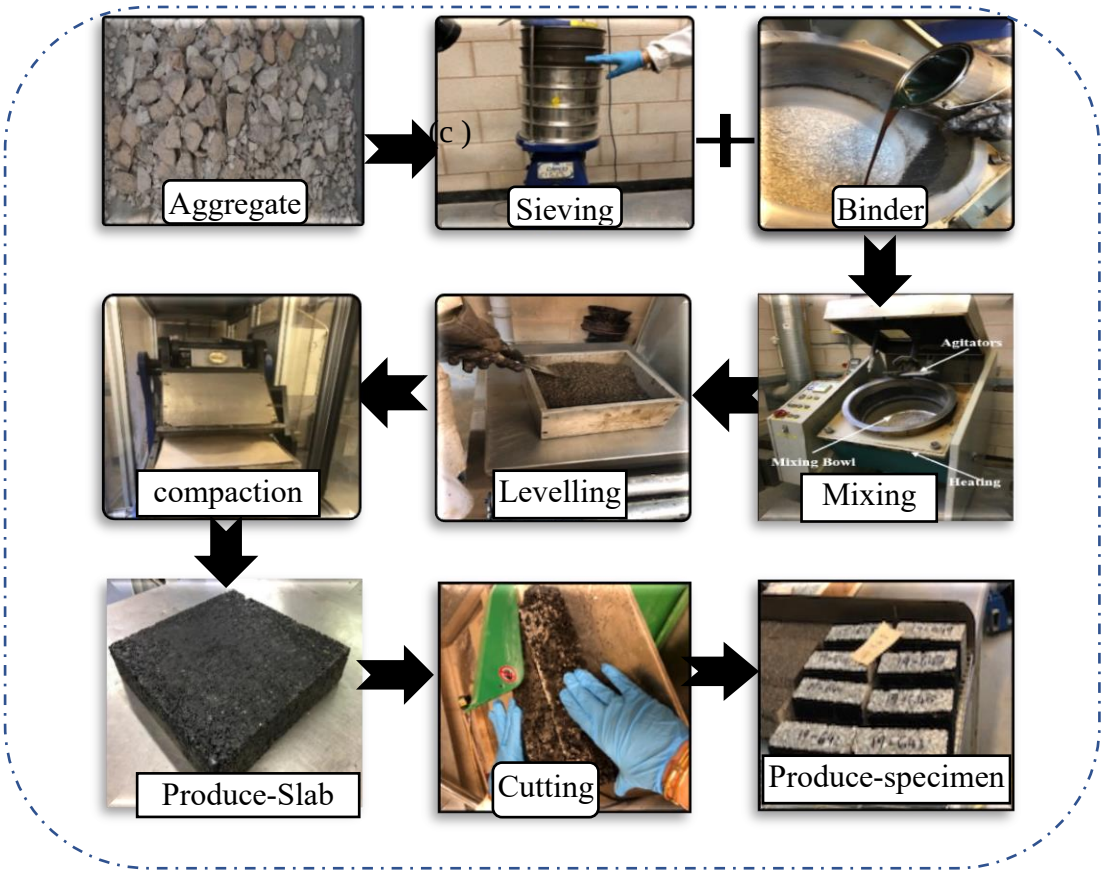


Figure B.2: Manufacturing of Hot Mix Asphalt

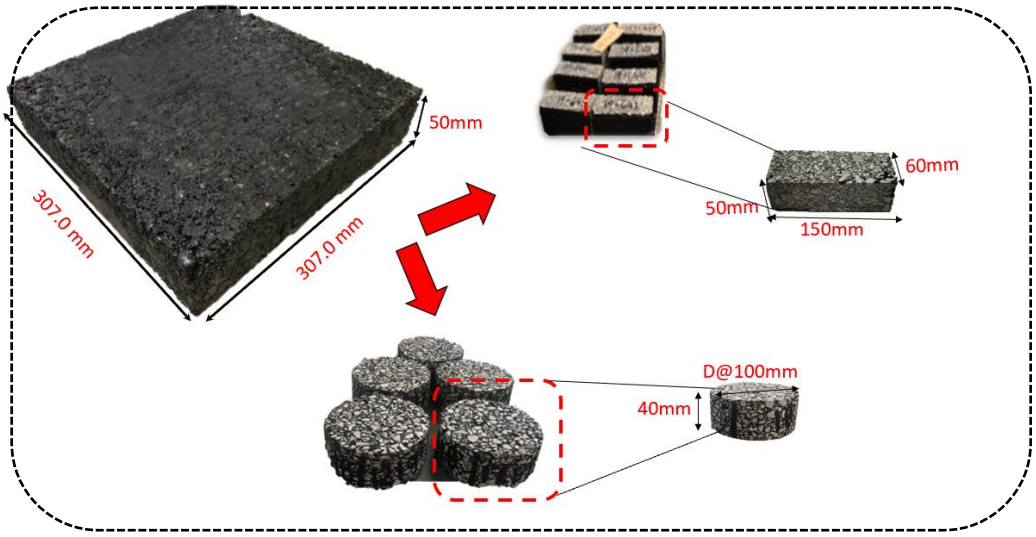
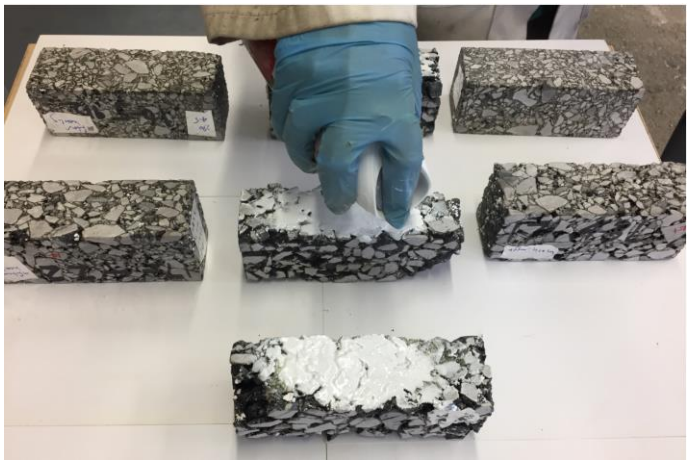
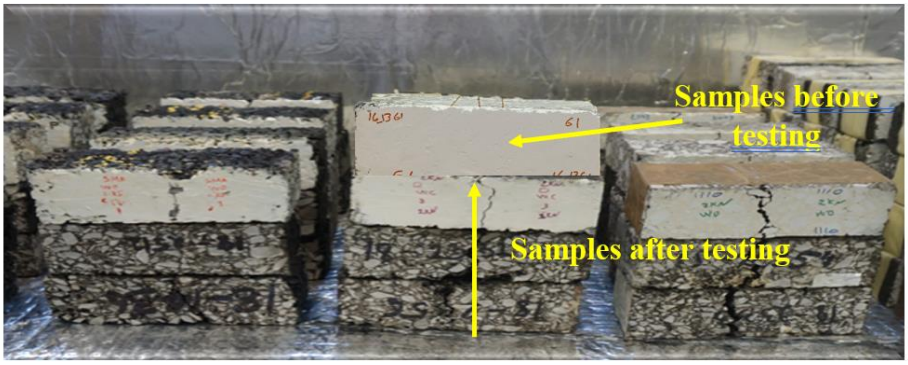


Figure B.3: Asphalt mixture slabs produced beams and cylinders.



(a)



(b)

Figure B.4: a)Example for samples (a)white marking spray paint, (b) Samples before and after testing.

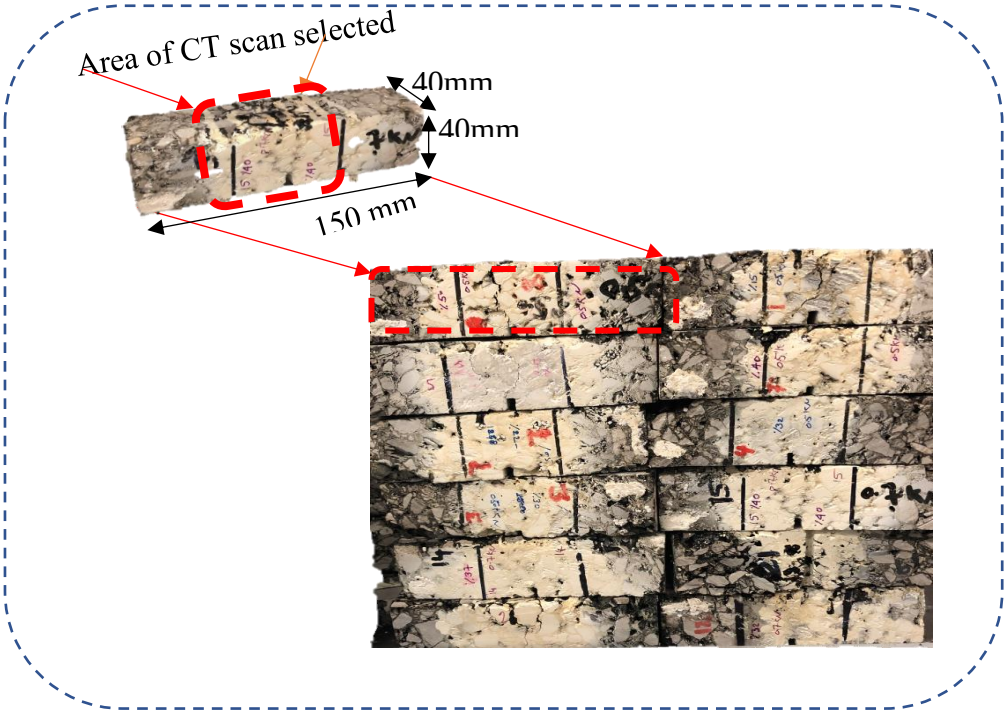


Figure B.5: Asphalt mixture beams for CTscan test for Chapter 5.

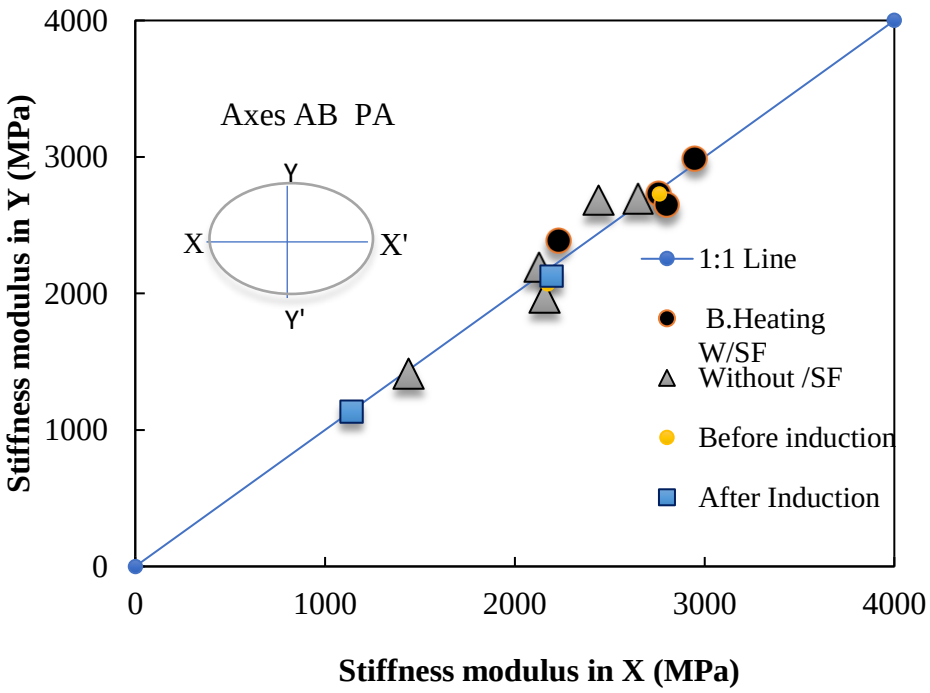


Figure B.6 : Average values of the stiffness modulus of PA specimens with (W/SF), and without (WO/SF), relationship between stiffness modulus of the PA specimens measured in longitudinal (Y) and cross (X) directions.

Appendix C:

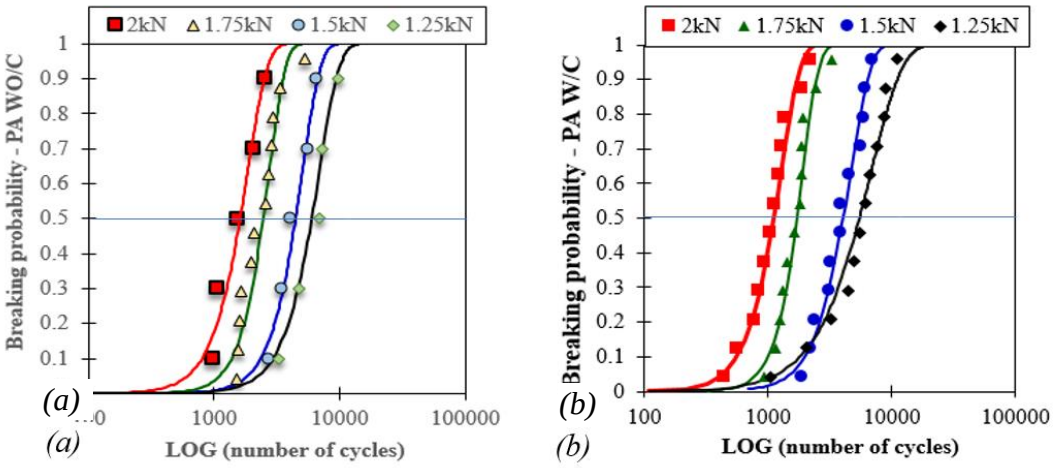


Figure C.1: Distribution functions of the number of cycles resisted by PA without capsules (WO) at different loading levels. (b), and Porous Asphalt (PA), with (W/C) capsules.

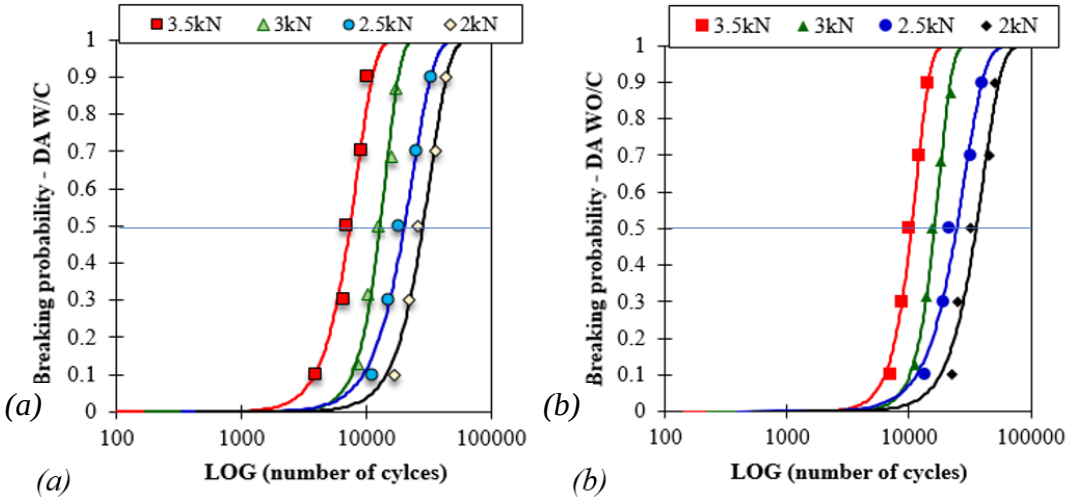


Figure C.2: Distribution functions of the number of cycles resisted by DA without capsules (WO) at different loading levels. (b), and Porous Asphalt (DA), with (W/C) capsules

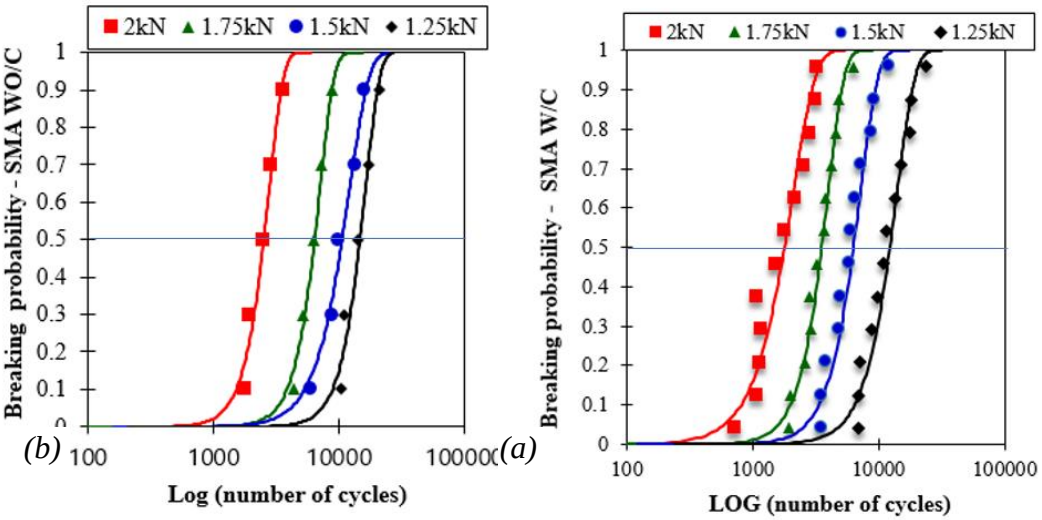


Figure C.3:Distribution functions of the number of cycles resisted by SMA without capsules (WO) at different loading levels. (b), and Ston Mastic Asphalt (SMA), with (W/C) capsules.

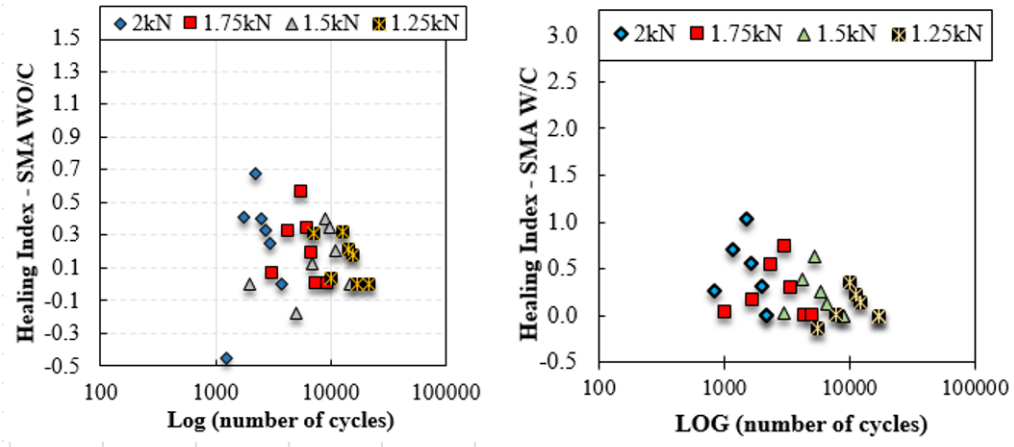


Figure C.4:Healing index vs number of loading cycles for, (a) SMA without capsules,(b) SMA with capsules

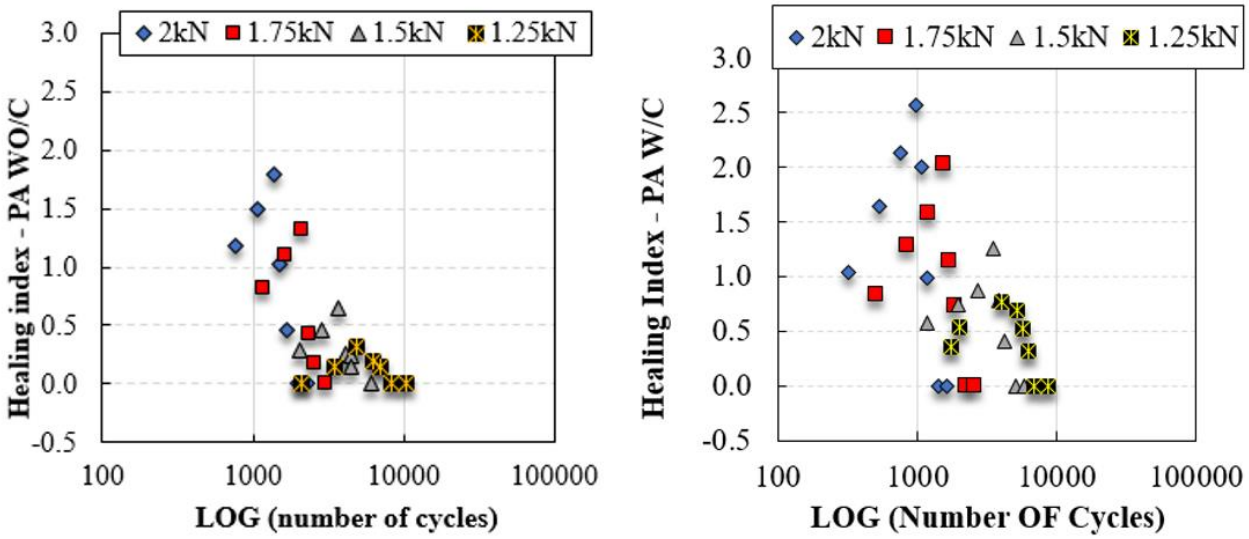


Figure C.5: Healing index vs number of loading cycles for(a) PA without capsules, (b)PA with capsules.

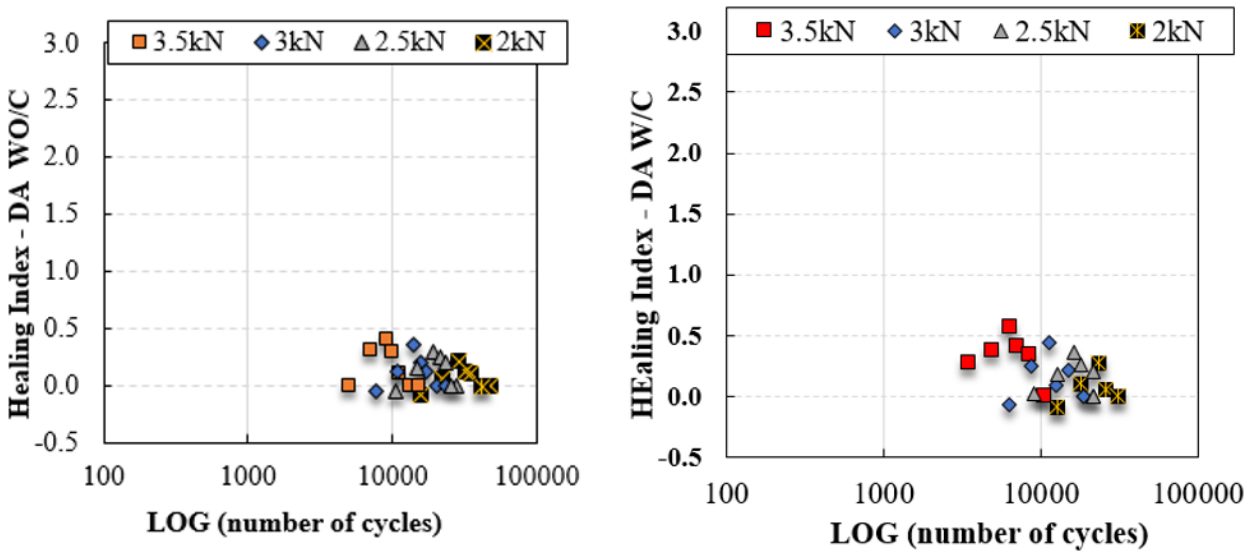


Figure C.6: Healing index vs number of loading cycles for(a) DA without capsules, (b)DA with capsules.

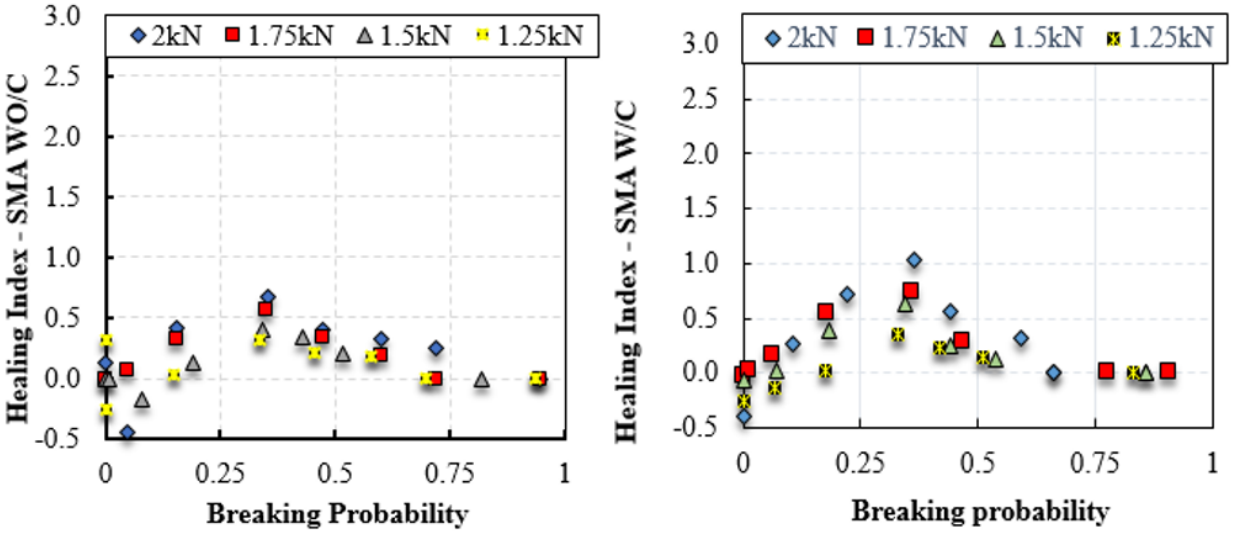


Figure C.7: Healing index vs probability of cracking for, (a) SMA without capsules, (b)SMA with capsule.

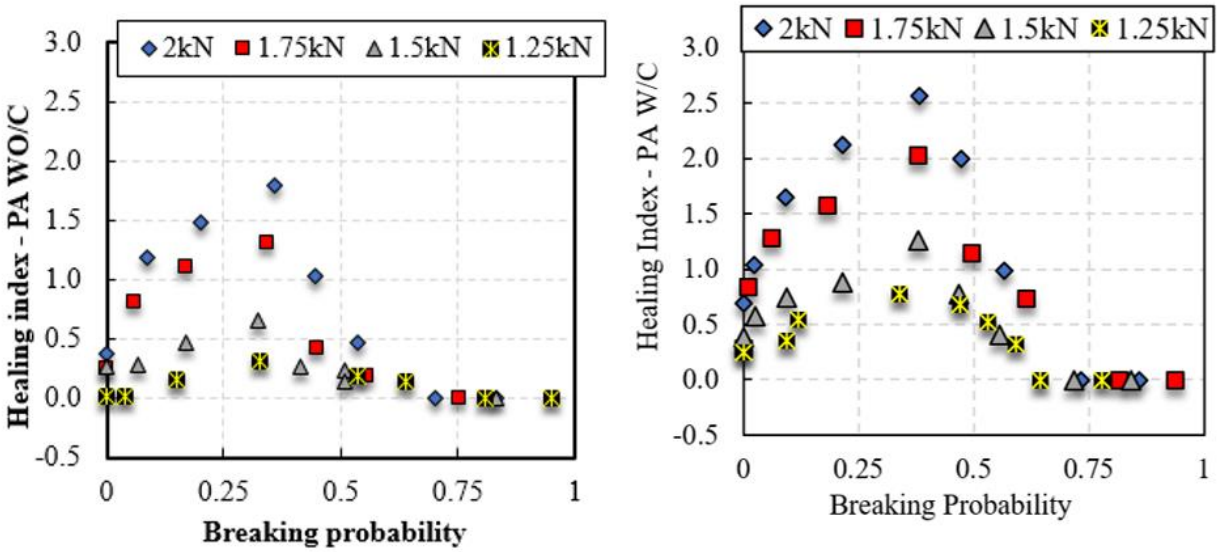


Figure C.8: Healing index vs probability of cracking for, (a) PA without capsules, (b)PA with capsule.

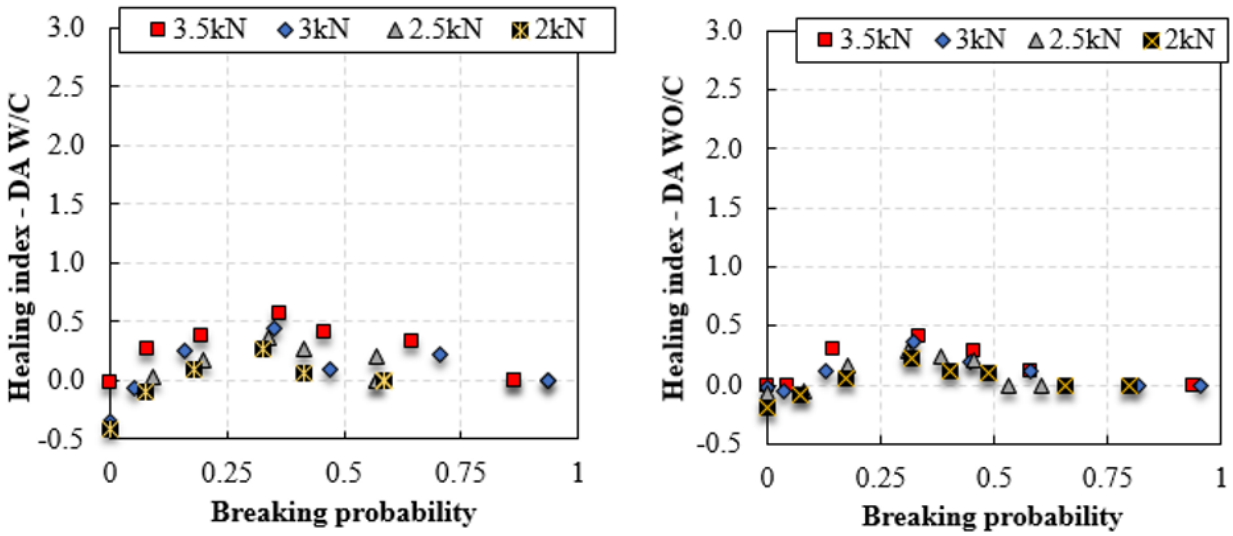


Figure C.9: Healing index vs probability of cracking for, (a) DA without capsules, (b)DA with capsule.